Erasmus hogeschool Brussel

upna Universidad Pública de Navarra Nafarroako Unibertsitate Publikoa

EXPERIMENTAL STUDY OF MICROTABS IN SMART BLADES FOR WIND TURBINES

DAVID SENOSIAIN SUESCUN & JOSEBA MORALES GOICOECHEA

10 JUNE 2013

MASTER THESIS SUBMITTED IN PARTIAL FULFILMENT OF THE REQUIREMENTS TO OBTAIN THE DEGREE OF MASTER OF SCIENCE IN INDUSTRIAL SCIENCES

ERASMUS STUDENT EXCHANGE PROGRAM 2012-2013

PROMOTERS AT EHB

DR. MARK RUNACRES

DR. TIM DE TROYER

PROMOTER AT UPNA

DR. PABLO SANCHIS GURPIDE

ACKNOWLEDGEMENTS

The accomplishment of this thesis would not have been possible without the invaluable help of many people who have supported us along this experience. It is not only our duty but a pleasure to thank all of them for their help.

In the first place, we would like to express our gratitude to the Erasmushogeschool Brussel for providing us the chance of completing our master degree in industrial science with the performance of the master thesis.

We want to show our gratitude to Dr. Mark Runacres, our promoter, and head of the IWT department at the EHB. We are really pleased to him for showing us how all our knowledge can be applied to the real life. And for providing us the chance of taking part in such a experimental project that would not have been possible at our home city university.

We would also like to be grateful with Dr. Tim De Troyer, our co-promoter, who has helped us during the entire project in all the difficulties we have had to face up. We also want to thank all the FabLab staff, especially Lieven Standaert and Serge Kubera, for supporting us in all the hours we spent in the FabLab in the last nine months.

Also, we would like to show all our gratitude to those people who have supported us from the distance. To our families and relatives, friends, both the ones in Spain, and all the new friends we have known in this amazing experience, and also to our promoter in the Public University of Navarra, Dr. Pablo Sanchís Gurpide for encouraging us to this experience and helping us in every step we made till the submit of this thesis.

David Senosiain Suescun and Joseba Morales Goicoechea

Brussels, 10 June 2013.

CONTENTS

FIGURES

GRAPHICS

TABLES

EQUATIONS

PREFACE

The goal of this thesis is to carry out an experimental study of the performance of smart blades reducing extreme and/or cyclic loads for their use in wind turbines.

First of all, theoretical research about wind turbines and smart blades was done. Some of this information is explained in the thesis in order to set the background and make it more readable and understandable (*Chapters 1 to 3*).

The next step was to choose a blade profile that would fit well the requirements of the experiments and the manufacture of the set up. Besides, one of the possible smart devices had to be chosen according to its expected performance and its feasibility. It had to be taken into account the technologies and tools that could be used for the construction of the set up, and the characteristics of the set up itself. Therefore, the main features of the set up had to be thought at this point, even though the final design was not decided.

After all the preceding work, the setup was defined and built (*Chapter 4*). It consisted in a GU25 (5) 8-11, a profile designed by the University of Glasgow that is quite thick, and has a C_L graph quite linear. It was made in balsa wood that would make it light and after sanding it the remaining surface would be reasonably smooth. Some holes next to the trailing edge were performed for the implementation of the microtabs. This blade was setup with a system for measuring the angle of attack in a test section, which included an aerodynamic balance for measuring the lift forces.

The experiments (*Chapter 5*) consisted in measuring the lift forces in the blade with and without microtab for different angles of attack, with a solidity ratio of 100%. Also different speeds were tested, as the behaviour of the profile changes extremely depending on the Reynolds number. The used microtabs were made in balsa wood cutting sections and gluing them altogether with a solidity ratio of the 96%. It was tested at the 90% of the chord length due to space requirements in the blade.

Finally, final conclusions (*Chapter 6*) and future research options (*Chapter 7*) are explained.

David Senosiain Suescun and Joseba Morales Goicoechea

Brussels, 10 June 2013.

1. INTRODUCTION

1.1 GLOBAL WARMING

Before the industrial revolution, the earth's atmosphere contained 280 ppm of CO_2. By the middle 50s this proportion had risen to 315. Nowadays, there are about 380 ppm and the concentration keeps rising around 2 parts per million every year [1]. The increase of CO_2 in the atmosphere is one of the factors that are leading to global warming [2]. The most visible signs of this problem are the decrease of North and South Poles surface, and the gradual extinction of more than half of the glaciers on Earth.

The industrial activity produces most of the gas emissions (such as methane, carbon dioxide, nitrogen oxide, etc.), which are the cause of the so-called greenhouse effect. Burning fossil fuels for energy production is the main cause of this phenomenon, with a much bigger impact than transport emissions [2].

It is at this point that renewable energies come into picture. The development and decrease of the cost of energy of these sources is the key to develop a sustainable model of energy consumption.

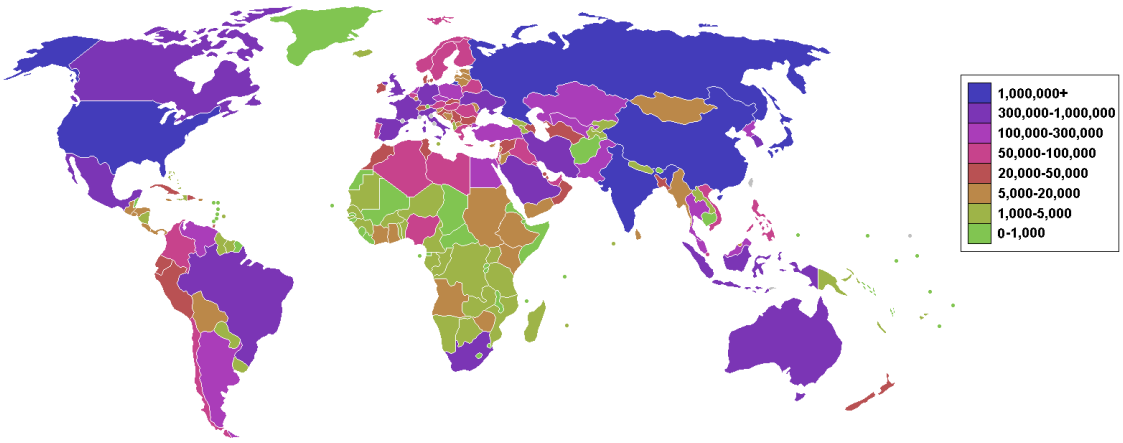

Figure 1 – World countries by CO_2 emissions [3]

1.2 WIND AS RENEWABLE ENERGY

As it has been explained in the section below, the global warming and the fact of the decreasing in number of fossil fuel reserves are one of the factors that started the development of renewable energies. There are different kinds of renewable energies: wind energy, solar energy, hydroelectricity, geothermal energy and biomass are the most important.

In this thesis the wind energy, all the technology about this field and the devices and innovation that are being performed are going to be explained and studied.

These are some advantages that wind energy has [4]:

- ✓ It is a green energy without CO_2 or any other green house effect gas emissions
- ✓ It is renewable; while the sun exists or till the atmosphere does not disappear there will be wind.
- ✓ The environmental impact of setting up a wind turbine farm is small compared to the set up of other energy plants.
- ✓ Easy to integrate in existing power grids
- ✓ It creates local work places
- ✓ The design of wind turbines is flexible and with a range of uses
- ✓ The costs of production have been decreased in a 80% in the last decade

The wind industry is one of the industries that more rapidly have grown in the last ten years.

2. WIND ENERGY

2.1 WIND CHARACTERISTICS

The wind is the result of air mass displacements, from cold regions (Earth poles) to warm regions (equator) [1]

2.1.1 WIND FLUCTUATIONS IN SPACE

The wind fluctuations in space are studied in two different scales: global scale, and local scale.

The global scale explains the wind circulation around the Earth, and as we have mentioned above, the wind moves from the Earth poles to the Earth's equator, following the inverse of the temperature gradient of the Earth. Once the wind is in the equator and it is hot enough it rises to the atmosphere and comes back to Earth poles. This phenomenon is shown in *figure 2*

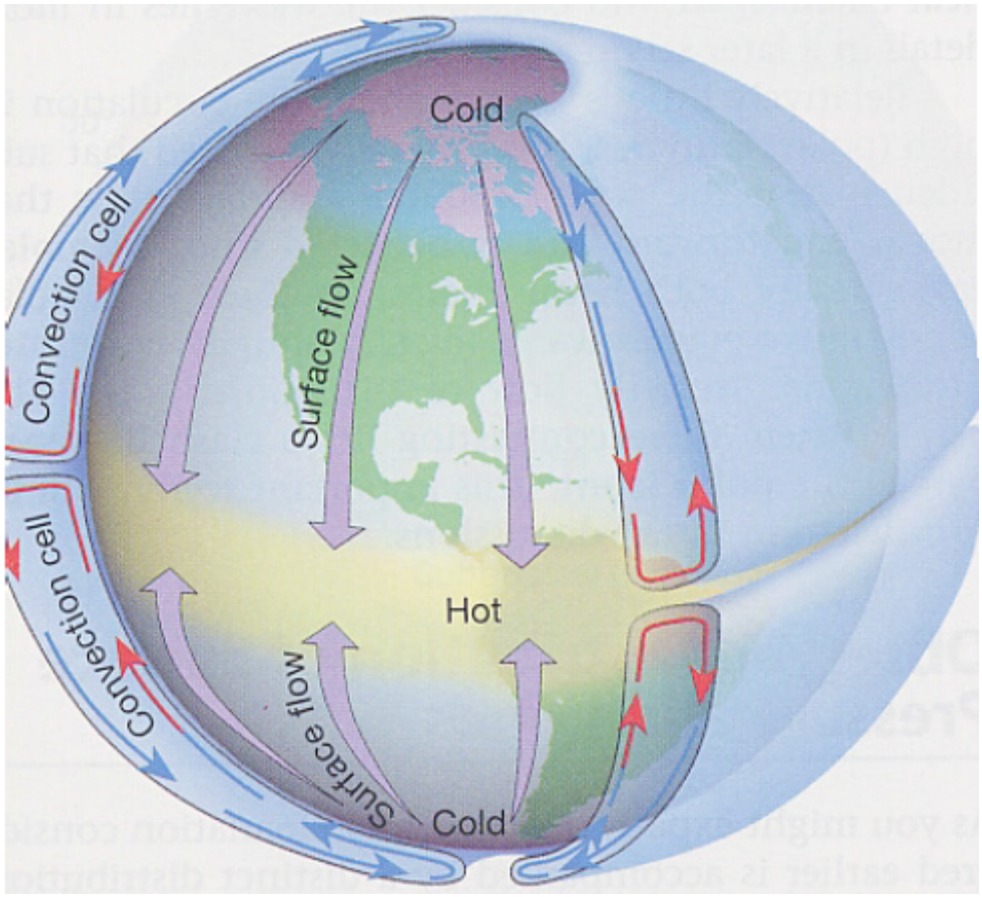

Figure 2 - Simplified model of the global wind flow [1]

However, since the Earth is rotating around its axis, the Earth is an accelerated system, so we have to consider, the effect of the Coriolis force. The Coriolis force changes the direction of the wind, so it does not flow parallel to the meridians, it bends the wind flow to the right side in the north hemisphere and to the left in the south one. This force is what causes the main wind flow directions of the earth as it is shown in *figure 3*

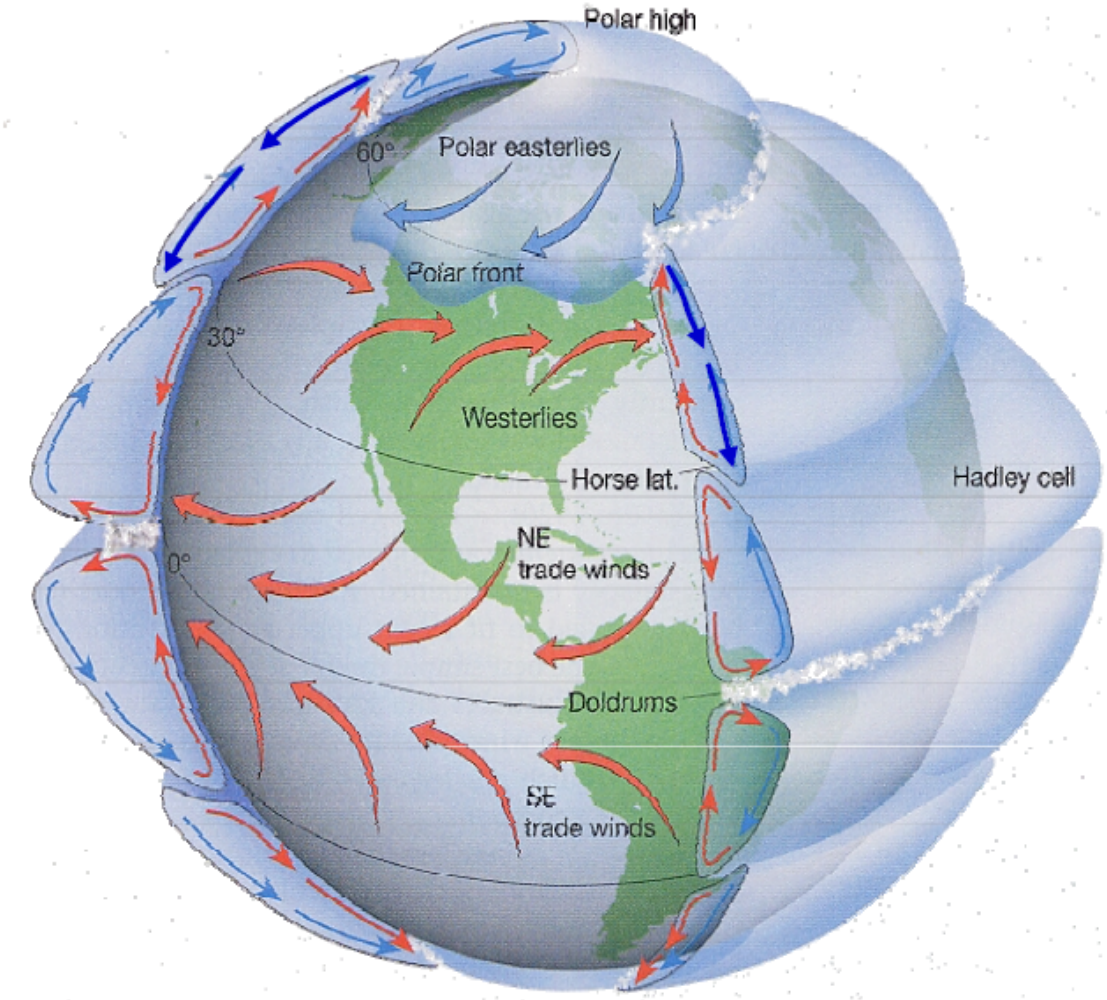

Figure 3 - Global wind flow model with the Coriolis force effect [1]

The local scale explains the wind flows fluctuations in smaller areas, for example, the fluctuation in a country due to the geology of the country (mountains, valleys, rivers etc.)

The complexity of the land affects the wind flow, and creates turbulence in the wind flow that are not desirable for the energy production, because these turbulence affects the structural loads in the wind turbine, and the energy generators work better in steady conditions. In *figure 4* is shown how the more complex is the land the bigger are the turbulences in the air. Turbulence is measured by the following expression [5]:

$$TI = \frac{\sigma_V}{\overline{V}}$$

Equation 1 –Wind Turbulence Intensity equation [2]

Where the TI, is the wind turbulence intensity, measured by the ratio of the standard deviation of the wind and the average speed of the wind.

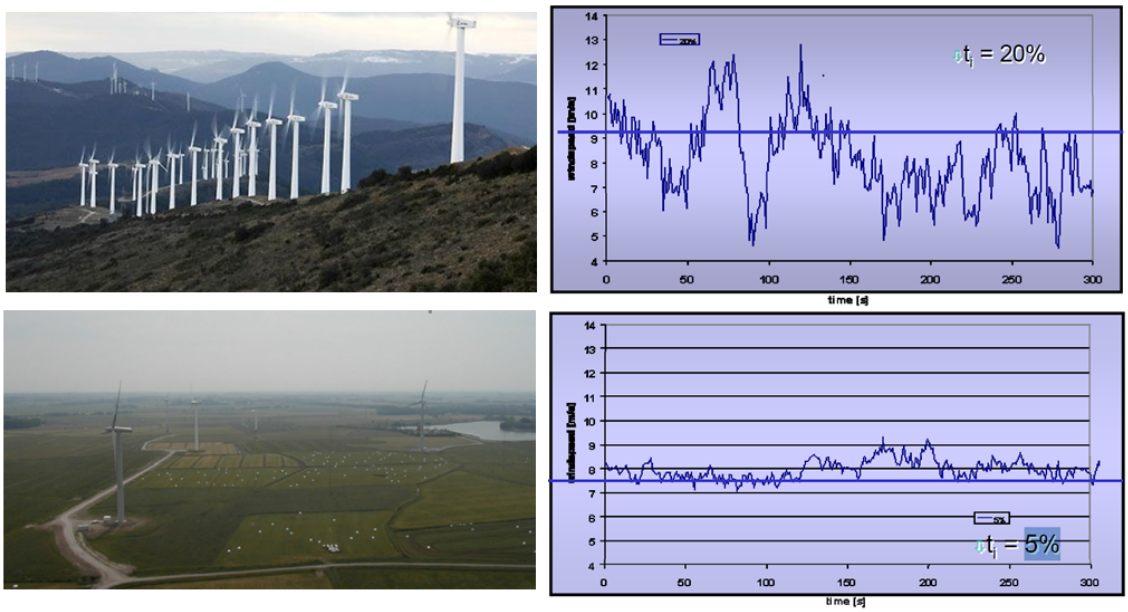

Figure 4 - Wind turbulence due to the land complexity [1]

If we study the graphics above, it is understandable why the off-shore wind turbines are now on the top of wind technology development, since wind above the sea as a really smooth land does not create almost turbulences in the air, and, in addition, the wind average speed is bigger in the sea (Figure 5), so in the sea there are the best conditions for wind energy.

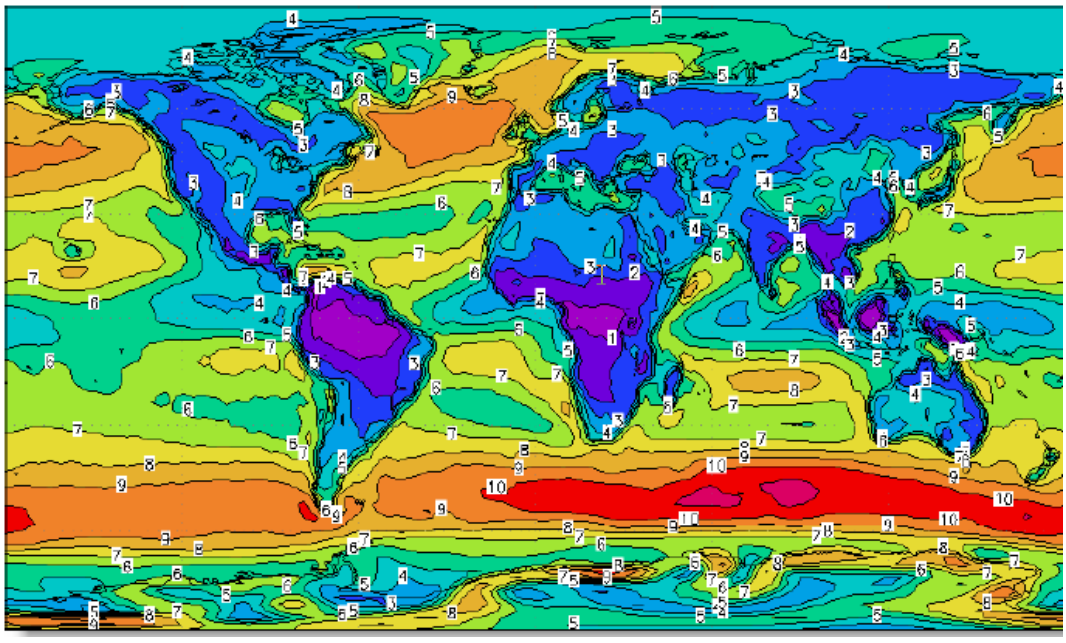

Figure 5 - Wind speed in different regions of the world. Scaled from 1 to 10 [6]

2.1.2 WIND FLUCTUATIONS IN TIME

As we have explained in the section before, the wind flows changes from site to site, but of course, for the same place there are wind speed condition fluctuations in time. For example, there is not the same wind flow in the morning and at night due to temperature variations. (Figure 6)

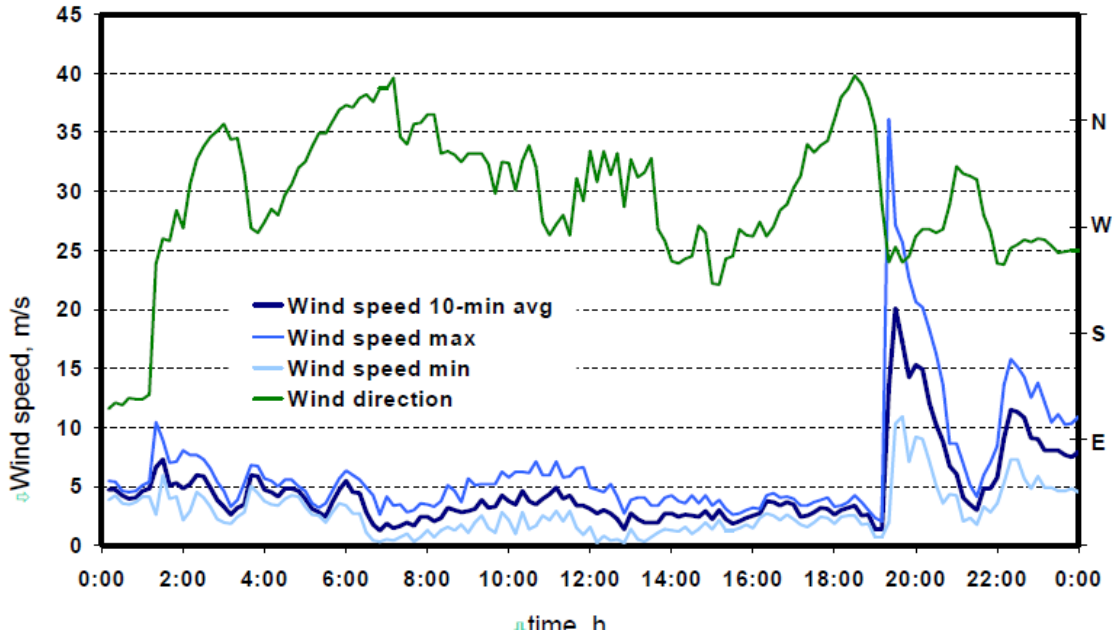

Figure 6 - Wind flow variation during the day [1]

In order to describe all this data in a statistical way, different statistical distributions were studied, and it came out that the distribution that explains better the behaviour of the wind variation along different scale of time is the Weibull distribution (Figure 7).

The Weibull function is given by:

$$f(u) = \frac{k}{A}\left(\frac{u}{A}\right)^{k-1} \exp\left[-\left(\frac{u}{A}\right)^{k}\right]$$

The scale parameter is given with A (scale factor), and the form/shape parameter k, which defines the shape of the Weibull distribution. For k = 1, the Weibull distribution becomes the exponential distribution, and for k = 2, the Weibull distribution becomes the Rayleigh distribution (Figure 7). [1]

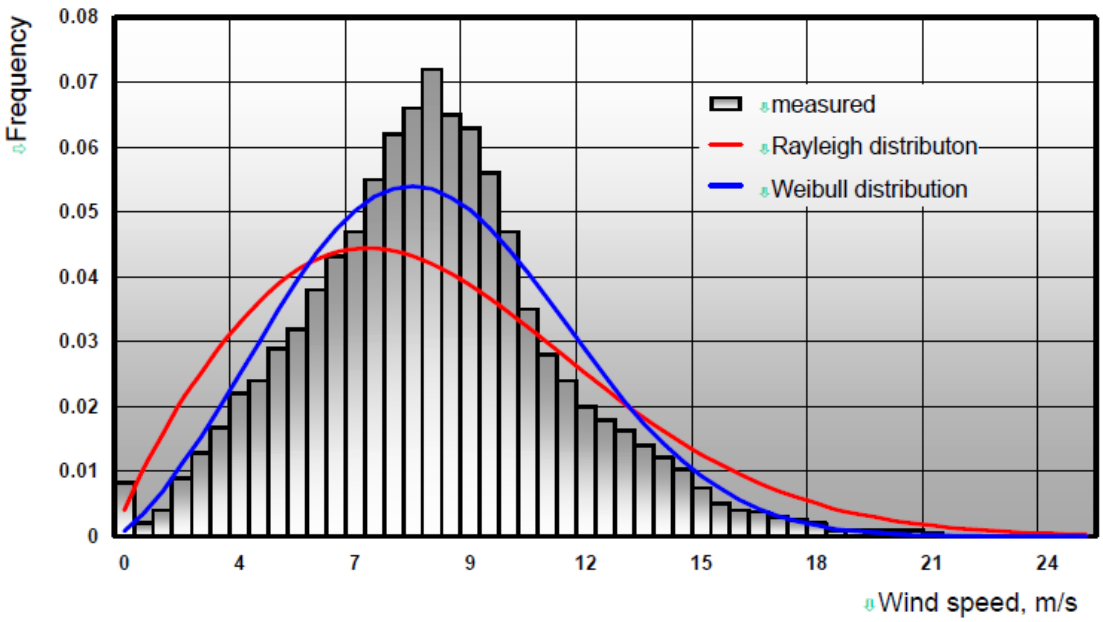

Figure 7 – Weibull and Rayleigh cumulative distributions for wind speed [1]

2.2 WIND ENERGY TECHNOLOGY

2.2.1 WIND TURBINE TYPES

We can classify wind turbines in two big groups: turbines with horizontal axis and turbines with vertical axis (Figure 8). The ones with horizontal axis are used more often, and within this group two different types are built: with the rotor upwind or downwind, being these last ones much more used. Also the wind turbine can be built with or without gearbox. Generally it is necessary a gearbox to get the high speed required by a standard generator. Although the gearbox is a critical part, the benefits earned make it worthy of consideration, and it is usually installed. [1]

Figure 8 – Different axis configurations

The number of blades used can also change (Figure 9). The three blades model is the most developed. There can be used more blades but the forces on the wind turbine will be increased so the lifetime of the wind turbine will be reduced. Several numbers of blades are used in small windmills in order to get a high torque with a small rotor.

The most used configuration is the three blades configuration; despite the most efficient is the downstream two blades offshore configuration. The two-blade configuration has the problem of instability when the blades are vertically, one positioned in the highest point and the other one in the lowest since there are unbalanced lift forces that make necessary the design of oscillating rotors.

After the good results obtained with this kind of turbines on the ground, new development in the field are trying to set wind turbines in the sea (Off-shore technology).

Figure 9 – Wind turbines with different number of blades [5]

2.2.2 WIND TURBINE COMPONENTS

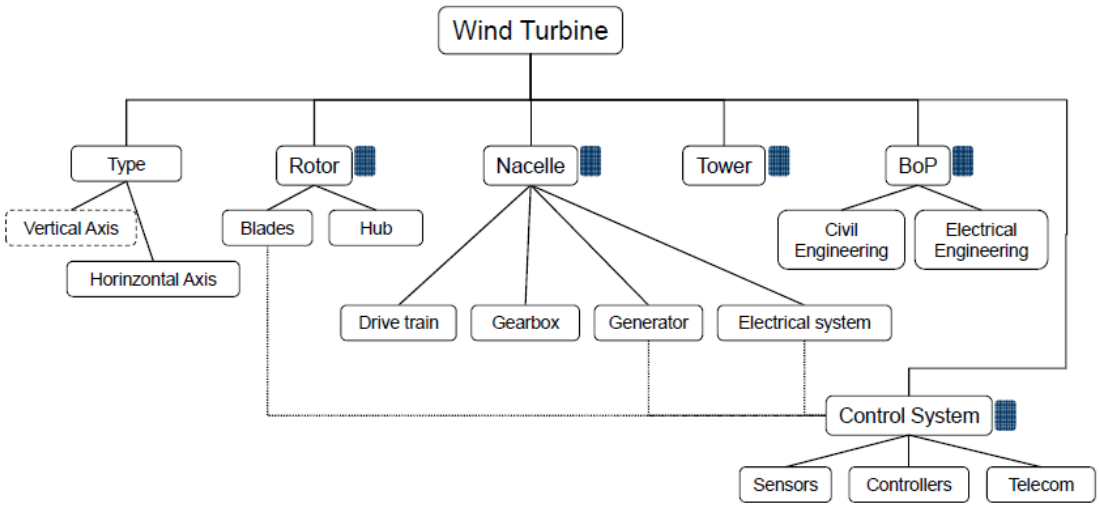

Figure 10 – Components of a wind turbine [1]

ROTOR

The rotors are made by attaching the blades to a hub that connect the blades to the main axis (Figure 11a). In the hub there are also placed all the sensors and actuators for the control of the blades (Pitch angle). (Figure 11b)

The blades are built in composite materials (Figure 11c); they are built with fibre or carbon glass matrix joined with a material such as polyester or an epoxy resin. When epoxy resin is used instead of polyester, the fibre matrix could be a carbon fibre matrix instead of a glass fibre matrix. This allows building a much lighter blade, but the cost of building it rises also. [5]

Figure 11 – a) rotor hub; b) rotor hub with actuators and sensors inside; c) mould for the construction of the blades [5]

NACELLE

The nacelle is the heaviest component of a wind turbine, it contains all the components that allow convert the wind mechanical energy into electric energy available for connecting it to the power grid.

Two of the main components in the nacelle are the gearbox and the generators. We can use two types of generators, synchronous and asynchronous.

Depending of what generator we use, there are some different configurations of the components of the nacelle (Figure 12).

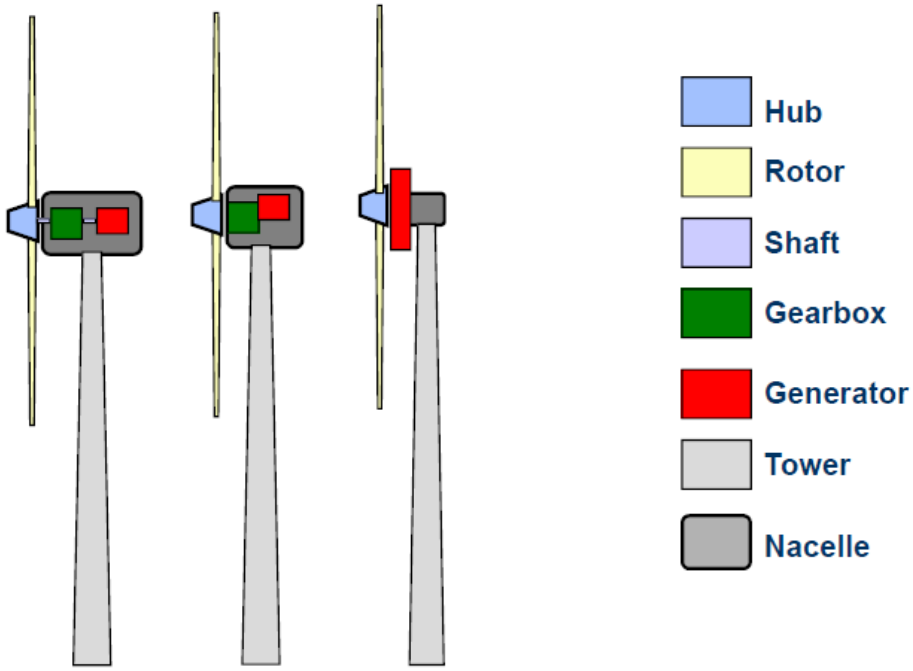

Figure 12 – Different nacelle configurations depending on the use of the gear box [1]

The first configuration is a fixed speed turbine (asynchronous) where the generator and the rotor are connected via the gearbox. In this case due to some small speed variations (up to 2.1%) reactive power is generated, this reactive power is compensated with a capacitors bench at the output of the generator. [5]

The second configuration is composed by a variable speed generator (synchronous) that is doubly fed by the gearbox that fixes the required generator speed and the power electronic converters that varies the electric resistance of the generator allowing rotor speed transitions up to the 10% of the nominal speed. [5]

Finally the third configuration is a variable speed generator connected directly to the rotor, and the output of the generator connected to power electronic devices that allow the generator being connected to the power grid. [5]

The nacelle also hosts the main bearings that stand for the main shaft, and other components, such a oil tanks for the greasing of the systems, torque converters etc.

TOWER

The tower is the structure on which the wind turbine stands. It must be stiff enough to support the rotor and the nacelle. The towers are built in different materials, in the first towers wood was used, but currently they are constructed in concrete or steel. [5]

The tower also contains the mechanisms for controlling the orientation of the rotor in the case of horizontal axis turbines (Yaw angle).

BALANCE OF PLANT (BoP)

In order to develop a wind farm, both civil and electrical engineering must be taken into account.

Civil engineering involves all the aspects related with the maintenance of the wind turbines, construction of the foundations and the crane platforms, and the construction of the access roads to the plant.

On the other hand, the electrical engineering includes aspects such as park cabling, the set up of transformer stations, grid connection etc.

2.3 COST OF ENERGY

With global warming and the limited supply of fossil fuels in mind, there is every reason to assume that wind energy will only become more important. In this context it is necessary to further improve the technologies, in order for wind energy to stay economically competitive with other means of energy production. In practice, this is done lowering the cost of energy (COE). This cost consists of three variables: the energy capture of the turbine over its lifetime, the capital cost of the turbine and the operations & maintenance (O&M) costs. This last variable can be further divided into scheduled and unscheduled costs. The COE can be expressed with a simplified formula [7]

$$COE = \frac{Capital\ Cost + O\&M\ Cost}{Lifetime\ Energy\ Capture}$$

Equation 2 – Cost of energy [9]

Equation 2 illustrates that there are several ways to reduce the COE. One way is to reduce the O&M costs by making turbines more reliable. Another is to reduce the amount of materials or improve manufacturing techniques to decrease the capital cost. Finally, the COE can be reduced increasing the energy capture during the lifetime of the turbine, for instance by increasing the rotor diameter and turbine size. However, the growth of turbines in size also means that the structural and fatigue loads become more pronounced [7].

2.4 AERODYNAMICS

2.4.1 LIFT AND DRAG FORCES

In order to understand the performance of a wind turbine, we should firstly understand the phenomenon that takes place in each blade, as it is the component that takes advantage of the wind to produce movement in the rotor.

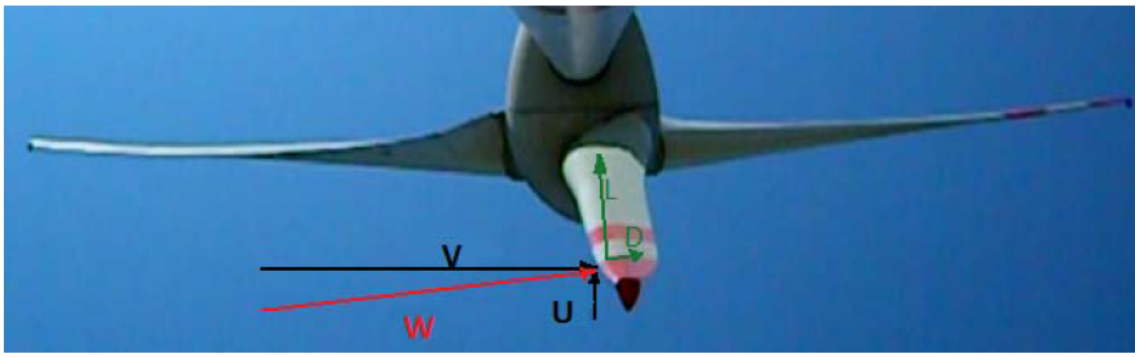

Figure 13 – Wind speed triangle and aerodynamic forces in an airfoil [1]

When the wind hits the blade two different forces are produced the lift (L) and the drag (D) (Figure 13) .The first one is normal to the relative wind direction, and is the result of the pressure difference between the suction side or extrados and the pressure side or intrados. The second one is parallel to the relative wind direction and is due to the resistance of the profile to the wind. The sum of both gives a resultant (R), which we can be divided into two forces according to the effect on the wind turbine (Figure 14) [1]

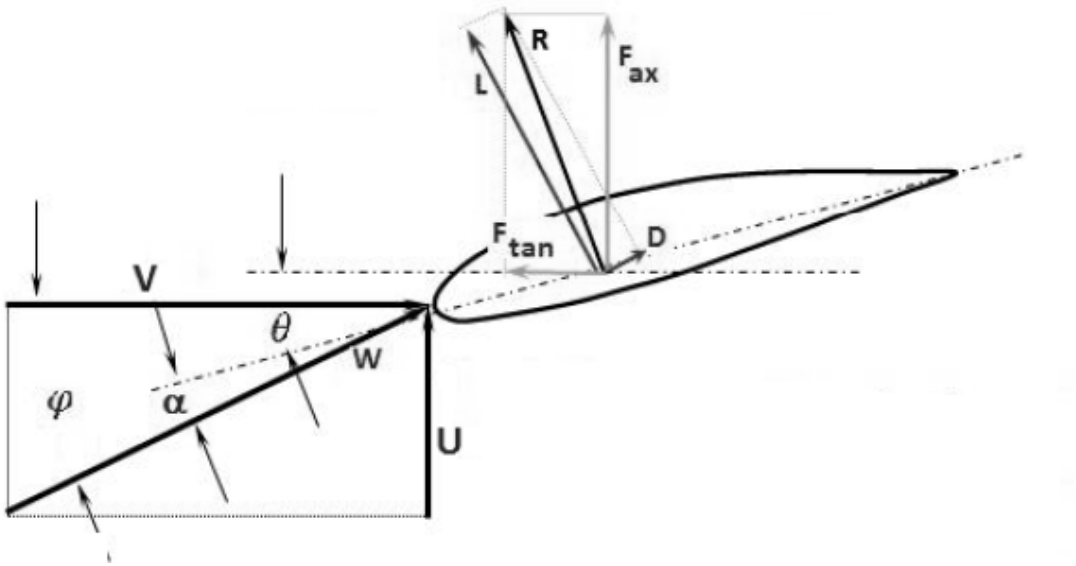

Figure 14 – Lif and Drag forces on an airfoil [1]

Where:

V is the blade speed
U is the wind speed
W is the relative speed between the blade and the wind or the wind speed that the blade sees.
α is the angle of attack
φ is the angle of inclination
L is the lift force
D is the drag force
R is the resultant force of the lift and the drag

Assuming the blade as a two-dimensional element, the differential forces of lift and drag are proportional to the pressure difference between the pressure and suction side and the airfoil surface projection in the plane perpendicular to the wind direction. In the same way, the surface is proportional to the chord, the radio and the angle of attack (Figure 15). They must be taken into account both lift and drag coefficients (C_L and C_D).

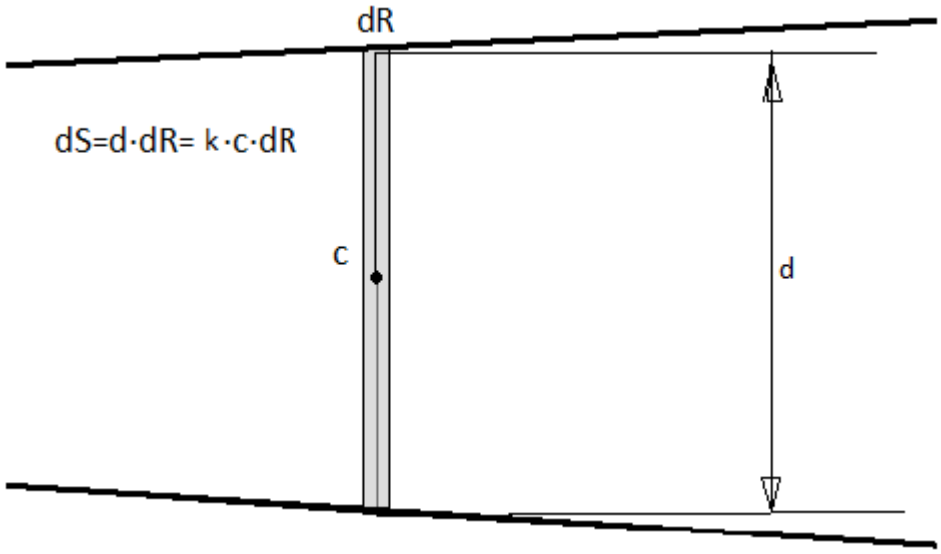

Figure 15 – Airfoil surface assuming the blade as a two-dimensional element [1]

Thus, the differential equations of lift and drag are:

$$dL = \frac{1}{2}\rho\, W^2 c\, C_L dR$$

$$dD = \frac{1}{2}\rho\, W^2 c\, C_D dR$$

Equation 3 – Lift and drag differential equations

The projection of these two forces in the rotation surface plane and the axial plane results in two forces:

- ✓ The tangential, related with the torque, that is located in the rotation surface.
- ✓ The axial, related with the thrust, that is perpendicular to that surface.

To develop the equation of both in the following lines, the angle of inclination (φ) is used. It is the sum of the angle of attack (α), and the angle of step (angle between the chord of the blade and the rotation surface). According to this, the forces can be written with the following expressions: [1]

$$dF_{\tan} = dL\sin\varphi - dD\cos\varphi = \frac{\rho W^2 c}{2}(C_L\sin\varphi - C_D\cos\varphi)dR$$

Equation 4 – Resultant tangential force on an airfoil [1]

$$dF_{ax} = dL\cos\varphi + dD\sin\varphi = \frac{\rho W^2 c}{2}(C_L\cos\varphi + C_D\sin\varphi)dR$$

Equation 5 – Resultant axial force on an airfoil [1]

Where w is the relative wind speed, ρ the air density, c the cord, C_L the lift coefficient, and C_D the drag coefficient. To obtain the final expression, it should be done the integral between 0 and the length of the blade.

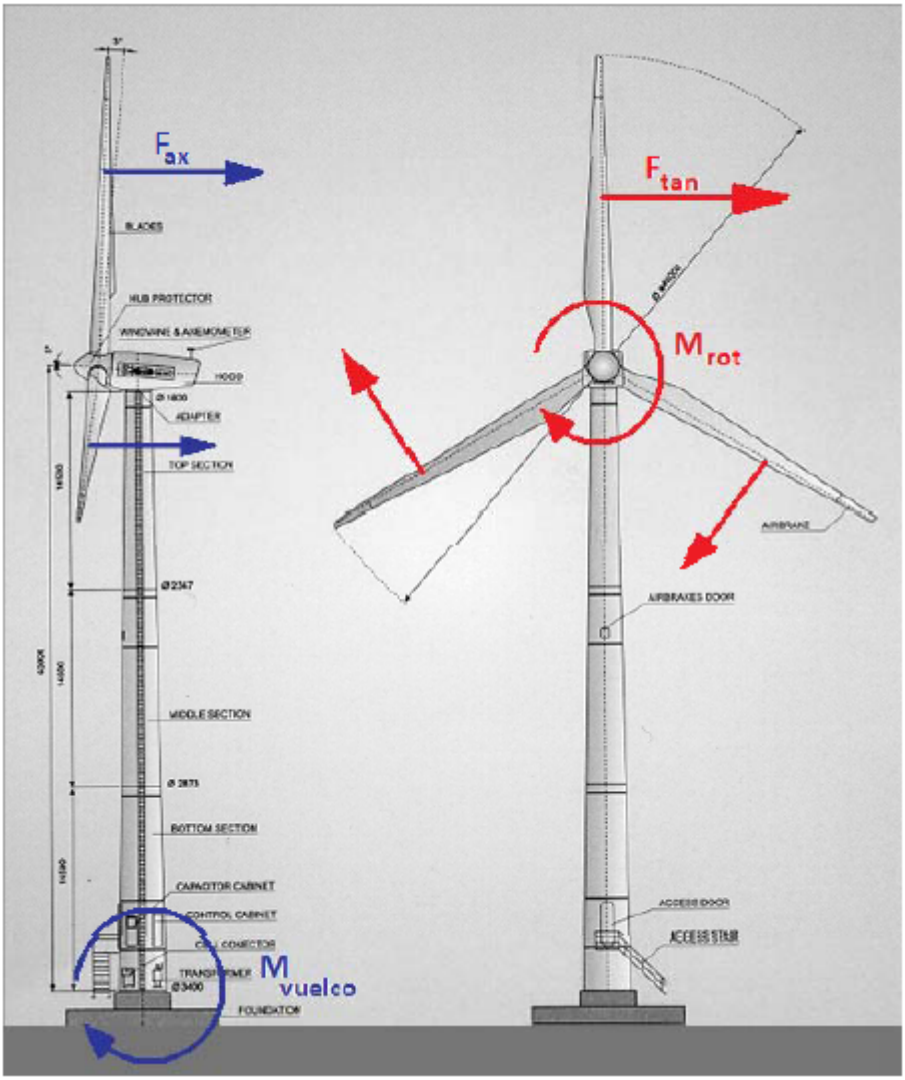

Figure 16 – Tangential and axial forces and torques in a wind turbine

The axial force pushes the whole tower (Figure 16), causing a torque that tries to knock over the structure. So it should be considered for the calculations of the wind turbine. It is obvious that the best case would be a wind turbine with null axial force, as it only causes problems. Unfortunately that is not possible, but a decrease can be achieved by both decreasing the lift or the drag. The lift is the one that makes the wind turbine work, so the only option is to reduce the drag.

The tangential force produces the moment that makes the rotor spin. According to *equation 4* the lift makes this force grow and the drag makes it smaller. So once again it is interesting to reduce the drag in order to improve the performance of the turbine. Taking into account these reasoning, it is interesting to develop devices that allow increasing the lift in those conditions the optimum is not reached. It could be also useful to create mechanisms that make possible to operate the wind turbine at speeds further than its original cut-out speed (this concept is explained in the next point), by reducing the lift and therefore the extreme loads in the turbine so the nominal energy could be produced in wider ranges of speed.

Using these devices could also affect the drag, which has also to be taken into account, as the higher it is, the stronger the structure should be and the more it will decrease the tangential force. Stronger structure means a more expensive wind turbine, and the reduction of the tangential force means a decrease in the efficiency of the machine.

2.4.2 AVAILABLE WIND POWER

It is very important to know how much energy is in the wind that can go through a turbine. Imagine a mass flow crossing a control volume that represents the rotor *figure 17*. The mass flow crosses the control volume (dV), which is a disk of area S and depth dL, with speed U (notice that U is used instead of V for velocity in order not to mix with volume). Applying the continuity equation of fluid mechanics and physics it can be determined the power of the air stream crossing the disk [1]

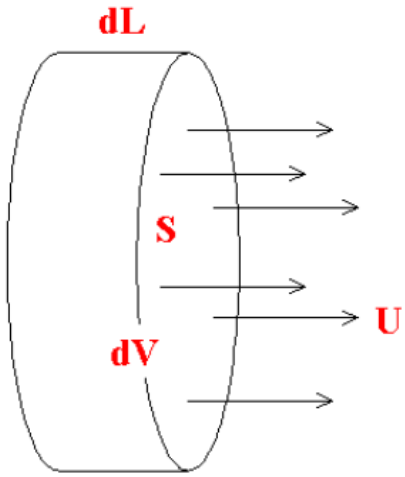

$$\dot{m} = mass\ flow = \frac{dm}{dt} = \frac{d(\rho V)}{dt} = \rho\frac{dV}{dt}$$

$$dV = SdL = SUdt$$

$$\dot{m} = \rho SU$$

$$E_c = \frac{1}{2}mU^2$$

$$P = \frac{dE_c}{dt} = \frac{1}{2}\dot{m}U^2$$

Figure 17 – Differential mass flow in the rotor [1]

$$P = \frac{1}{2}\rho A V^3$$

Equation 6 – Wind power [5]

The kinetic energy per unit time (or the power of the flow) is given by the equation above. There are three important conclusions that can be made from this:

- ✓ The wind power is proportional to the density of the air. This implies that the location of the wind turbine is important as the air density depends on it, for example it is bigger at the sea level than in high mountains.

- ✓ Power from the wind is proportional to the area swept by the rotor or the rotor's radius squared. So the bigger the rotor is the bigger the power that can be obtained will be. The effect of the rotor diameter increase is more important than the air density effect, due to the radius squared dependence.

- ✓ The wind power is also proportional to the wind velocity cubed. Obviously, this is the most relevant parameter because a small change in the air velocity means a big difference in the obtained power. Again the importance of the wind turbine location is shown, and this is the reason why long-term wind data from the location is studied before installing any wind turbine.

The kinetic energy per unit time calculated in *equation 6* is not the maximum that can be obtained from wind by a turbine. This is the power that the wind has, but it is impossible to take advantage of all this energy with a wind turbine.

2.4.3 POWER CURVE AND PERFORMANCE COEFFICIENT (CP)

The relationship between the wind speed and the power that a turbine can get is fundamental. As a consequence one of the most important plots for every wind turbine is the power curve, in which the power output of the turbine is represented as a function of the wind speed. In *figure 18* is shown a typical power curve with its most important points and zones [7]

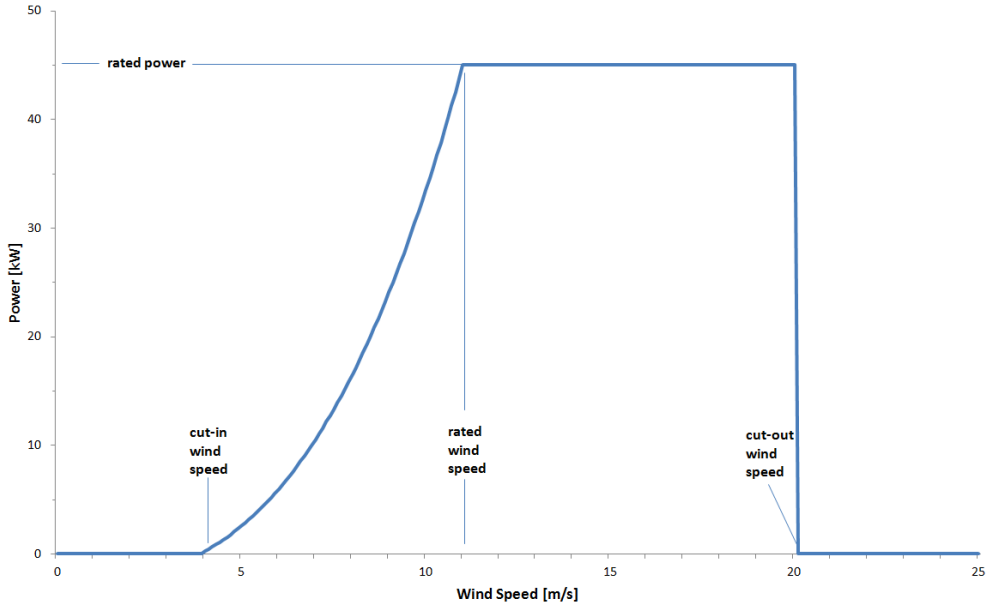

Figure 18 – Power curve of a wind turbine [1]

At very low wind speeds, there is insufficient torque exerted by the wind on the turbine blades to make them rotate. However, as the speed increases, the wind turbine will begin to rotate and generate electrical power. The speed at which the turbine first starts to rotate and generate power is called the cut-in speed.

As the wind speed rises above the cut-in speed, the level of electrical output power rises rapidly as shown in *figure 18*. In this figure is also appreciable that the power available in the wind raises with the cube of the speed, this is an ideal behaviour, in real cases the curves never reaches the ideal one shown in the figure is always below it or in the best cases is equal. However, although this curve represents the maximum power available for a wind speed, the slope of the real curve can locally be greater than the one shown in *figure 18*. However, due to the wind speed increase the power output of the turbine can reach the limit of the electrical generator. This limit of the generator output is called threated power output and the wind speed at which it is reached is called the rated wind speed. At higher wind speeds, the design of the turbine is arranged to limit the power to this maximum level and there is no further rise in the output power. There are two typical ways in wind turbines to keep the rated power at a constant level, by controlling the pitch angle or by controlling the stall.

Once the rated power of the wind turbine is achieved the wind turbine can still work in higher wind speeds than the related to the rated power, but there is a critical wind speed in which the turbine must stop, as the generated forces can damage the turbine structure and induce the collapse of the wind turbine. This is called cut-out

speed. The efficiency or, as it is more commonly called, the power coefficient, C_p, of the wind turbine is simply defined as the power delivered divided by the available power.

$$C_P = \frac{Delivered\ Power}{Available\ Power} = \frac{P}{\frac{1}{2}\rho S V^3}$$

Equation 7 – Power coefficient [1]

2.4.4 BETZ LIMIT

There is a theory about the maximum possible energy that can be delivered by a "hydraulic wind engine", or wind turbine, that is called Betz's law. Decades before the arrival of the modern 3-blade wind turbines used to generate electricity, Albert Betz developed Betz's law in 1919. According to Betz's law, no turbine can transform more than 59.3 % of the kinetic energy in wind [1]

In order to calculate the maximum theoretical efficiency of an ideal rotor (for example a wind turbine), it is replaced by an actuator disc that withdraws energy from the fluid that goes through it. The upstream flow has higher velocity (V_1) than the one in the rotor section (V), and at certain distance behind the rotor section the fluid flows with a smaller velocity (V_2). These velocities are represented in the *figure 19.*

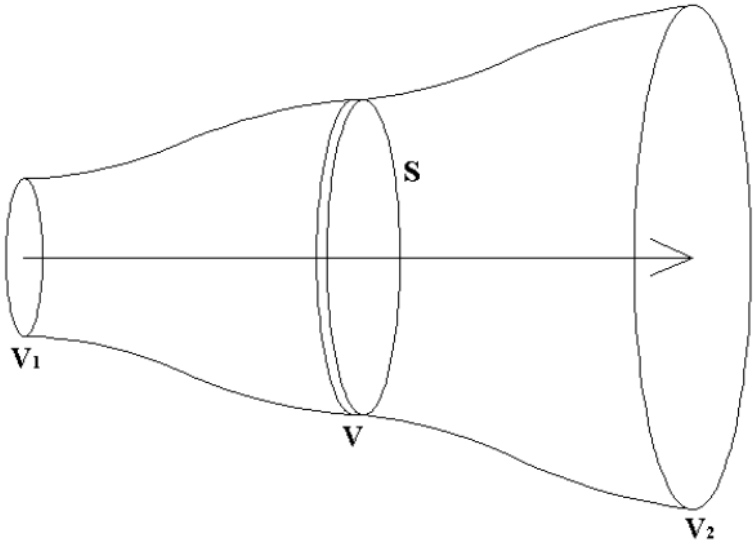

Figure 19 – Scheme of wind flow distribution

To describe Betz's theory we need to do some assumptions:

- ✓ First of all, the rotor is an ideal rotor, with an infinite number of blades that have no drag. Any resulting drag would only lower this idealized value.

- ✓ In addition, the flow into and out of the rotor is axial. This is a control volume analysis, and to obtain a solution the control volume must contain all the flow going in and out (not taking into account the whole flow would violate the conservation equations).

- ✓ The flow is considered incompressible. The density remains constant, and there is no heat transfer from the rotor to the flow or vice versa.

Once those assumptions are done, the expression that describes the power in a wind turbine is explained:

Applying conservation of mass to this control volume, the mass flow rate (the mass of fluid flowing per unit time) is given by:

$$\dot{m} = \rho A_1 V_1 = \rho S V = \rho A_2 V_2$$

Equation 8 – Continuity equation

Where V_1 is the speed in the front of the rotor and V_2 is the speed downstream of the rotor, and V is the speed at the fluid power device. ρ is the fluid density, and the area of the turbine is given by S. The force exerted on the wind by the rotor may be written as:

$$F = m \cdot a = m\frac{dV}{dt} = \dot{m}\Delta V = \rho S V (V_1 - V_2)$$

Equation 9 – Wind force equation

The work done by the force may be written incrementally as:

$$dE = F \cdot dx$$

$$P = \frac{dE}{dt} = F\frac{dx}{dt} = F \cdot V = \rho S V^2 (V_1 - V_2)$$

Equation 10 – Wind power equation

However power can be computed in another way, by using the kinetic energy. Applying the conservation of energy equations to the control volume yields:

$$P = \frac{\Delta E}{\Delta t} = \frac{1}{2}\dot{m}(V_1^2 - V_2^2)$$

Looking back at *equation 8* a substitution for the mass flow rate yields the following:

$$P = \frac{1}{2}\rho S V (V_1^2 - V_2^2)$$

Equation 11 – Wind power equation II

Both of these expression for power are completely valid, one was derived examining the incremental work done and the other by the conservation of energy. Equating these two expressions yields:

$$P = \frac{1}{2}\rho SV(V_1^2 - V_2^2) = \rho SV^2(V_1 - V_2)$$

$$\frac{1}{2}(V_1^2 - V_2^2) = \frac{1}{2}(V_1 + V_2)(V_1 - V_2) = V(V_1 - V_2)$$

$$V = \frac{1}{2}(V_1 + V_2)$$

Therefore, the wind velocity at the rotor may be taken as the average of the upstream and downstream velocities. This is often the most argued against portion of Betz' law, but as you can see from the above derivation, it is indeed correct.

Returning to the previous expression for power based on kinetic energy:

$$\dot{E} = \frac{1}{2}\dot{m}(V_1^2 - V_2^2)$$

$$\dot{E} = \frac{1}{2}\rho SV(V_1^2 - V_2^2)$$

$$\dot{E} = \frac{1}{4}\rho S(V_1 + V_2)(V_1^2 - V_2^2)$$

$$\dot{E} = \frac{1}{4}\rho SV_1^3\left[1 - \left(\frac{V_2}{V_1}\right)^2 + \left(\frac{V_2}{V_1}\right) - \left(\frac{V_2}{V_1}\right)^3\right]$$

If we optimize this formula, it is shown that the maximum value for the power happens when:

$$\frac{V_2}{V_1} = \frac{1}{3}$$

Substituting these values in the power expression we obtain the maximum power in function of the air density, the rotor area and the upstream wind velocity cubed. This equation is the same as the *equation 6* multiplied by a number that represents the coefficient of performance. Betz proved in his theory that the coefficient of performance has a maximum value of 16/27 (0.593). According to this, the maximum power that can be obtained by an ideal wind turbine is:

$$P = \frac{16}{27}\cdot\frac{1}{2}\rho SV^3$$

Equation 12 – Maximum obtainable power [1]

In the *figure 20* the differences between the available power in the wind, the theoretical maximum usable power and the real power curves in conventional stall controlled and pitch controlled turbines are shown.

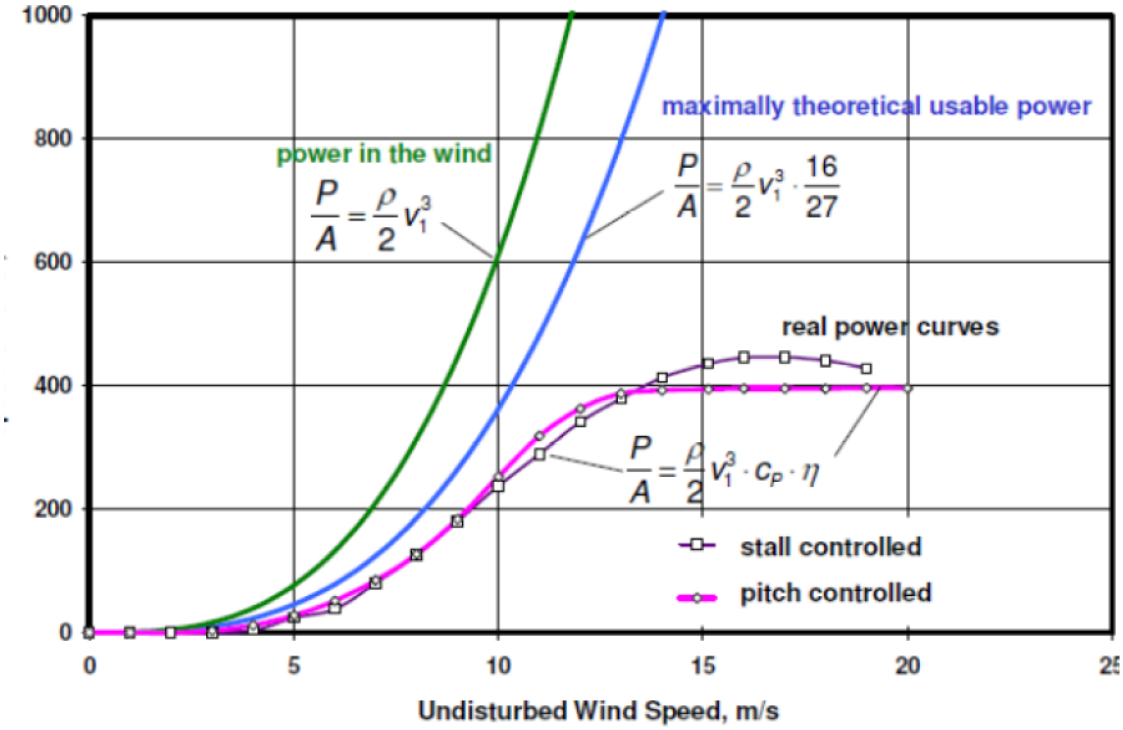

Figure 20 – Power curves [1]

3. SMART BLADES

In the previous chapter some basic wind turbine theory, with special emphasis on the loads of a turbine, has been explained. In this chapter we describe how smart blades can be used to alleviate these loads.

3.1 THE CONCEPT OF SMART BLADE

Smart blades include devices that are either passively or actively controlled and can adapt their performance so that the power can be obtained more efficiently and in a wider range of wind conditions. There are several goals that can be achieved using this type of blades:

- ✓ To settle the cut-in speed at lower wind speeds.
- ✓ To settle the cut-out speed at higher wind speeds.
- ✓ To reduce some of the extreme and cyclic loads in turbines.

Usually smart blades are like the classic blades used for turbines but with devices installed to improve the performance. These devices are groups of sensors that are able to measure the working conditions and through a software analysis give the optimal response to some actuators also installed in the blade. The actuators change the performance of the blades, and indeed, the performance of the whole turbine, raising its effectiveness.

Another type of smart blades is the one in which intelligent materials are used in the manufacture. This allows the blades modifying their profile depending on the wind conditions. Normally blades of this kind are not controlled actively; in fact, they are classified as passive control blades. For a deeper analysis in smart blades it is necessary to study the way that wind turbines are controlled.

3.2 EVOLUTION OF THE CONTROL TECHNIQUES IN WIND TURBINES

The turbine control is divided into two main groups: passive control turbines and active control turbines (Figure 21). Concerning to the classification of control types, when the control over the blade is done without any external energy support is called passive control. Some well-known passive controls are the yaw movement of a free to yaw downwind rotor, which allows orientating the turbine in wind direction, the aero elastic blade twist (in small wind turbines) that could increase the performance all along the blade and the flexible blade.

If an external energy support is needed for the control of the turbine, it is said that active control is being used. Pitch angle control and variable rotor speed control are examples of active control. In *figure 21* is shown the classification of different control types. The smart blades would be included in the active flow control group.

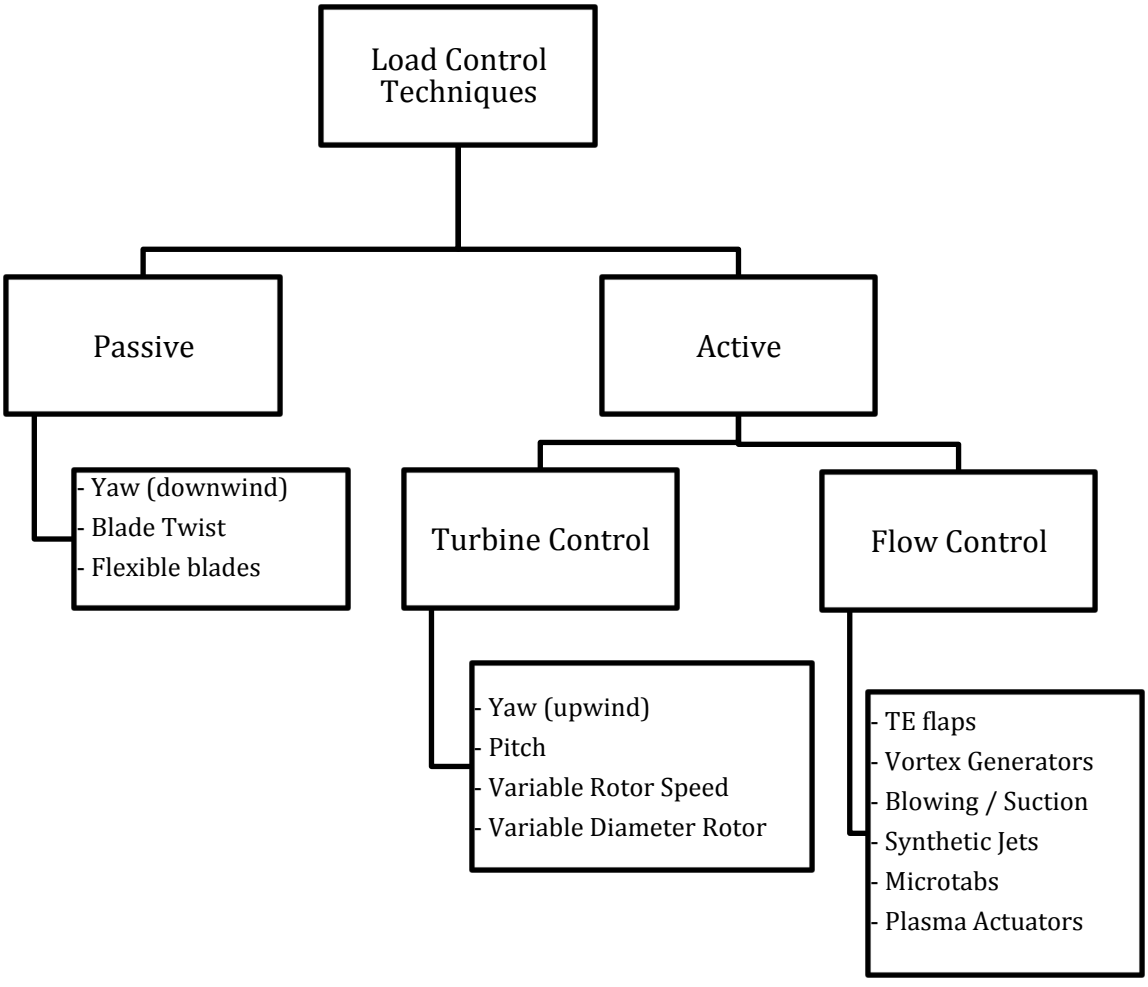

Figure 21 – Scheme of the load control techniques [7]

The goal of wind turbine control is to balance the following requirements:

- ✓ Setting upper bounds on and limiting the torque and power experienced by the drive train in order to prevent the turbine from collapse.
- ✓ Minimizing the fatigue from the rotor drive train and other structural components due to changes in wind direction, speed (including gusts), and turbulence, as well as start-stop cycles of the wind turbine.
- ✓ Maximizing energy production.

In this chapter some active and passive control systems were described, but the need to increase the power production pushed engineers to design new systems to improve the effectiveness of turbines and also to make higher size growth feasible. In these new huge machines it is sometimes very difficult to handle the control of oscillatory loads that cause fatigue in the structure. These loads occur as a result of rotor yaw errors, wind shear, wind up flow, shaft tilt, wind gusts, shadow effect and turbulence in the wind flow. For this purpose it is not enough with the pitch controlled or variable rotor speed wind turbines used until now and more complex controls are required. The following several control methods are able to handle this kind of problems.

3.2.1 ADVANCED PITCH CONTROL

Traditional pitch control is based on rotating all the blades around their spanwise axis. That way the angle of attack is modified and the generated lift changes. It is used to limit the peak power in order to prevent the generator from powers above the rated one, optimize the rotor efficiency and also slow down the rotor.

By comparison, the advanced pitch control technique allows each blade to rotate independently. This means that some oscillatory loads can be alleviated. For instance, fatigue loads due to rotor, tilt, and yaw errors, can be reduced by pitching the blades in this way.

The goal of this advanced control is to combine both systems, where collective pitch is used to keep the power at a desired level (adjusting pitch based on the mean wind speed) while the individual pitching is used to modify this pitch angle independently for each blade to minimize fatigue loads without affecting the power output. This kind of control is already used in helicopters but not yet applied to commercial wind turbines.

3.2.2 BLADE TWIST CONTROL

This advanced passive control is possible thanks to the recent advances done in the last years in composite materials. The implementation of these new materials allowed creating aero elastic tailored blades. These elastic blades are able to modify their twist distribution along the blade depending on how much they are bent as a consequence of the aerodynamic loads, reducing fatigue loads. In addition to this, the temporary loads caused by wind gusts are also mitigated with this control system. At the same time the pitch activity is reduced. [7]

However the blade twist control has some negative issues that should be noticed. First of all, the blade which includes these materials has a reduced energy capture. This is because part of the wind force is converted to deformation because of the lack of stiffness in those materials in the blade, instead of being used for power production purposes. Secondly, the capital cost increases as a result of the use of more complex materials. In addition to this the blade integrity becomes weaker, affecting the maintenance costs also.

3.2.3 VARIABLE DIAMETER CONTROL

As it has been explained before in this document, the energy capture in a wind turbine depends on the size of the rotor area. It means that making the rotor blades larger or smaller changes the power output. Under such circumstances, there are some designs done about systems that allow the blade to increase its size obtaining variable diameter turbines. This implies that energy capture can be improved for low wind speeds and also the extreme loads in high wind conditions can be reduced.

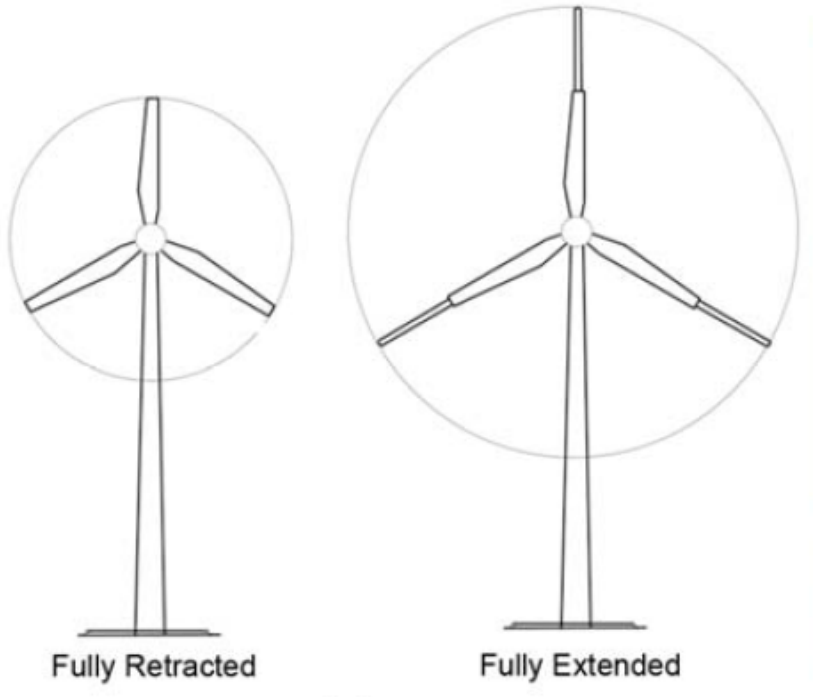

Figure 22 – Variable diameter wind turbines [7]

3.2.4 ACTIVE FLOW CONTROL (AFC)

One way to improve the performance of the turbine is to control the airflow that surrounds the blades. This technique allows decreasing extreme loads and fatigue loads, as both of them take place due to the action of the wind in both normal and high-speed wind conditions. This is the main goal of the AFC, and in order to achieve it, the blades must be provided with sensors that recognize changes in the local flow and actuators that react in response to the readings of the sensors, counter acting the conditions that cause the loads.

More specifically, what the flow control devices do is to delay or advance the transition between laminar and turbulent regime, to suppress or enhance turbulence and prevent or promote boundary layer separation. The effects pursued with the use of the devices in order to reach the goal are: lift enhancement, drag reduction, flow-induced noise reduction and mixing augmentation. It has to be taken into account that improving one of these objectives may interfere with one of the others, so it is the responsibility of the engineer to find a balanced solution.

Besides, installing AFC systems can result in secondary effects that can be very beneficial. Bigger rotors can be built as the AFC allows reducing loads, which means that more wind energy can be transformed by one wind turbine. They also can make the turbine more productive in low speed wind conditions by reducing the cut-in speed values. Nevertheless, this improvement in low speed productivity can lead to higher drag forces. More over, if the flow is kept in laminar regime the noise will be reduced and the aerodynamic performance improved.

The active flow control is composed by three categories:

1) *Control and sensors:* the sensors give the controller the information about the operational conditions. The information stream is continuous, so that the controller can adjust the operation in every moment.

2) *Actuators and devices:* actuators receive orders from the controllers, and their mission is to deploy the devices, which produce the effect in the airflow.

3) *Flow phenomena:* the interaction with the devices produces a change on the flow. The sensors register this change, and then the loop is closed and starts again.

According to what explained in this point, different solutions have been found and researched, in order to mitigate loads and improve the performance of the turbines. In the next pages, different types of AFC systems will be analysed making possible the choice of the best one for the study considered in this project.

The active flow control methods can be organized in the same way as the load control ones, either passive or active. Passive techniques involve geometry manipulation or fixed mechanical devices. Active techniques can be divided into predetermined or interactive, as shown in *figure 23*.

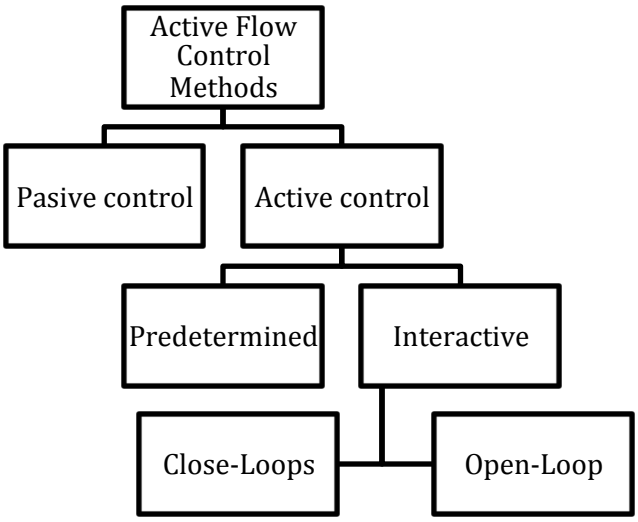

Figure 23 – Active flow control techniques [7]

Predetermined means that the system has two positions, "on" and "off", so it works depending on the wind conditions, but it always works in the same way. An interactive system is the ensemble of a sensor, an actuator and a controller; therefore the response is given according to every condition. Open loop means that the effect of the response is not measured, so the system cannot correct itself, while close loop does that is the reason because a close loop system is without any doubt the best way to reach the objectives accurately, because the response is always measured and compared with the reference.

3.3 SMART DEVICES

This compilation of devices and the way to separate them into categories is based on the *SANDIA* Report: "*Active Load Control Techniques for Wind Turbines*" [7]

Before starting the analysis of the devices, a little further explanation is needed, so that it will be easier and faster to understand how each one works. Four different points will be explained, for the classification of the systems:

1) *Actuation:* there are two different kinds, geometric (G) / fluidic (F). The geometric devices are those that move an external section of the blade in order to change the shape of the profile and achieve wind-flow attachment. The fluidic ones blow or suction air from the wind-flow to modify it. Some devices can be considered to be of both types, or not included in this classification.

2) *Location:* according to the location of the device, it will be considered near the leading edge (LE), in the mid-chord (MC), or near the trailing edge (TE).

3) *Lift curve adjustment:* this curve is moved in two different ways by the deployment of the AFC systems. Firstly, the curve can be lifted up or down. When is lifted up, it is called increasing lift (I) and the opposite is called decreasing (D). If a device is able to do both it will be marked with (I/D). Secondly, the lift curve can be extended so that it goes into stall at higher AoAs, which is called delay stall (DS).

4) *Movement:* if the device operates in a specific position, it is called steady (S) and if it has continuous movement it will be considered unsteady (U).

Even though each system has different characteristics and fundamentals in its way of working, there are some points to take into account in every device to obtain useful results.

- ✓ The size of each device has to be as small as possible, so that it can be installed along part of the span to obtain different control depending on the section. It also has to be scalable, so that it can work properly no matter how long the chord of the section is.
- ✓ Fast activation speed is needed, to provide the capacity of countering oscillating loads at the appropriate frequency.
- ✓ The energy consumed by the activation of the device must be low; therefore the activation forces must be low, as well as the power requirements. The energy consumed must be lower than the energy gain, or at least equal.
- ✓ The system has to be reliable and dependable, so that the turbine maintains operation if one or more devices fail.
- ✓ The system has to be able to support the environment surrounding the turbine, and the lifetime has to be similar to the lifetime of the turbine and its components.
- ✓ The device has to be easy to integer in the manufacture, assembly and maintenance of the turbine blade.
- ✓ It has to be able to reduce the cost of energy, as it is the main factor behind the research of these devices.

Now, several types of devices will be explained to proceed to the selection of the most interesting for this project.

✓ ***Traditional Trailing-Edge Flaps:*** *(G, TE, I/D, S)* These well known devices are commonly used in aircraft technology and they can be also used for wind turbines. They are surfaces located in the trailing part of the wing that can deflect towards the pressure or the suction side. This control method has a slow response, implies big actuators and as a consequence there is an important increase of the weight. The created noise is also another problem for this kind of actuator. The targets of these devices are usually aerodynamic braking and load control.

✓ ***Non-traditional Trailing-Edge Flaps:*** *(G, TE, I/D, S/U)* They are very similar to the previous ones, but these introduce newer materials and technologies, such as small piezoelectric devices and flexible materials. They are shorter, faster, and lighter and sometimes even there are no gaps between the flap and the blade and their main purpose is to counter the extreme loads and the fatigue loads. Compact Trailing-Edge Flaps, Adaptive Trailing-Edge Geometry and Adaptive Compliant Wing are inside this group.

✓ ***Microtabs:*** *(G, TE, I/D, S/U)* They are very small tabs located near to the trailing edge of the wing and deployed perpendicular to the surface. These devices are located inside the airfoil and when needed they are able to slide out of the wing surface. These smart devices will be studied more later in this document because of their interesting performance in load alleviation.

✓ ***Miniature Trailing-Edge Effectors (MITE's):*** *(G, TE, I/D, S/U)* They are very similar to microtabs, but in this case they are located in the trailing edge of the wing. They are able to slide up or down with a translational movement. The effect of this device is to enhance or mitigate the lift.

Figure 24 – Miniature trailing-edge effectors

✓ ***Microflaps:*** *(G, TE, I/D, S/U)* Again they are very similar to Microtabs and MITE's. In these devices the movement instead of a translational is rotational but the achieved effect is the same.

✓ ***Active Stall Stripes:*** *(G, LE, D, S)* They are another kind of very small tabs that can slide out perpendicularly to the wing. The difference is that they are located near to the leading edge of the wing and that they promote flow separation.

✓ ***Vortex Generators:*** *(G, LE, DS, S)* Active vortex generators are very small solid tabs mounted on the airfoil surface. Their main goal is to delay the stall by mixing the airflow in the boundary layer. They increase the lift but also the drag in blades.

✓ ***Blowing and Suction:*** *(F, LE/TE, DS, S/U)* The main idea of blowing and suction is to introduce some properly located slots in the airfoil surface (it can be near to leading or trailing edge). Thus, momentum (in blowing devices) or low momentum (in suction devices) is introduced or removed from the boundary layer through these slots. The target is to delay the boundary layer separation.

✓ ***Circulation Control:*** *(F, TE, I/D, S)* The circulation control is derived from blowing and suction theory. Basically they are very small jets introducing high momentum air tangentially to the rounded trailing edge of an airfoil. This device increases the circulation and as a result the lift, but it requires the installation of air ducts inside the blade making them much more complex and also the trailing edge has to be rounded which increases the noise and drag.

✓ ***Plasma Actuators:*** *(P, LE, DS, S/U)* This non-fluidic device (since it does not affect directly to the wind flow) allows to create a high momentum air stream converting electricity into kinetic energy. An "electric wind" stream is created between an anode and a cathode guided by the electric field when applying a large voltage difference. That way the boundary layer airflow is modified and the separation point of the flow can be delayed.

✓ ***Vortex Generator Jets:*** *(F, LE, DS, S/U)* It consists in jets of air. The air comes out through the airfoil surface, and it hits a cross flow, that is the air running along the surface. The result is a dominant streamwise vortex. The characteristics of the vortices can be controlled, allowing modifying the flow in different ways.

✓ ***High-Frequency Micro Vortex Generators:*** *(G, LE, DS, U)* This is a mechanical element, which oscillates in high frequency, inside the boundary layer thickness. The frequency is settled to a certain value, so that it generates periodic vortices. The result is high-momentum streamwise air that has to be focused into the surface, in order to give more energy to the boundary layer and reduce its separation.

✓ ***Synthetic Jets:*** *(G/F, LE, DS, U)* The purpose of this device is to create streamwise vortices similar to the ones obtained with the PVGJs. Instead of using compressed air, the vortices are created by the movement of a diaphragm inside the airfoil. It sucks and ejects air from the airflow periodically, creating vortices that interact with it. The jet is generated by the interaction and advection of the vortices, and it moves the streamlines producing the same effect as a change of shape in the airfoil. Significant lift increase can be reached.

✓ ***Active Flexible Wall:*** *(G, LE, DS, U)* It can detect when the boundary layer starts to separate, and disturb it to avoid separation. It is an assembly of transducers embedded in a flexible housing, which has a thickness of microns. Thanks to this, it does not affect the airflow when it is not activated. When boundary layer separation is detected, the transducers vibrate to counter it. The device is able to decide which transducers need to vibrate to obtain the wished result. Stall can be delayed and the lift increased a little bit.

✓***Shape Change Airfoil:*** *(G, MC, I, S/U)* This setup consists in some piezoelectric actuators assembled inside the airfoil, covered with a latex membrane to make the surface of the airfoil continuous and avoid seams. When the system is deactivated, the shape of the profile is the regular one. When activated, the actuators push the upper side of the airfoil, changing the shape and thus generating a change of camber and vortices in the flow. The movement is adaptive and fast. Higher lift coefficients and smaller flow separation area can be obtained.

After this quick analysis, the decision of which device will be studied can be made. Due to the complexity of some of the setups, and the impossibility of acquiring certain materials or technologies and working with them, the best decision is to work on one of the geometric devices of which performance relies on simple mechanisms. Between these, the choice is to study the microtabs for several reasons. First of all, the benefits obtained with this device are very interesting in order to alleviate loads and improve the performance of a wind turbine, they are also easy to manufacture with the tools available in the FabLab, and the implementation in the blade is also easier.

3.4 MICROTABS

As it has been explained before in this document, microtabs are geometrical devices that are located near to the trailing edge of a blade. The tabs are very small in height (usually around the boundary layer thickness) and they can be as long as the blade allows. Thanks to a translational movement they can be deployed perpendicularly to the wing surface modifying its aerodynamic performance. The tabs can be installed in both the suction and the pressure sides of a blade, in order to achieve different aerodynamic performances. Controlling the device actively means that the tab deployment can be adpated according to lift or other characteristics, and that it needs to use some energy supply.

The implementation of this small device causes a very important change in the aerodynamics of an airfoil. When located in the pressure side of the airfoil, the flow separation point changes from the trailing edge to the end of the smart device (it changes the Kutta condition). Altering the flow separation and changing effectively the camber results in modification of the lift coefficient. Experimental studies done in 2000 [8] show that a 30-50% increase in the lift coefficient can be achieved, using a microtab with a height of 1% of the chord and located in the pressure side. Lift enhancement is achieved by deploying the tab on the pressure (lower) surface and lift mitigation is achieved by deploying the tab on the suction (upper) surface. In *figure 25* it is shown how the flow separation is displaced by the microtab, as shown by the flow streamlines over an airfoil.

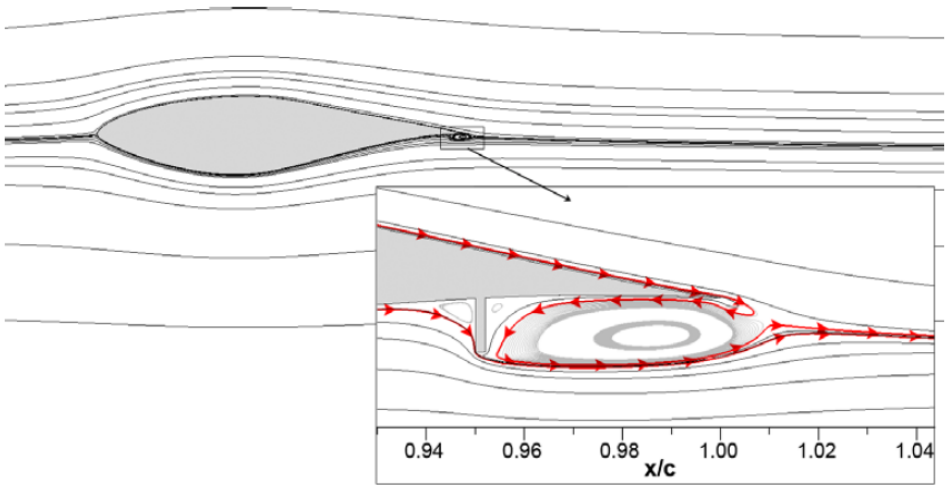

Figure 25 – Flow separation detail due to the effect of the microtab [7]

The aforementioned studies related to microtabs show the importance of the size and location of these devices. In these situations, it is indicated that the best compromise between size and location is a height of 1-2% of the chord located at 95% of the chord in the pressure side, and at 90% of the chord in the suction side, so that the balance between lift, drag and volume constraints is optimal. Moreover, the space covered by the tab along the span-wise of the blade it is also important for the microtab effectiveness. The conclusion of the study done was that tab effectiveness is reduced as the gap size between the microtabs is increased. The amount of gap can be identified with a solidity ratio, defined as:

$$SR = \frac{Covered\ \ Span\ \ By\ \ Tabs}{Span\ \ Of\ \ The\ \ Blade}$$

Equation 13 – Span ratio

The results said that it is highly recommended to maintain an 85% solidity ratio or higher for a proper effectiveness. In case of a 75% solidity ratio, the gaps between microtabs allow the flow to reattach in the trailing edge and it causes a big reduction of the blade performance.

In conclusion, microtabs can be used for load alleviation in wind turbines and lift enhancement. Modification of the lift and drag coefficients when needed can remove, or at least alleviate, some cyclic loads in turbines. For instance, installing a smart microtab in the suction side and deploying it every time the blade passes in front of the tower could alleviate the fatigue loads due to the shadow effect. This will smoothen the lift variation.

The main advantage of microtabs for their implementation is that they are able to cause big changes in lift. The abovementioned studies [8] report lift increases up to 22% when deployed in the pressure side and lift decrease up to 30% when deployed in the suction side. These lift modifications are only comparable to ones obtained by much more larger flaps, but the microtabs need less external power to be deployed and they are also faster. On the other hand the main problem of these smart devices are the gaps created between the tabs and the airfoil surface. The air leakage going through them negatively affects the blade performance and it also generates aero-acoustic noise.

4. SETUP

In the previous chapters the current situation of the wind energy, as a renewable energy source, the technology behind this energy, and especially the technology that involves the smart blades have been explained. This chapter will describe what we have been built and set up for the performance of the tests in the wind tunnel.

The main purpose of this project is to check the effect of the microtabs on the lift force of an airfoil. For succeeding in this project, it was necessary to build a blade, the micro tabs, a system for measuring and keeping under control the angle of attack, an aerodynamic balance for measuring the lift forces, and we have had to set up the wind tunnel.

In the following selections all the procedures that led to the final set up are explained. This chapter could be especially interesting for those people that have to build a setup with no previous experience in this field.

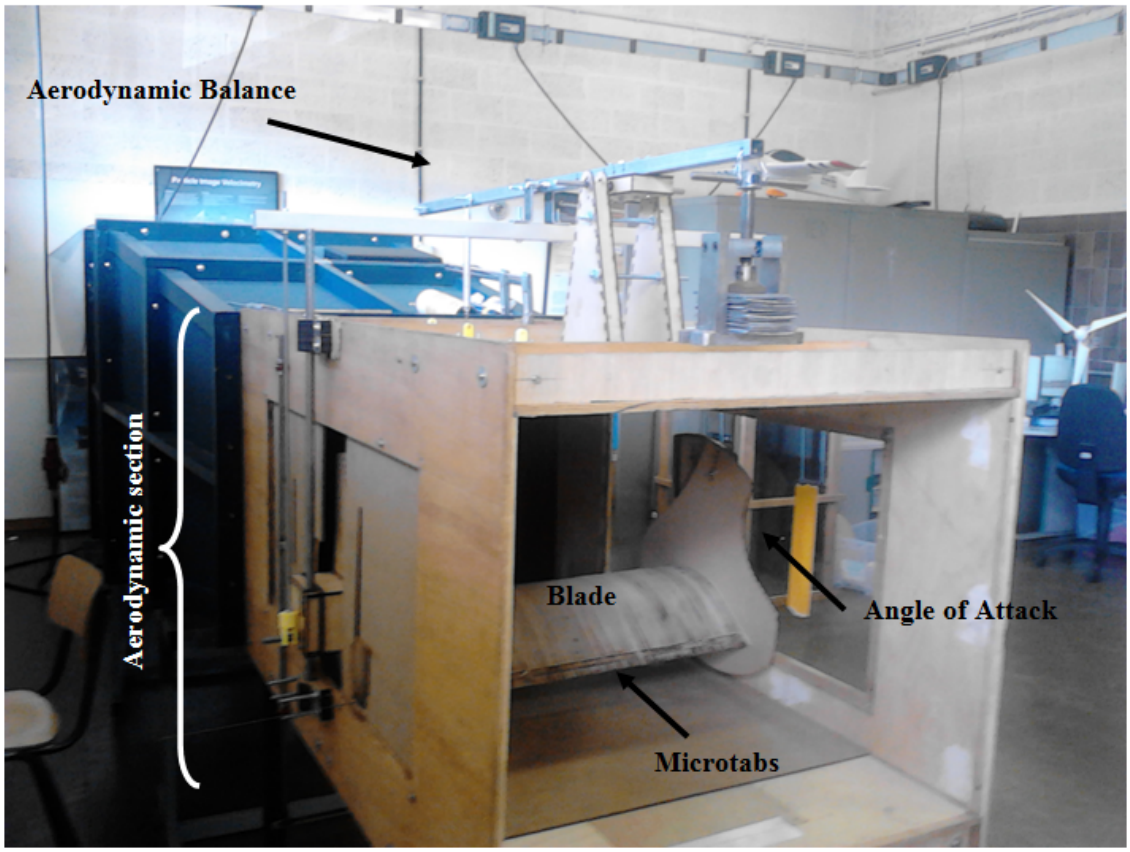

Figure 26 – The set up of the smart blades with the microtabs and the angle of attack system into the aerodynamic section connected to the wind tunnel, at the top the aerodynamic balance

4.1 THE BLADE

First of all, we started by constructing the blade, so the first step to do that, was choosing the profile of the blade. One of the most common profiles used in wind turbines are the NACA profiles, nevertheless, we bet on the GU 25(5) 8-11. The University of Glasgow developed this profile and we choose it since it is wider in the trailing edge zone, so there is more space to install device inside. This is important since, as we are going to set up microtabs in the trailing edge, we have to think that this microtabs need an actuator system to deploy and retract them, and this actuator needs space.

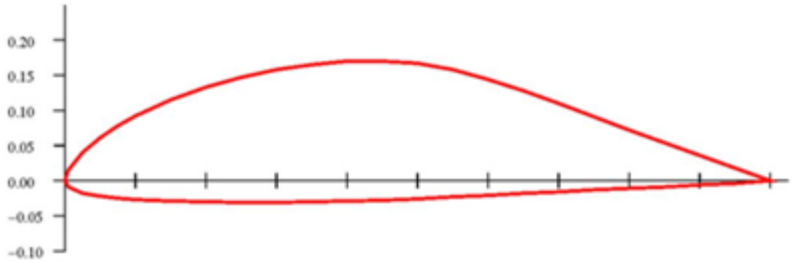

Figure 27 – GU 25(5) 8 -11 air profile

Once we decided what profile we were going to use to construct the blade we looked for information in the internet about the profile, and we get from the web page of the University of Illinois the coordenates of the profile [9]

After that, we started thinking about the manufacturing of the blade. There were two main options of building the blade with the tools and machinery available in the FabLab. One option, was cutting wood sections using the laser cutter, and then join all the sections. Another option was making a mold with foam using the milling machine and then build a composite blade using the mold.

Another option was using a 3D printer. In the FabLab there is available a 'Dimension Elite' 3D printer. This printer can build models up to 203 x 203 x 305 mm in size. Using the fused deposition modelling process, this 3D printer builds models layer by layer, from the bottom up. Each layer has a thickness from 0.178 mm to 0.254mm; this is a parameter that can be chosen. Generally, using thinner layers results in a smoother surface, especially when building small models. The layer material is acrylonitrile butadiene styrene plus (ABSplus), which is a durable thermoplastic. Due to the limitations on the maximal dimensions of a single model in the printer, the total wing should be divided into 3 pieces that would later be joined together. Each piece would have the same chord length as the complete model but would have a smaller span so that the height limitation of 305 mm of the work plane of the printer is matched. The manufacturing cost of this technique is about 1€/cm^3, so building the whole blade with the 3D printer would have an average cost of 2000€, which is too expensive.

Finally, another option would be building the blade in aluminium by an extruding process, this process could not be realized in the FabLab due to the lack of machinery, but we think that if it could be, the process would provide a fast and cheap prototype with a regular and uniform shape and a really smooth surface.

We decided to build the blade using the laser cutter, in the begining, making it with composite material would give us a smoother surface, but the manufacturing process was much more difficult and also it was more difficult to implement the microtabs inside the blade. So, we started building the blade with wood using the laser cutter and we kept the possibility of the composite and the milling machine in case that the smoothness achieved by the laser cutter was not good enough.

Figure 28 – The laser cutter in the FabLab and cutting wood sections

The next step was to decide what kind of wood we were going to use for building the blade. In previous thesis MDF was used, but in this case, we used balsa wood. This kind of wood is much more expensive that the MDF but it is also much lighter and easier to sand. Finally, the achieved smoothness after sanding the balsa wood was much better than the one with MDF.

So we started drawing blade sections in AutoCAD with different microtab configurations, we cut them in the laser cutter and then we tested it. Finally you can see in the *figure 29* the blade section used.

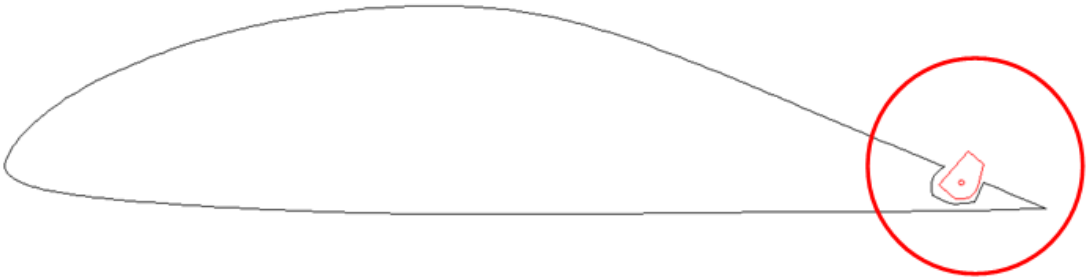

Figure 29 – Blade section used in the laser cutter with the hole for the microtab

So, once we had all the necessary information for the manufacturing of the blade we started cutting the sections and joining them with glue. In the *figure 30* and *figure 31* we show the process of building the blade.

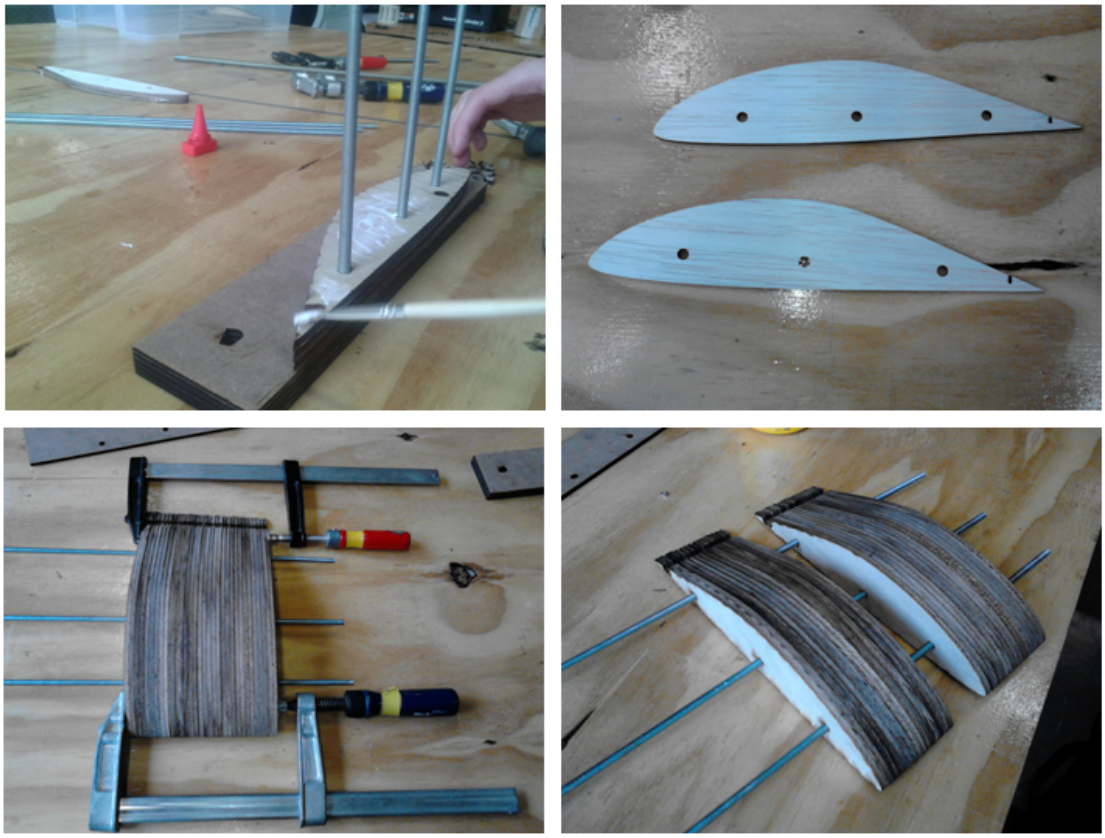

Figure 30 – First steps of building the blade

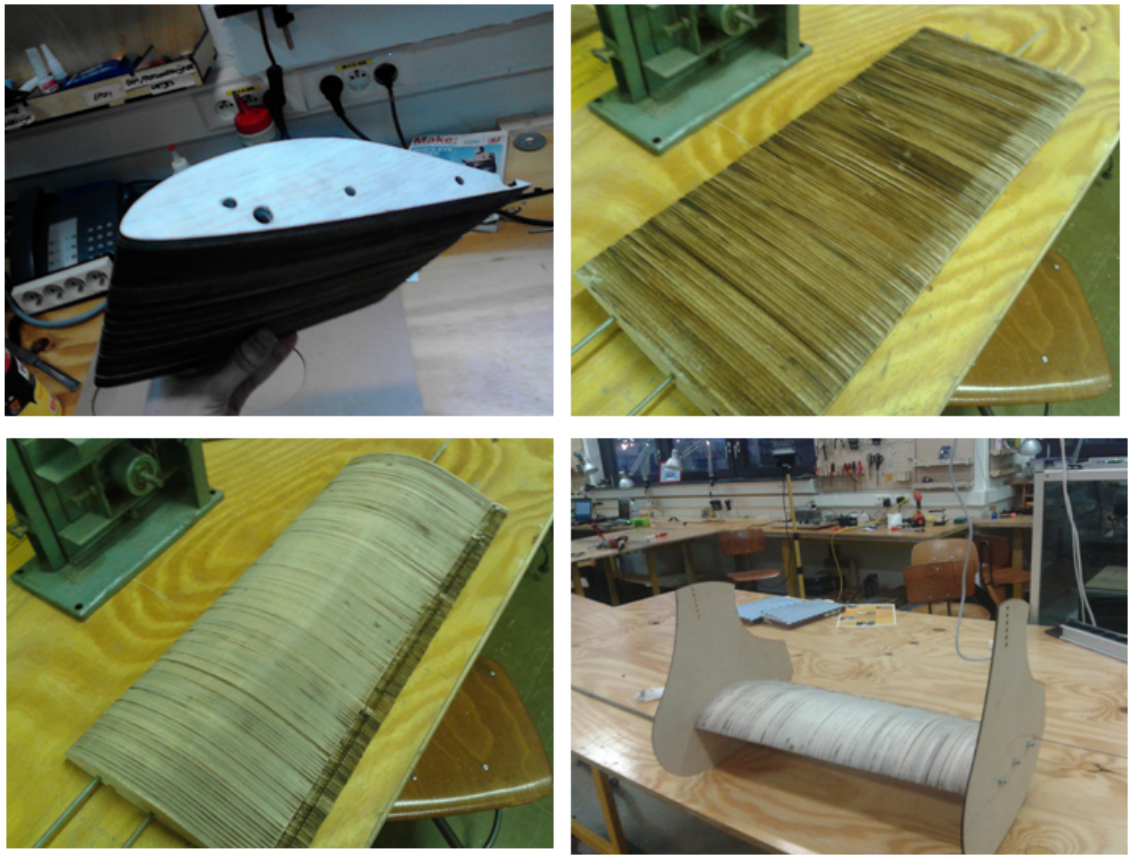

Figure 31 – Last steps and the blade sanded

In the top left corner of *figure 31* there can be seen four holes we made in to the wood sections. The three little ones are common to all the sections and are the ones we used in the beginning just for guiding the sections using metal rods when we were gluing them. We left the metal rods inside the blade in order to give to the blade more stiffness. The biggest one is a hole we made where we set up the metal rod we use for rotating and changing the angle of attack, and we just made it to the sections in the right and left side (7 cm from every corner) of the blade.

As it also can be seen in the *figure 31* we sanded the surface of the blade, and, as expected we got a really smooth surface, smooth enough for our purpose, so we decided to discard the composite and milling machine manufacturing option.

Finally, we joined two wood walls, these walls are part of the angle of attack system, but they also match another requirement of the blade. We built a 0,25 m chord length blade since the space at the end of the profile is proportional to the chord length and we need a minimum space to install devices there, we need a 1,5 m span length blade in order to try to keep an aspect ratio of 6 that would decrease the tip effects of the wind flow (Figure 32) since the these loses are inversely proportional to the aspect ratio. But due to the dimensions of the wind tunnel and the aerodynamic section, the built blade is just 0,6m span length, so, with these wood walls we avoid wind trespassing from the pressure side to the suction side.

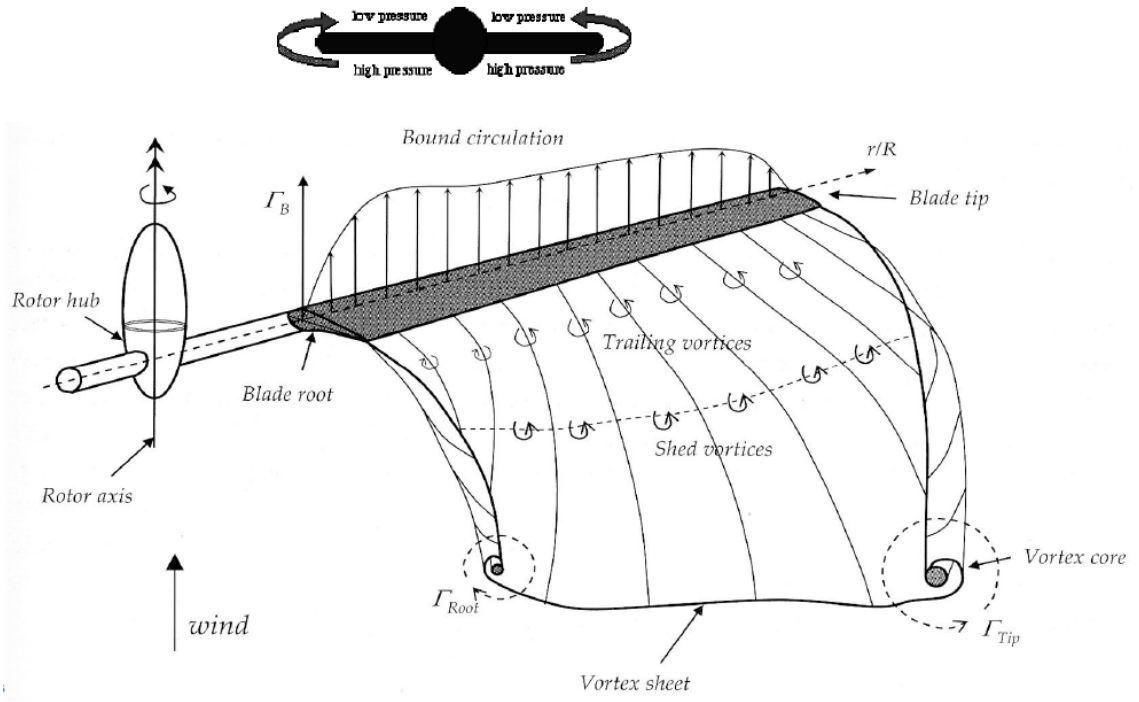

Figure 32 - Demonstration of the tip effect [1]

4.2 MICRO TABS

As it has been explained in chapter 3, (micro tabs sub-section), the micro tab itself is just a piece of material that rises perpendicularly to the wind flow from the blade. There are plenty of different configurations available both in the design of the micro tab and in the design of the actuation system. We will explain here some of the systems we considered and our final choice.

We considered two main actuator systems for the micro tabs. The first one was a rotating system, so that, the microtabs would be connected to a rod that would be connected at the same time to a servo engine that will rotate the rod and would deploy or retract the micro tabs (Figure 33).

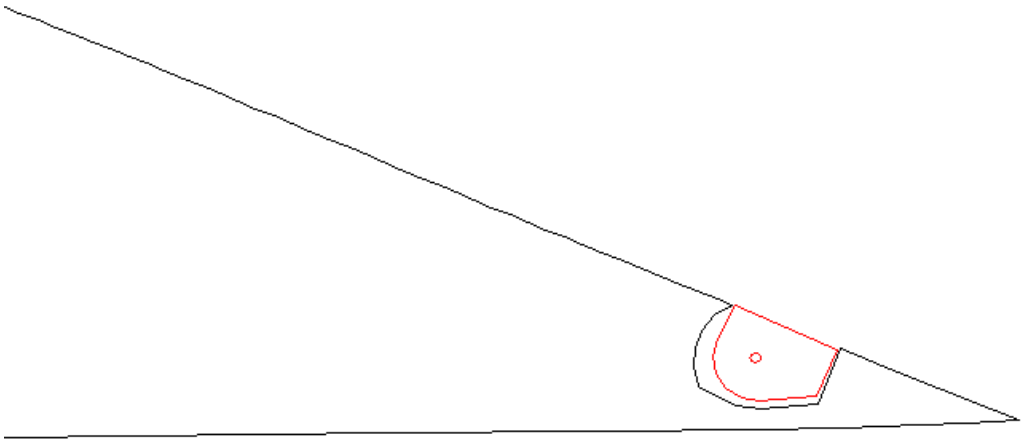

Figure 33 – Micro tab rotating system

The second system would be a linear actuating system, in this case, we would use some kind of actuators and rods connected to the microtabs and a balance point that could allow the micro tabs deploy or retract perpendicularly from the surface of the blade instead of rising with a rotating movement (Figure 34).

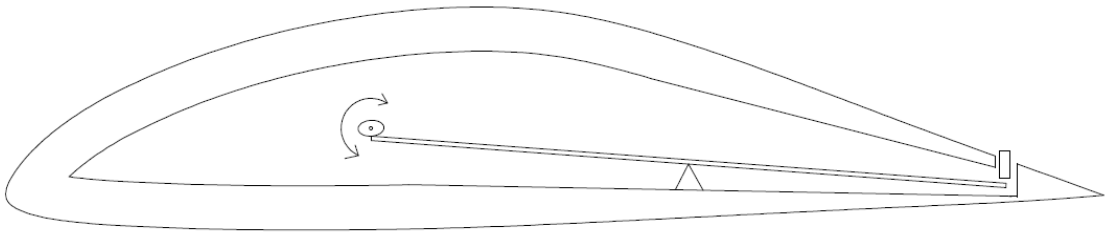

Figure 34 – Micro tab linear actuation system with balance

Finally in *figure 35* it is shown a combination of the two previous systems, a linear actuation system but without balance, using a crank connected to the servo engine

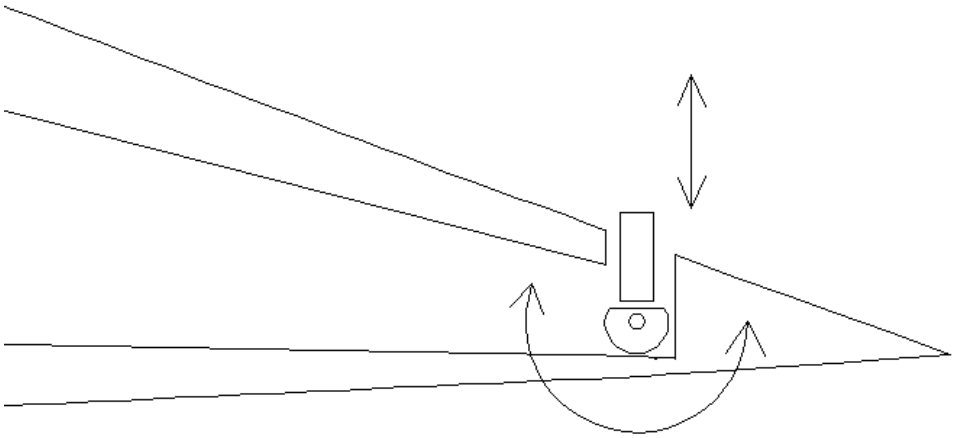

Figure 35 – Micro tab linear actuator system with crank

The first system has the advantage of simplicity, it is a more simple to implement, there is no need of cranks or balance points and the micro tabs rotating axis could be connected directly to the servo engine. On the other hand, as a rotating movement it could cause some transient effects from the retracted position to the deployed position in the wind flow.

The other two system as linear actuating system would produce less transient effects than the rotating one, but it has more disadvantages than advantages. For example, it is more complicated to implement, it needs more material inside the blade, and both systems would need the help of springs for keeping the contact between the actuators and the engine, with the amount of friction that would entail.

So we decided the most convenient choice was to use the rotating system.

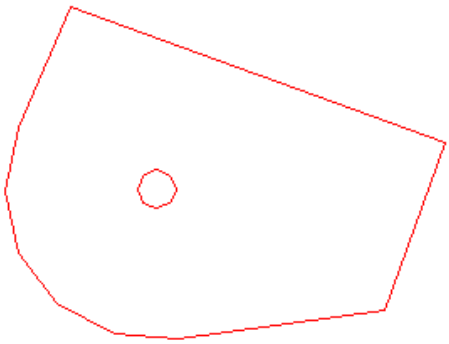

Figure 36 – Microtab

Once we have decided the kind of actuating system for the microtab, we started thinking about how to build it. Since the microtab would be implemented in the blade, the construction of the blade would be affected by the construction of the microtab.

As it is shown in *figure 33*, we had to design the hole that would host the microtab in the trailing edge of the blade sections. One of the facts we had to face up with was the localization of microtabs and also the height of the microtab itself. Considering that we are looking for a configuration where the microtabs are located in the upper surface of the blade, the best localization for the microtabs is at 90% of the chord length [7]. For the height of the microtabs, the best results are obtained for a height of 1-2 % the chord length [10]. So, in our case we designed the microtabs and the blade sections in a way that when the microtabs would be deployed, the microtabs would be located at 25 mm from the trailing edge, and with a height of 2,5 mm.

Finally, we had to decide the material for the microtabs. Since we wanted a surface as equal as possible to the one of the rest of the blade, we decided to build the microtabs in balsa wood, the same as the blade.

So we started cutting microtabs sections in the same way as we did for the blade with a hole inside for hosting a 1 mm diameter metal rod. Once we obtained enough microtabs section to cover almost all the span of the blade we started joining them with the metal rod and gluing the sections (Figure 37a).

Instead of covering the whole span with microtabs, we set up some supporting points in the blade span for helping the metal rod in its guiding axis work (Figure 37b). The placement of these gaps in the span, not covered by the micro tabs it is not significant for the effectiveness of the microtabs, since computational researches concluded that a solidity ratio higher than the 85% maintains the full effectiveness [7]. In our case the span ratio is around 95%.

Figure 37 – The microtabs joined in the metal rod (a); gaps in the blade span (b)

4.3 ANGLE OF ATTACK SYSTEM

The main purpose of this project is to prove the effectiveness of the micro tabs in the mitigation of the lift forces in a blade, and how they work at different pitch angles. So for the experiments we were going to make in the wind tunnel, we needed to build a system to:

- ✓ Fix the angle of attack in an easy way.
- ✓ Avoid differences between results when an experiment is repeated.
- ✓ Have at least an accuracy of 0.5 degrees.
- ✓ Be able to cover the pitch angle from -6 to 24 degrees.

So, we thought about two different systems and discussed which of them was the most appropriate.

4.3.1 GEAR – ZIP SYSTEM

One option would be to build a gear-zip system. The gear would be fixed to the blade and would rotate in the same axis and a fixed zip would control the movement of this gear.

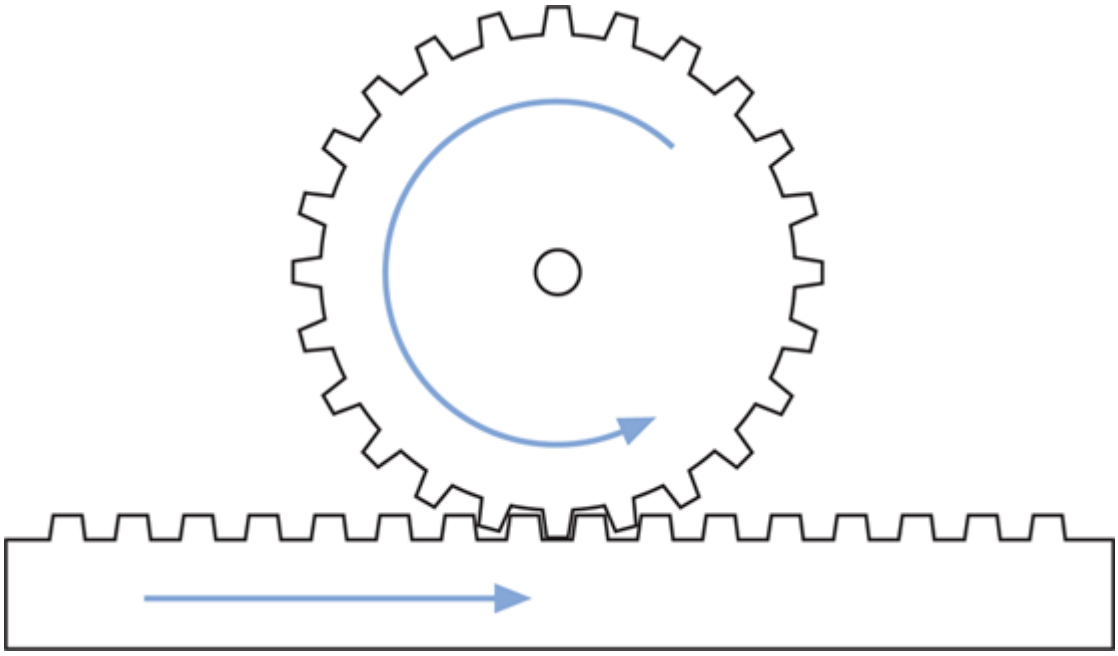

Figure 38 – Gear – zip system

The advantages of this mechanism are: It is easy to setup the required angle of attack, and it is also easy to build it with the tools available in the FabLab.

On the other hand, in this design, it is difficult to have a good adjustment between the gear and the zip, so there would be movement between the parts and this would result in a lack of accuracy.

4.3.2 COAXIAL SCREW-FIXED DISCS

In this case, we would take two wood plates, one with a number of holes, one per half degree, fixed to the aerodynamic section, and the other one with just a few holes, for fixing the angle with the still disc, fixed to the blade.

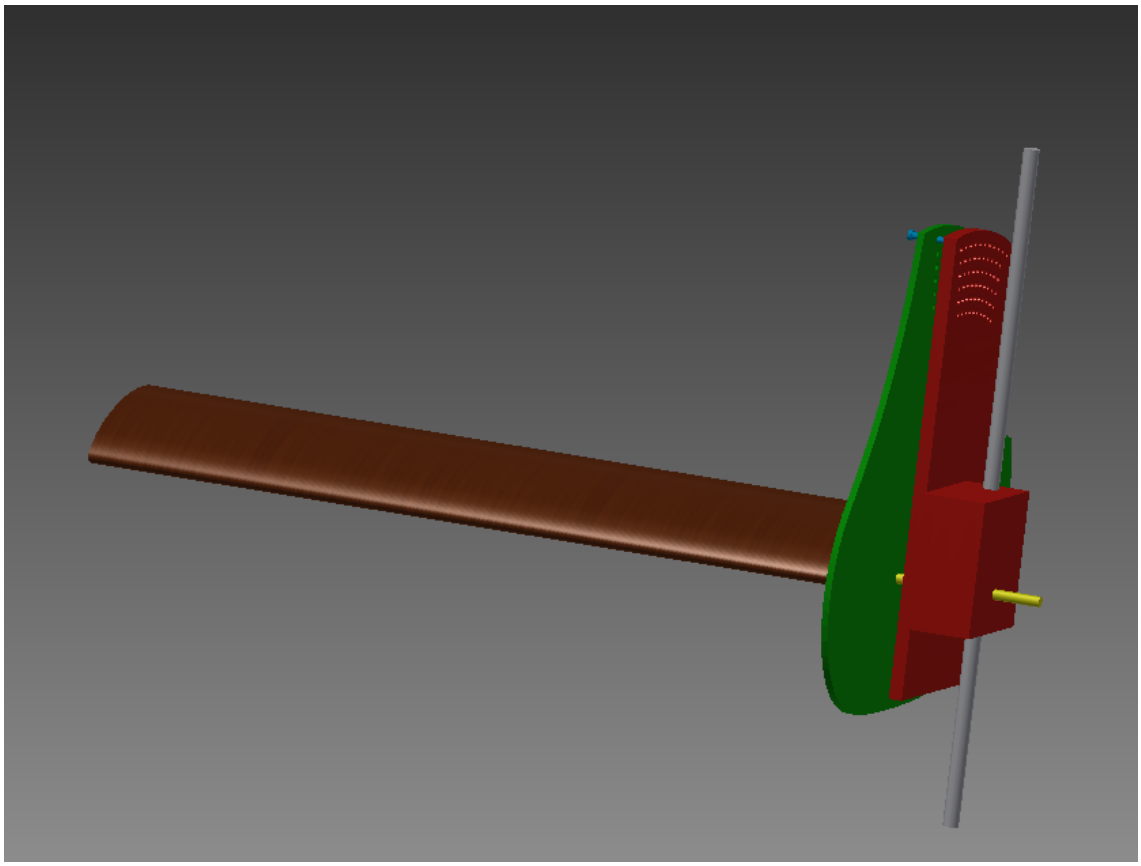

Figure 39 – The two discs system

As it is shown in *figure 39*, the red disc is the one fixed to the aerodynamic section and remains without rotation due to the metal rod (in grey). The green disc is the one fixed to the blade and they rotate in the same axis (in yellow).

The advantages of this system is the good accuracy we should get, since fixing the matching holes with screws we could get a very good adjustment between the two discs without movement as it would happen with the other system.

The main disadvantage is the complexity of fixing the required angle of attack.

Because of the bigger accuracy that would be achieved, we decided to construct the coaxial screw-fixed discs system.

Figure 40 – The system built and set up in the aerodynamic section

As it can be seen in the *figure 40* the fixed plate has holes with a range of half a degree, from -6 to 24 degrees, and the rotating plate has just five holes to fix with the holes of the fixed plate distributed in five rows.

When the angle of attack is set by matching the holes of both plates, the two plates are screwed to avoid movement between them, and so also to avoid changes in the angle attack during the measurements in the experiment.

An electronic angle meter checked this system and it resulted satisfactory, since we constructed a system with a resolution of half a degree, and when it was checked with the electronic angle meter that has a resolution of 0.1 degree fixing it in the blade, the lectures in our system matched with the ones in the electronic angle meter. In the case that it had been resulted not accurate enough, we had thought about duplicating the system with another set of holes so the fix with screws would be better.

Figure 41 – Electronic angle meter

4.4 AERODYNAMIC BALANCE

Once we built up all the components for the experiments we needed to measure the lift forces in the blade, and do it for different angle of attacks. At this point we had to decide between two options:

- ✓ Measuring the aerodynamic forces in the wind tunnel of the VUB, which has a load cell.
- ✓ Build a system that would be able to measure the lift forces

The wind tunnel at the VUB is more advanced than the one at the EhB, since the aerodynamic section is larger and the turbulence intensity is much smaller. It would be interesting testing the system there, since the load cell is more accurate. But the challenge that could suppose building our own system for measuring aerodynamic forces encouraged us to choose the second option and build our own aerodynamic balance at the EhB.

Last year master thesis Asier Herrero and Iñigo Solana designed a way for measuring forces using pressure taps. So they measure the pressure difference between the upper and lower surface and then they integrated the pressure along the surface so they get the resultant lift force in the airfoil. [11] This thesis was a good starting point to develop our own system

Building an aerodynamic balance similar to the one that can be seen in the *figure 42* was chosen.

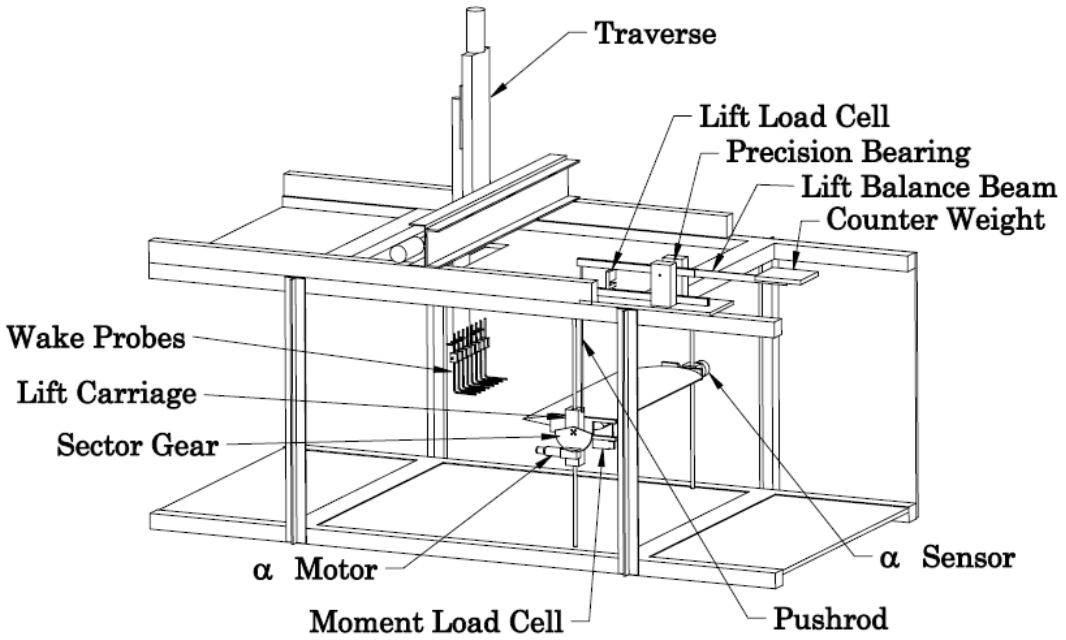

Figure 42 – Aerodynamic balance [12]

The first step (Figure 43) was setting the vertical metal rods outside the aerodynamic section; we used an electronic angle meter to assure that the rods were kept perpendicular to the horizontal. This allows the blade to move in the vertical axis, and that would also guide the lift carriage.

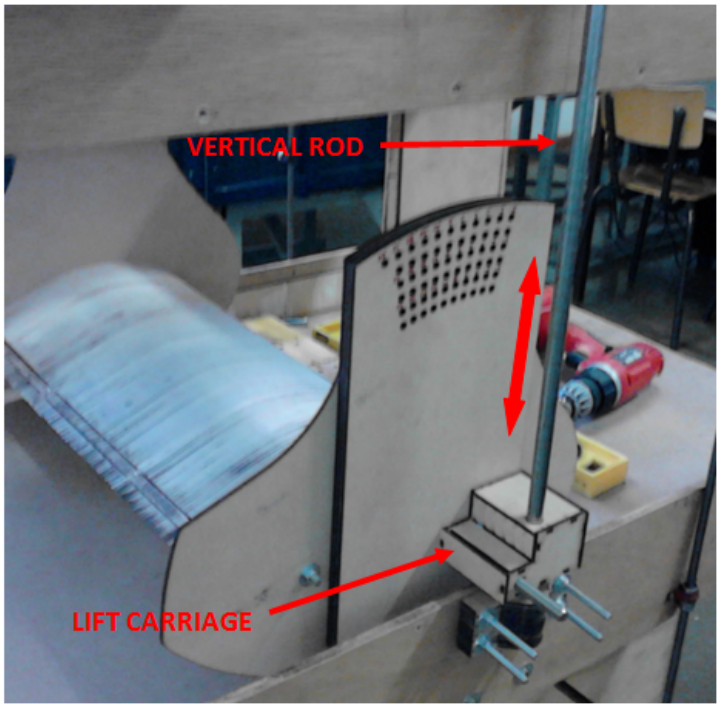

Figure 43 – First step of the aerodynamic balance

The problem with this design was the high friction caused by the wood-metal contact between the rod and the lift carriage. So we designed a new lift carriage system built with linear bearings to reduce the friction (Figure 44).

Figure 44 – Final lift carriage system

Once we had a correct vertical movement of the system along the metal rods we set up some push rods for actuating over the balance, we used the 3D printer available in the FabLab for building two supports for the pushing rods. (Figure 45)

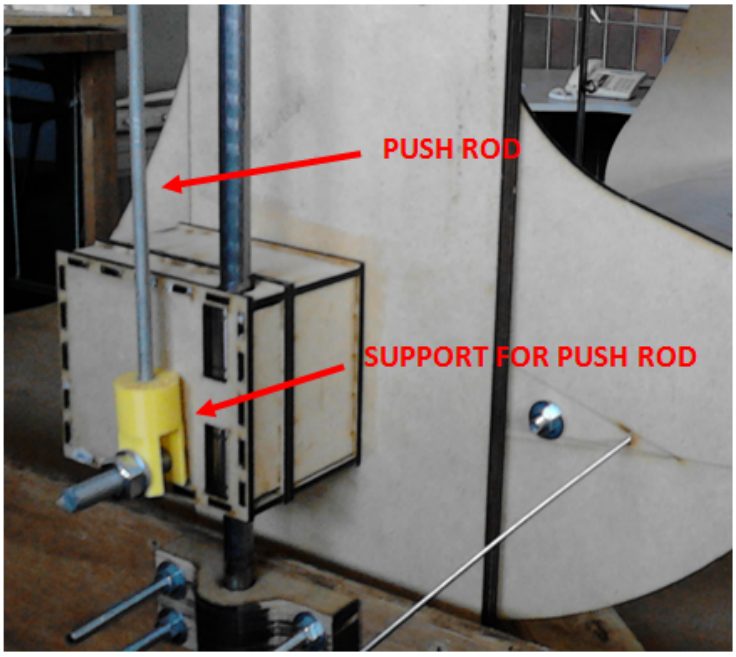

Figure 45 – Push rods and the support

Next step was set up the balance: Construct the balance point, add the main rod where the push rods, the counterweight and the force measuring system were going to be set up, and design the way to join the push rods to the main rod.

The first idea for joining the push rods to the main rod, was to build wood triangles that would be stiff enough not to flex too much when the push rods actuates over the balance in order to avoid the position of the lift forces actuation point or the symmetry of the lift forces of both rods (Figure 46a). But the system did not work, and we replaced the two wood triangles by a square aluminium rod where the push rods and the main rod would be screwed in (Figure 46b).

Figure 46 – The two wood triangles and the square aluminium rod

As it can be also seen in both figures above, for the balance point we used just two triangles to raise a small axis to the height of the aluminium rod. In *figure 46b* also are shown the way we fixed the balance point and the aluminium rod to the main rod.

After that, we designed the force measurement system. A good system would be to use extensometer gauges, but they are really difficult to calibrate and can lead to hysteresis problems.[12] Furthermore, there was a dynamometer that can measure up to 25N already available in the aerodynamics lab, so we chose to use it for the balance (Figure 47).

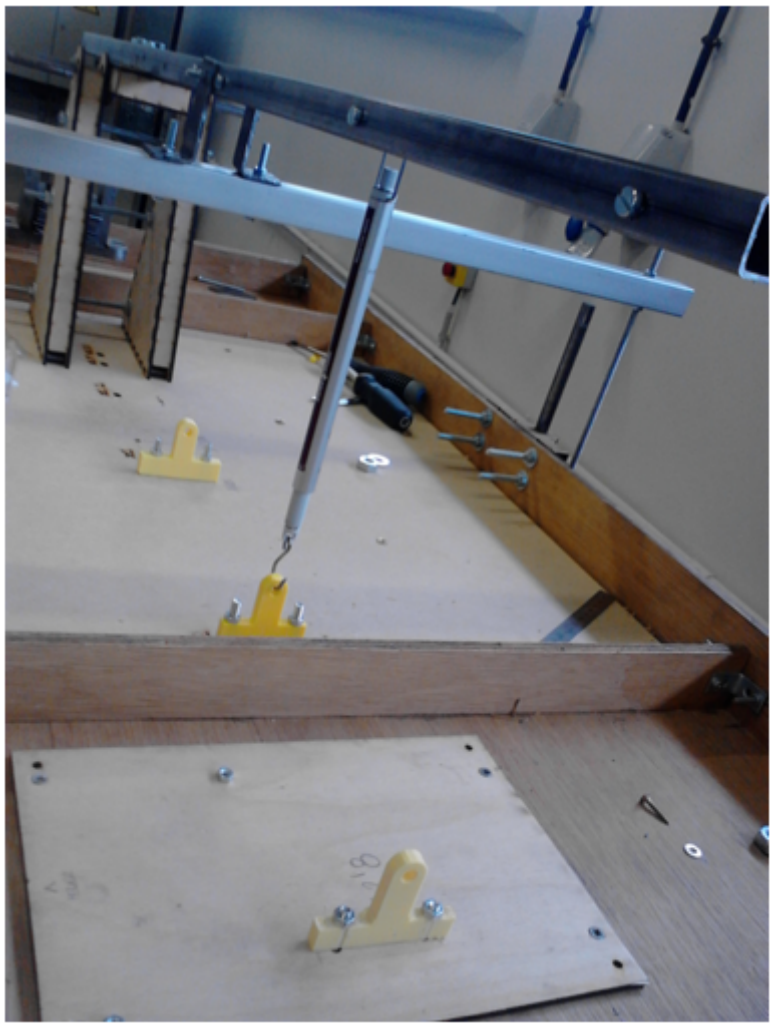

Figure 47 – Dynamometer with different support for different distances.

Since the lift forces we were going to measure could reach levels of 35-40N we adjusted it by changing the distance of the dynamometer to the balance point. In the *figure 47* there are shown also the different supports for the dynamometer depending on the distance we wanted to use for the measuring.

We ended up setting up the dynamometer at the double distance from the balance point than the aluminium rod (i.e. the lift force actuation point) was, so the lift forces measured in the dynamometer are the half of the real lift in the blade.

Finally we designed the counterbalance for the system, we took a support from the FabLab, and we added weight-known steel plates till the total weight of the system was compensated. There are some calculations about the friction that have taken into account for the counterbalance that will be explained in the next chapter.

A picture of the whole balance with the counterweight included can be seen in the *figure 48.*

Figure 48 – Aerodynamic balance with all its components set up.

4.4.1 LIMITATIONS OF THE AERODYNAMIC BALANCE

This sub-section explains the limitations of the aerodynamic balance due in major part to the friction of the linear bearings with the metal rods that allow the blade move vertically.

In our set up, a dynamometer compensates the torque that the lift force produce over the balance, so, the lift force can be obtained with some simple procedures once we know the force in the dynamometer, in our case, since the dynamometer is acting at a double distance from the balance than the lift force does, the force measured in the dynamometer is half the force of the lift, in order to maintain the equilibrium.

But since there is friction in the metal rods that are used for allowing the vertical movement of the blade, the dynamometer will measure less force than it should, and there could be cases where the static friction force will be big enough to compensate small lifts and keep the blade in the origin. So, it is necessary to study the friction force of this set up, know its value and determine whether its big enough or not for taking it into account.

FIRST MEASUREMENT OF THE FRICTION

The static friction is going to be measured by adding or subtracting weight from the counterweight system. The friction works always against the movement, when the blade is moving up because of the lift, the friction is added to the system weight, but when the blade is moving down as the lift decreases, the friction is subtracted to the system weight. So, since it is difficult to calculate the weight of all the system, we are going to measure two situations. (1) Beginning in a steady position, it is going to be measured how much weight have to be put in the counterbalance system for start moving the blade up, in that case the equation will be:

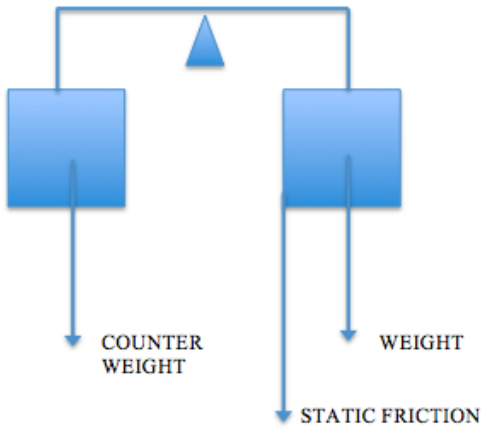

$$CW_1 = W + SF$$

(2) With the system unbalanced to the counterweight side, weight was subtracted until the system start moving down, in this case, the equation will be:

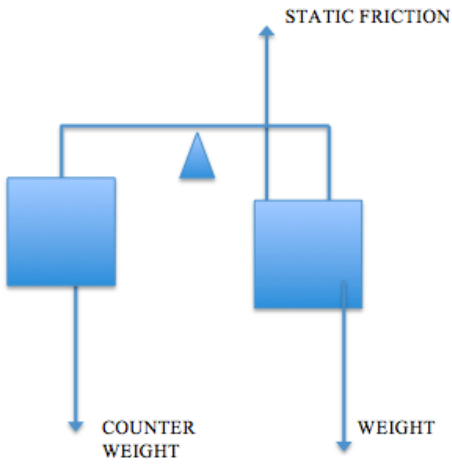

$$CW_2 = W - SF$$

For the counterweight system, there were used steel plates of 100 gr. (plus minus 10g) and a support for engaging them to the main rod, but since we do not know the weight of the support, we can not measure the counterweight itself, but what we can do is measure the difference between the two situations, i.e., how much weight do we

subtracted from the counterweight, until the system passed from being unbalanced in the counterweight side to the blade side:

$$CW_1 - CW_2 = 2 * SF$$

So, the weight subtracted for going from the first situation to the other is the double of the friction. And in the first case the friction had a value of 4 N.

This value was unacceptable, since the lift forces that were going to be measured in the greatest cases will be of 30 N.

SECOND MEASUREMENT OF THE FRICTION AND PROPOSED SOLUTION

Since the value of the friction was not acceptable, it was necessary to improve the system in order to decrease the system's friction. It was decided that the first attempt could consist in greasing the metal rods and improving the bearings in the balance. In the second case the friction was reduced in 0.25 N, to 3.75 N, that it was still not adequate.

Finally, the solution was to add enough weight in the counterweight system for compensating the weight of the system and at least the 75% of the friction (3 of the 4 N). The difference between the first situation (system unbalanced in the counterweight side) and the second situation were 800 g. So, since 1N=100 g (assuming g = 10 m/s^2), 700 g of weight had to be added in the counterbalance when it was in the second situation (remember that the second situation is just when the system starts moving down), so, there will be only 100 g (1 N) still to be compensated by the lift force, and in this case this error will be acceptable.

Nevertheless, the vibrations in the aerodynamic balance in high-speed wind conditions due to the turbulence made the lecture in the dynamometer unsteady, so the static friction is diminished. And in low-wind speed conditions the static friction was avoided as much as it was possible by tapping the balance so there was movement when the lectures were taken and the movement diminished the static friction.

Finally in chapter 7 (Future researches) some improvements are proposed for the aerodynamic balance.

4.5 WIND TUNNEL CALIBRATION

Finally, before to start with the experiments, we decided to calibrate the wind tunnel. The main intention with this calibration is obtaining wind speed fields and calculate from them an average wind speed for the wind force expression, and from it, the C_L expression.

This machine (Figure 49) works in open circuit and subsonic regime; in a range of speeds from 0 up to 22 m/s. It means that the air comes from the outside and goes out again, without having control of the characteristics of the incoming air. This will result in a possible variation of the results, related with the atmospheric conditions, any variation in the speed rate of the fan or possible alterations in the air due to human activity. Therefore, the conditions in every experiment have to be known in order to correct the effect of the environmental conditions in all the measurements and adapt them to obtain comparable results.

Figure 49 – Wind tunnel with the aerodynamic section at the wind output.

For the calibration of the wind tunnel, we used a wood frame with a metal wire grid (Figure 50a) for dividing the exit section of the wind tunnel, and in this way organize the measurements. And for taking the measurements of the wind speed we used a hot wire anemometer (Figure 50b).

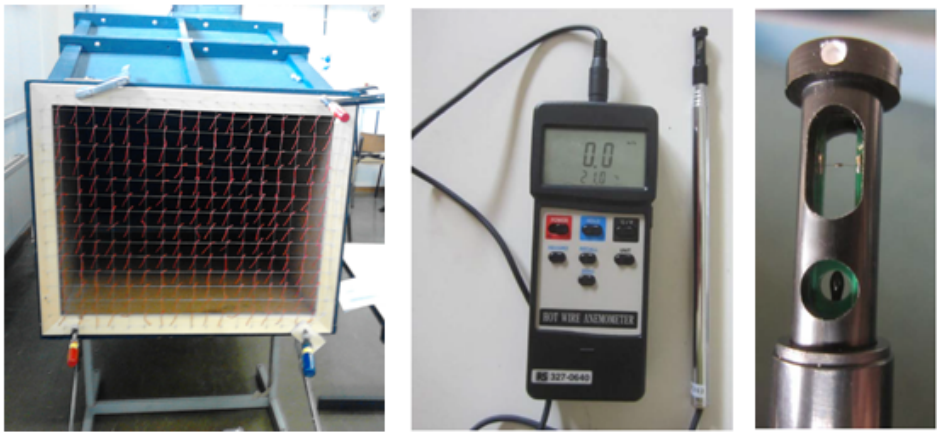

Figure 50 – Grid in the output of the wind tunnel; the hot wire anemometer; the hot wire sensor

The anemometer allowed us to measure the speed of the airflow. To do so, a wire is heated (Figure 50c), and the heat transference due to the interaction with the air stream is measured and translated into wind speed. The anemometer used for the measurements gives also the environmental temperature, which is very useful data as far as measurements made in different days need to be compared.

To provide control of the spin velocity in the fan, it is linked to a computer. A controller has been implemented with the software LabView 2010 (Figure 51). It allows controlling the fan speed; in a range from 0 to 5, where 0 means that the fan is stopped, and 5 is the maximum velocity.

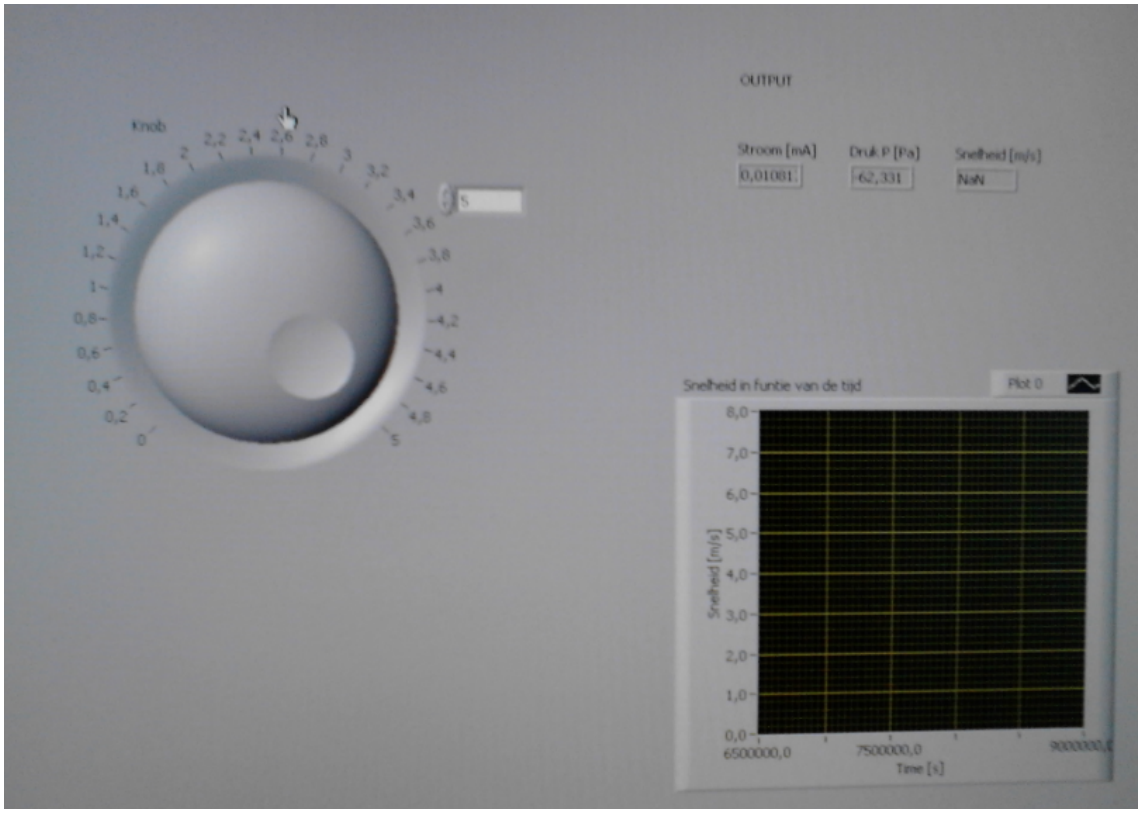

Figure 51 – LabView software with the wind tunnel control knob

We made five measurements, for wind speeds corresponding to wind tunnel levels: 1, 2, 3, 4 and 5.

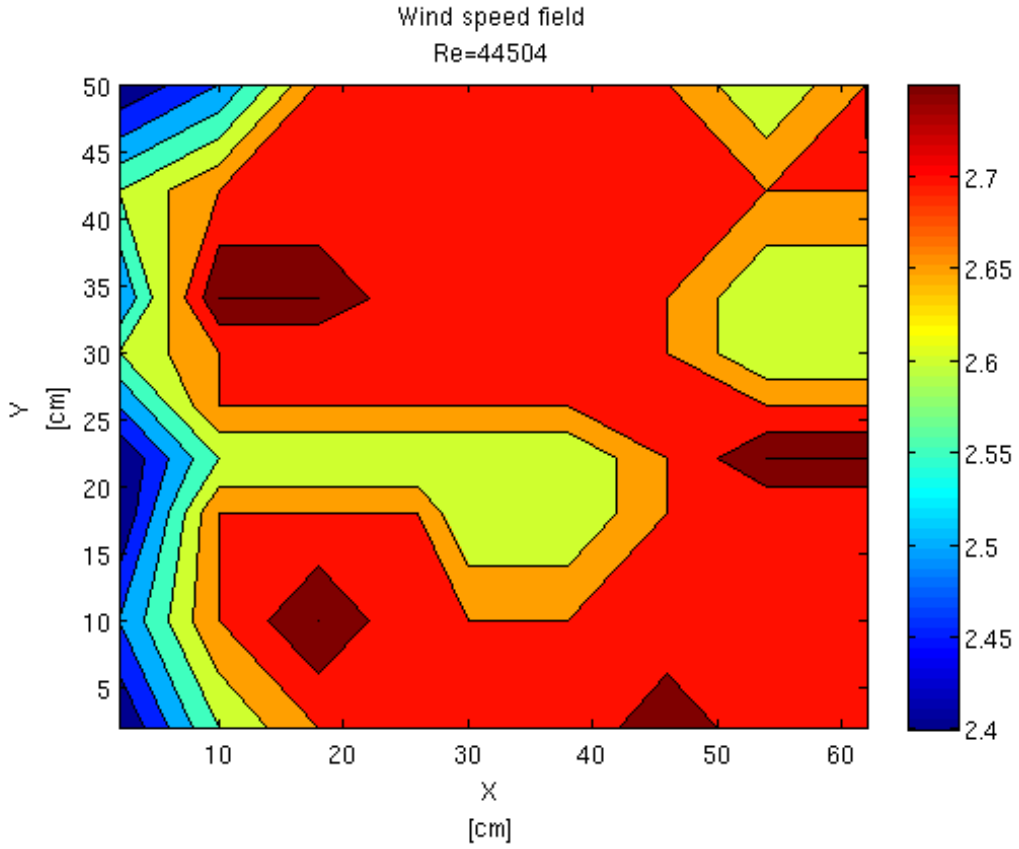

Figure 52 – Wind speed field for a Reynolds number = 44504 corresponding to the wind tunnel power level 1

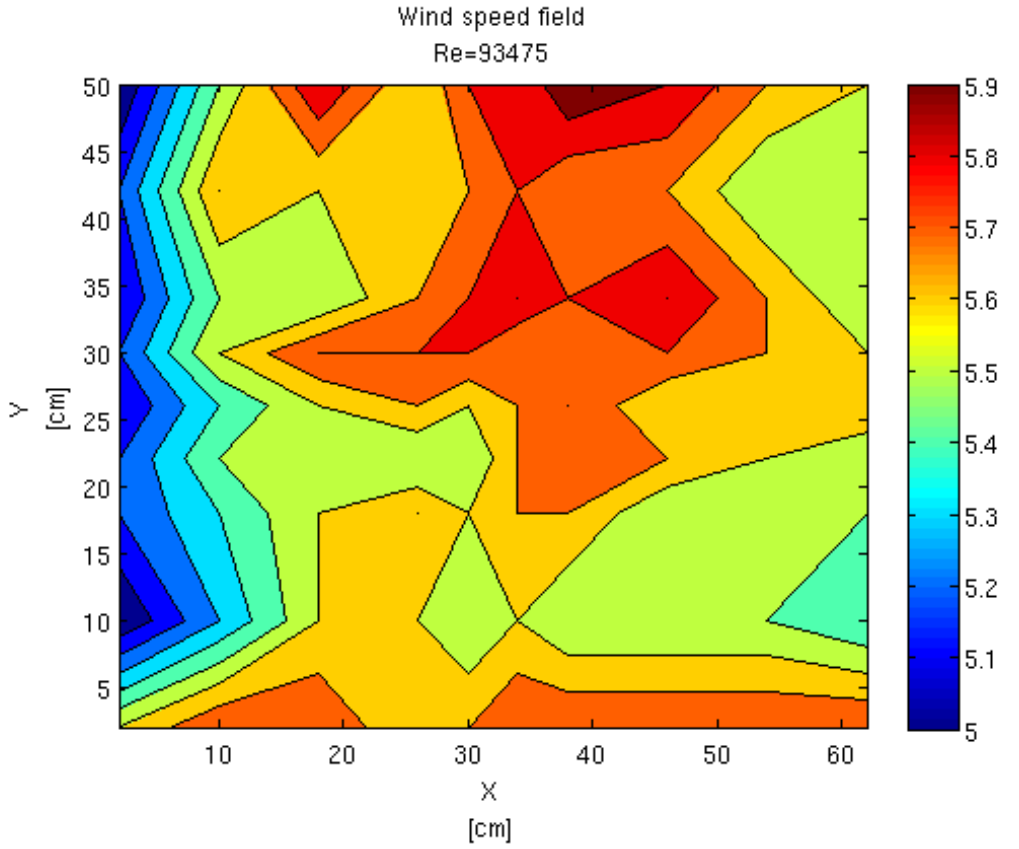

Figure 53 - Wind speed field for a Reynolds number = 93475 corresponding to the wind tunnel power level 2

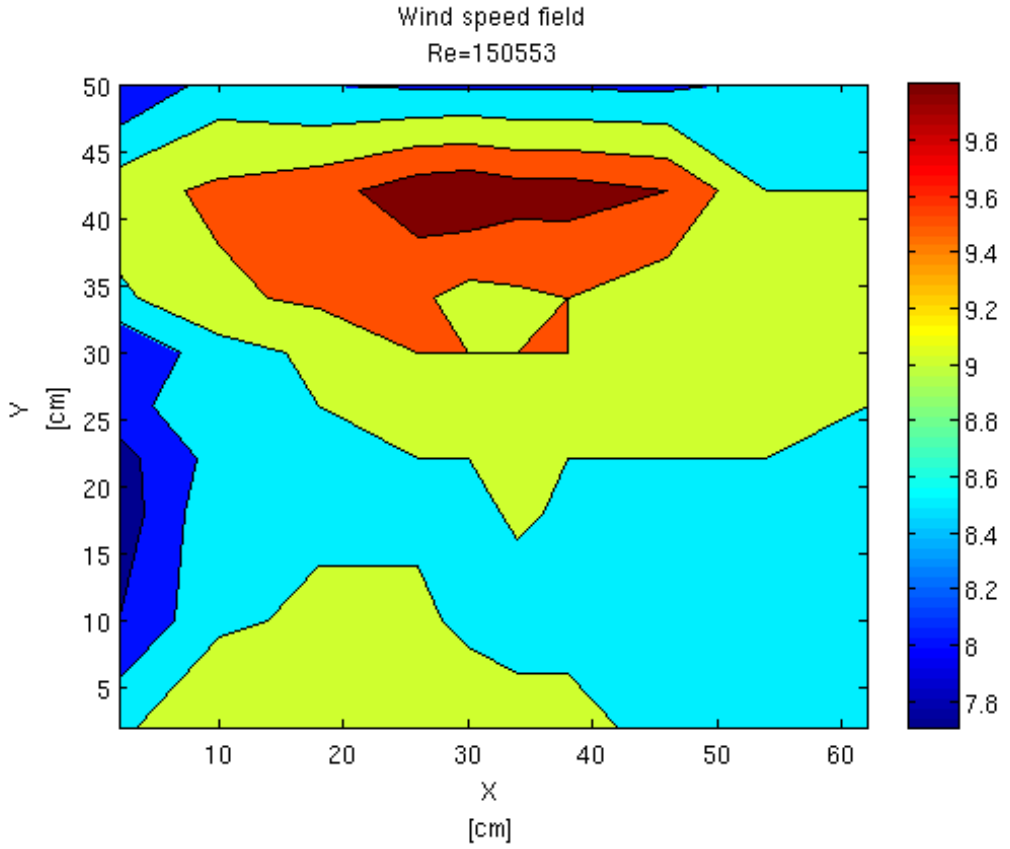

Figure 54 - Wind speed field for a Reynolds number = 150553 corresponding to the wind tunnel power level 3

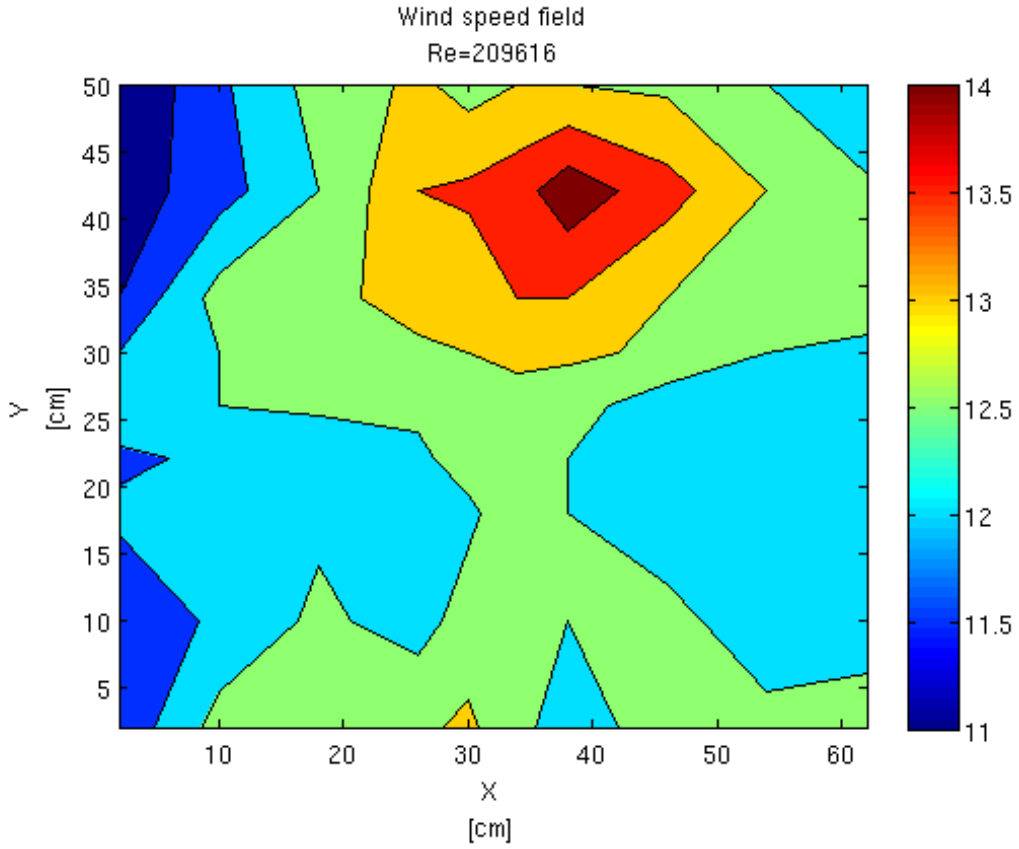

Figure 55 - Wind speed field for a Reynolds number = 209616 corresponding to the wind tunnel power level 4

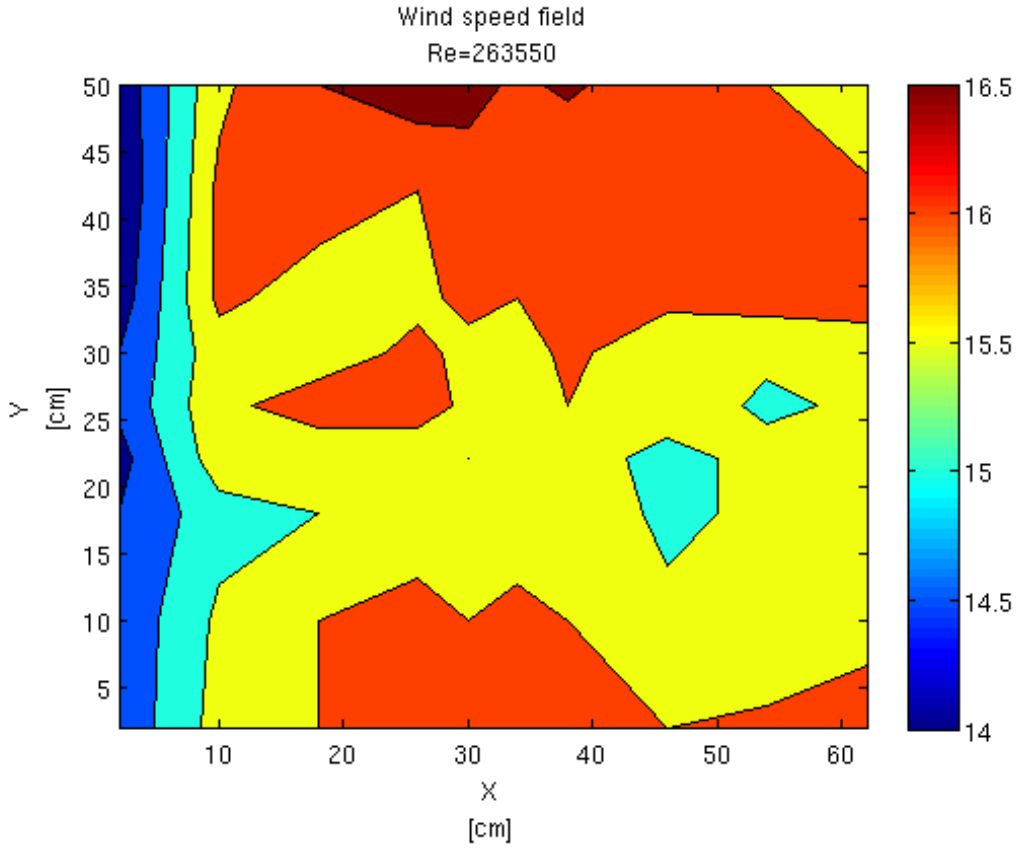

Figure 56 - Wind speed field for a Reynolds number = 263550 corresponding to the wind tunnel power level 5

It can be seen that there is a trend that the lowest speed are concentrated in the left side of the section, but in the rest of the section the field is almost uniform so we can assume that the wind speed is constant in the section.

For each wind tunnel level we calculated an average wind speed without taking into consideration de data of the first column in the left side that showed non-significant data.

Level	Reynolds Number	Average speed [m/s]
1	44504	2,69
2	93475	5,65
3	150553	9,10
4	209616	12,67
5	263550	15,93

Table 1 – Average speeds for different wind tunnel levels

But all this measurements where calculated with the output of the wind tunnel free, without the aerodynamic section. When we started with the experiments we realized that the speed is altered by the presence of the aerodynamic section and the blade, so we measured again the wind speed with the section at the output. This new speed values are displayed in the experimental results chapter.

5. EXPERIMENTAL RESULTS

This chapter describes the experiments performed in the wind tunnel of the Erasmushogeschool Brussel, the obtained results and some discussions and conclusions.

The goal of this master thesis is to study the effect of the microtab to reduce lift in a controllable way in a smart blade.

5.1 EXPERIMENT 1

5.1.1 SET UP

First step was setting up the GU25 (5) 8-11 profile into the test section with the balance and the angle of attack measuring system. (Figure 57)

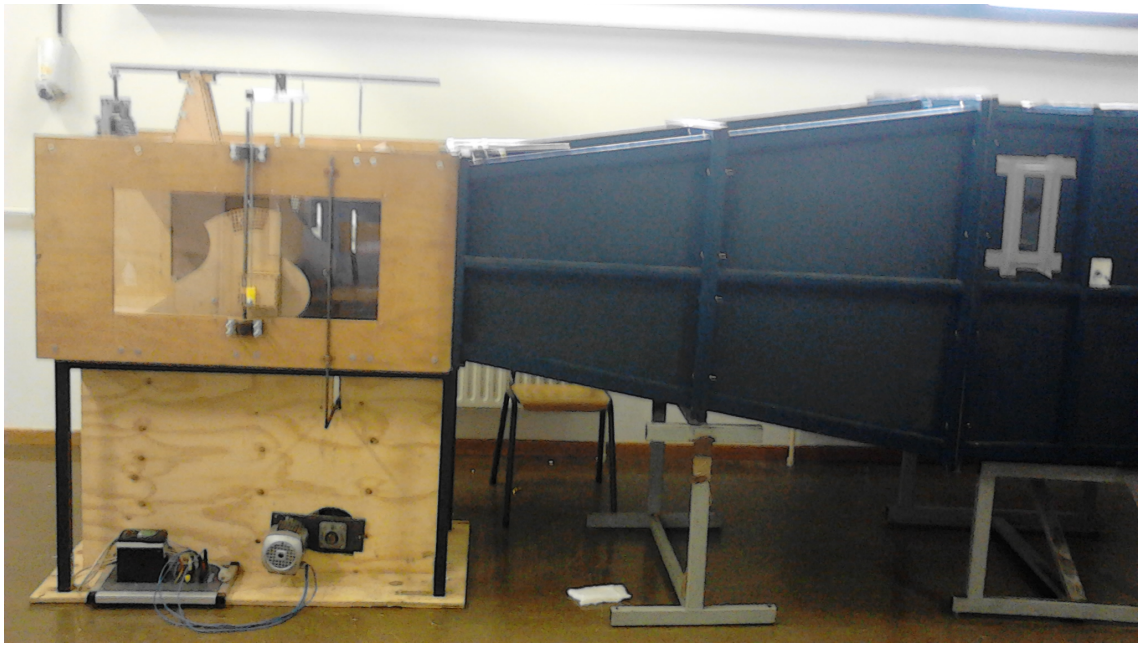

Figure 57 – Aerodynamic section set up in the wind tunnel.

The measurements were taken in an angle of attack range from 0º to 20º in steps of 2º. The lift forces were measured from the lecture of the dynamometer in the aerodynamic balance and then the lift coefficient was calculated with the wind force (Equation 14)

$$C_L = \frac{Measured\ Lift\ Force}{\frac{1}{2}\rho A V^2}$$

Equation 14 – Lift coefficient

Where:

ρ = air density measured with the pressure and the temperature of the aerodynamic lab

A = surface of the blade (chord * span)

V = undisturbed wind flow speed

As it was explained on pages 60-61, the wind flow speed of the wind tunnel for different wind tunnel power levels was calculated (Table 1 – Chapter 4 Section 4.5).

In this case, the levels of interest were from 3 to 5, since the wind flow speeds associated to the discussed Reynolds numbers (Equation 15) were in this range.

$$\mathrm{Re} = \frac{\rho V l}{\mu} = \frac{V l}{\upsilon}$$

Equation 15 – Reynolds number

Where

ρ = air density measured with the pressure and the temperature of the aerodynamic lab

V = wind flow speed

μ = dynamic viscosity of the wind

l = the characteristic length, in this case the chord

υ = kinematic viscosity of the wind

The first experiment was made by measuring the lift forces with the dynamometer and then calculating the lift coefficient (C_L) and plot it against the angle of attack (AOA).

The average speeds shown in *table 1* were measured without taking into consideration the blockage effect of the blade in the test section, i.e., without putting the blade at the exit of the wind tunnel. So, new wind flow average speeds were measured with the blade located at the exit of the wind tunnel, this was done making some holes in the aerodynamic sections located before the blade (Figure 58).

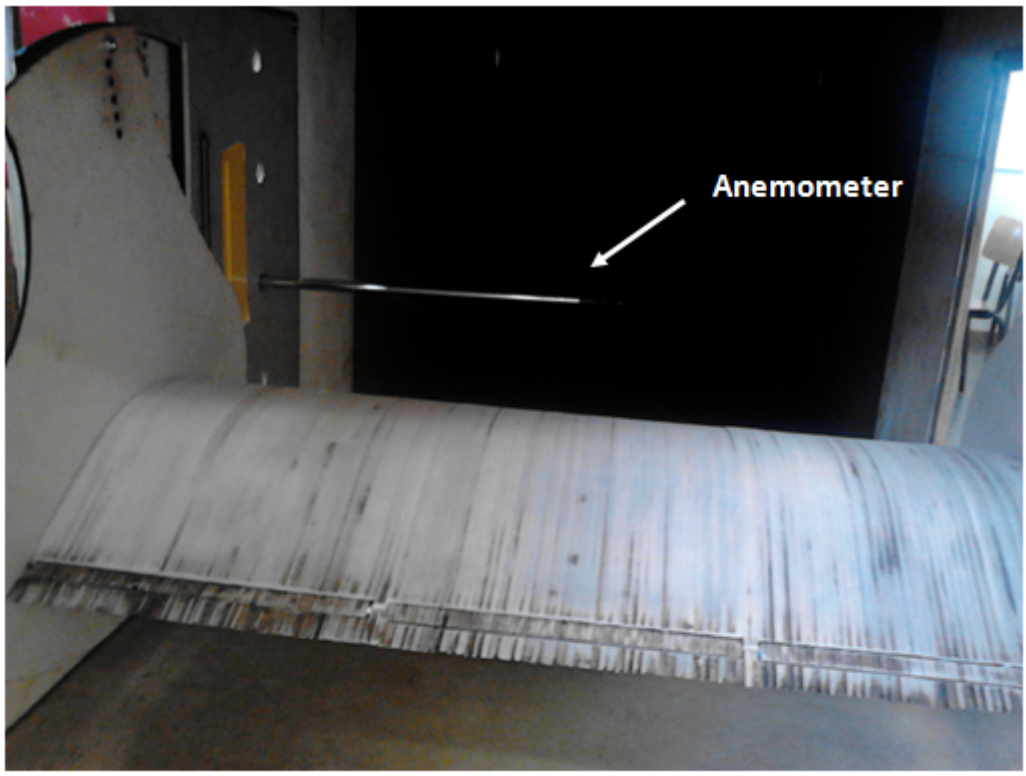

Figure 58 – The aerodynamic sections with the holes for the anemometer

5.1.2 RESULTS

The wind tunnel was tested for levels 3, 4 and 5, and the results were:

Level	Reynolds number	Average speed [m/s]
3	165442	10
4	227483	13,75
5	287043	17,35

Table 2 – Corrected average wind flow speeds

The wind speed is higher with the blade blocking the exit of the wind tunnel. This statement agrees with the literature, where it is explained that wind airfoils with a considerable size, i. e, those ones that take the most part of the aerodynamic section as in our case, where the blade occupies the whole width of the section and 20% of the height, may cause blocking effects that change the wind flow speed field, increasing the speed in the test section [13], so the wind forces are bigger than expected before, and the current lift coefficients are smaller.

So, it was decided that the lift coefficients were going to be calculated with the average speeds shown in *table 2* that takes into account the blockage effect of the blade at the exit of the wind tunnel.

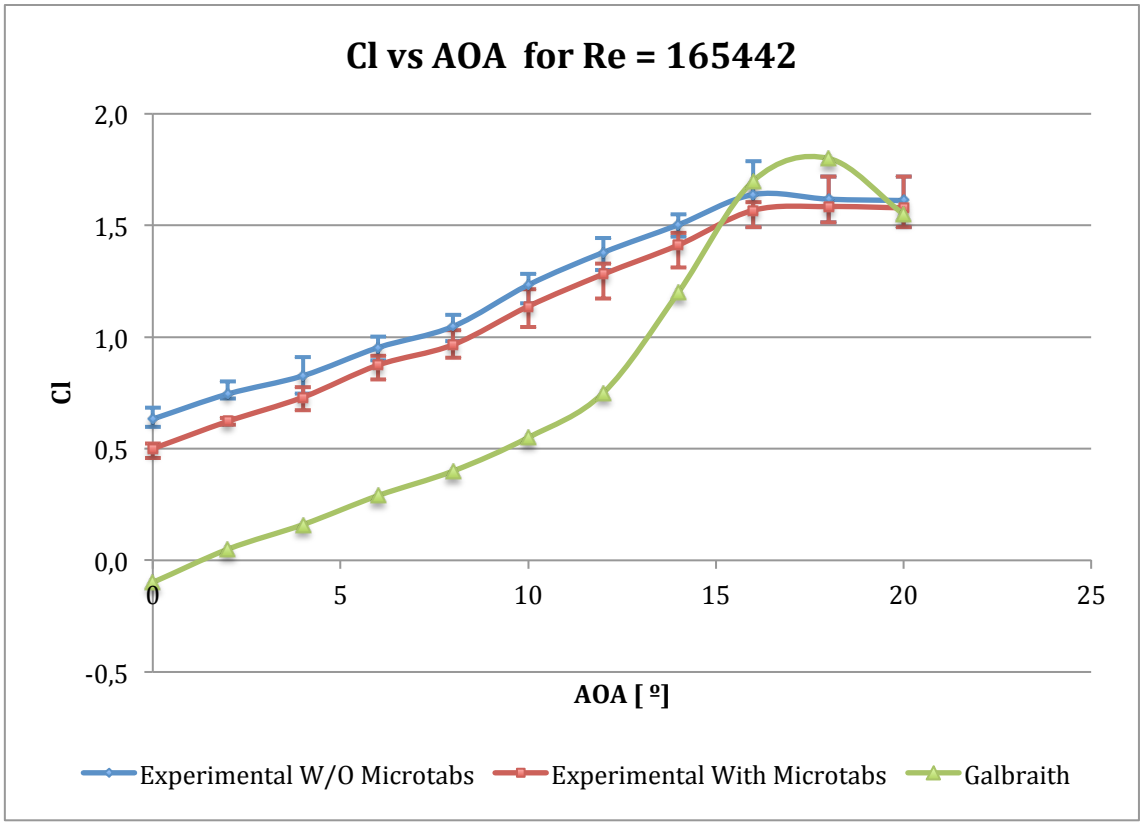

Graphic 1 – Lift coefficient curves for Re = 165442

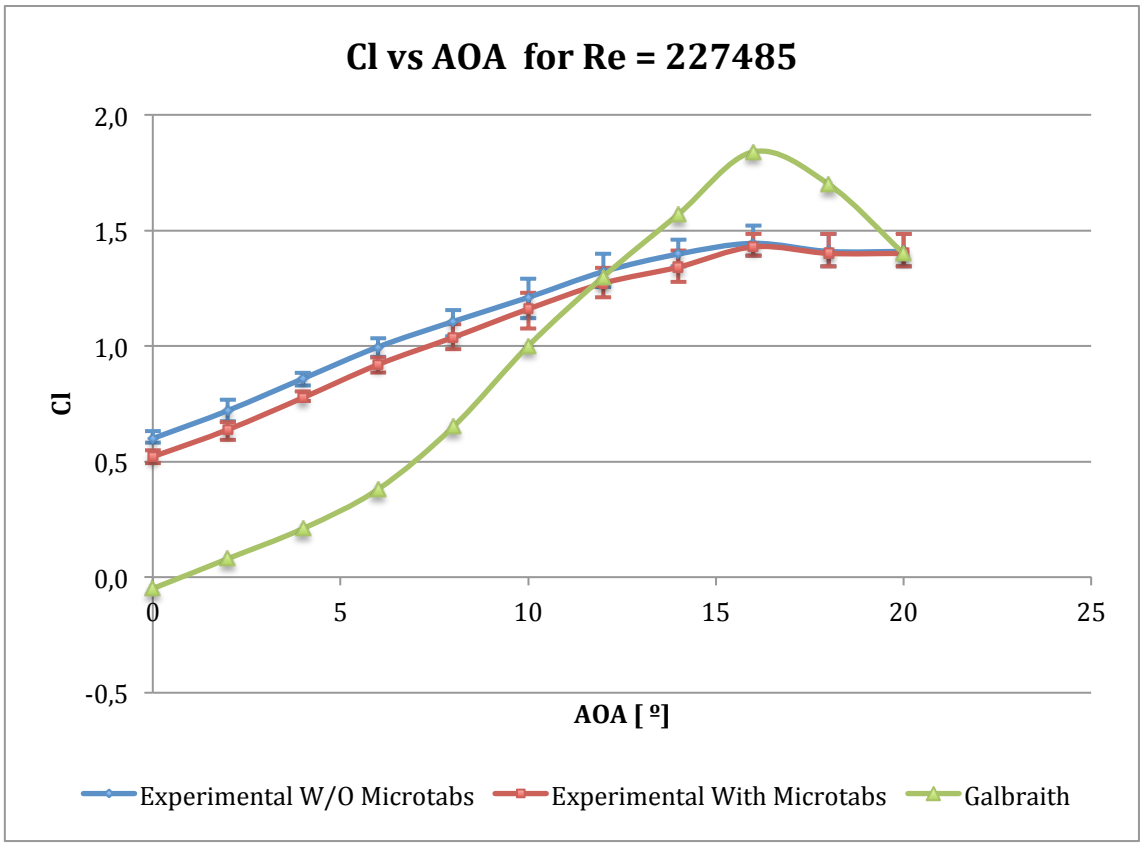

Graphic 2 - Lift coefficient curves for Re = 227485

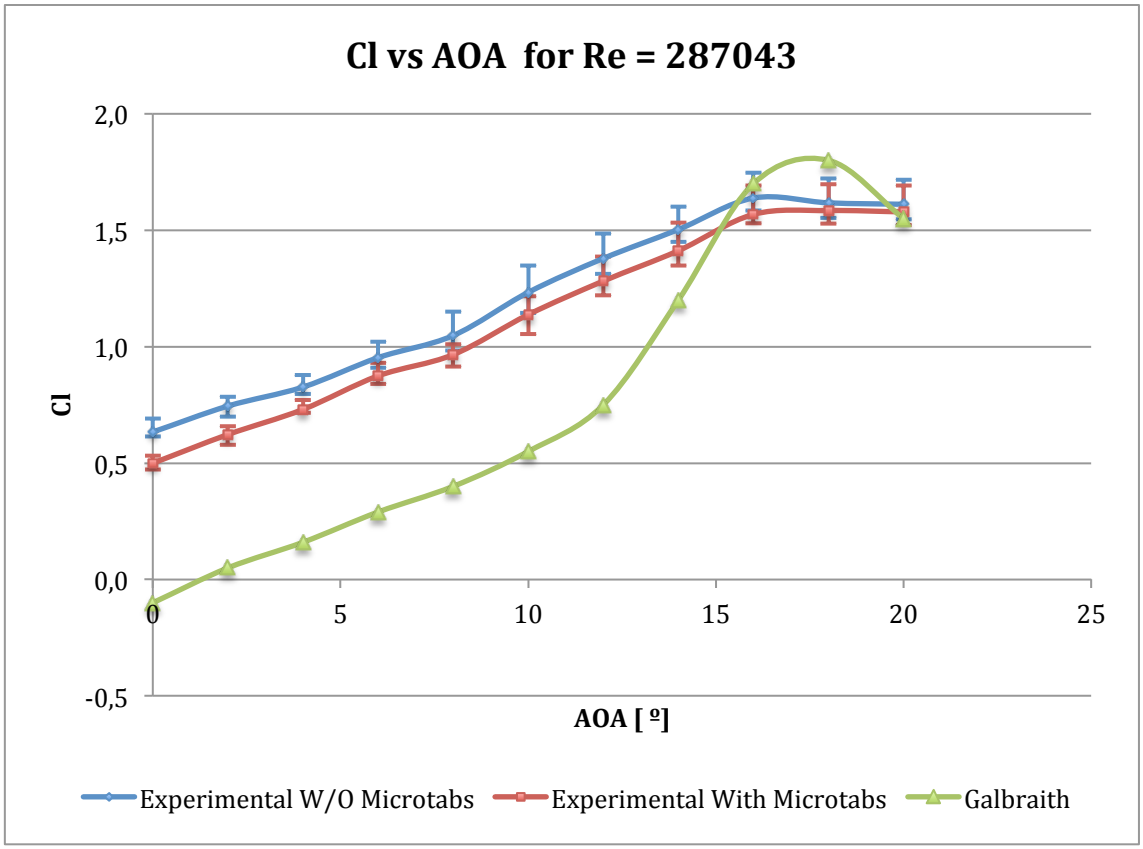

Graphic 3 - Lift coefficient curves for Re = 287043

5.1.3 DISCUSSION AND CONCLUSIONS

Four tests were performed; each one was performed using different methods:

1. Fixing the wind tunnel level and testing for each AOA
2. Fixing the AOA (0º - 20º) and testing for each wind tunnel level
3. Fixing AOA but for decreasing AOA numbers (20º - 0º)
4. Fixing AOA but with the dynamometer zero position modified

Then, the mean and the standard deviation for the C_L value for every angle of attack and for each wind tunnel level were calculated. The plotted graphics show the mean values calculated with error bars for each measured angle of attack point.

The error bars were calculated just plotting the mean of the value and then setting as the error boundaries the maximum and the minimum value of the 4 tests, for each angle of attack.

The experimental and theoretical lift coefficient curves differ in several ways. Despite the maximum C_L peaks match and the slope in the first 6-10 degrees of the angle of attack are the same, there are large differences between the experimental and theoretical curves in all the graphics. In this section we will explain some possible causes for these differences

First, there is a difference in the intercept of the lift curve, in all the experimental curves the C_L starts at 0.5, and in the Galbraith's ones at 0. One cause for this offset could be a mistake in the fixed Reynolds number. The calculated Reynolds numbers are, for the wind tunnel levels 3 to 5, 165442, 227485 and 287043 respectively. Some possible facts that could explain the difference between the experimental and the Galbraith curves are:

1. The blade surface is not perfectly smooth
2. The blade is not small enough comparing with the aerodynamic section so the boundary effects are negligible

In our case, the blade was made in balsa wood, cutting sections and then gluing them. After that we sanded the surface for achieving a surface as smooth as possible. However since the achieved surface was quite smooth, maybe it was not enough. Furthermore, the cut sections at the beginning were 4 mm thick sections, but when FabLab run out of 4 mm balsa wood, it was necessary using 2 mm balsa wood. This wood when it was sanded was not as smooth as the 4 mm one, so there was a smooth difference in a third of the blade.

As it was explained in pages 63-64 the blockage effect of the blade must be taken into account. This blockage provokes restrictions in the flow and produce extraneous forces in the airfoil. Also the effect of the wind tunnel boundaries must be sum up. These effects are minimized when the model is small to the size of the test section.[13]

Finally, the aerodynamic section was anything but perfect, there were a lot of gaps and irregularities that can affect the wind flow (Figure 59), and the connection to the exit of the wind tunnel was not perfectly closed, so this also could affect the wind flow increasing the turbulence character of the flow.

Figure 59 - Gaps and defects of the aerodynamic section

The second main difference is that the C_L values drop when the stall zone is approached, i.e., in all the cases the maximum lift coefficients are smaller than those in Galbraith's curves.

There are some possible explanations to these differences, first the way the lift forces were measured, in the Galbraith paper, the lift forces were measured using pressure gaps in the middle of the blade span.[14] The measured data relates to the conditions at the mid span of the model and no account was taken of any span wise variation.

In the other hand, data measurements in this thesis were taken with an aerodynamic balance. And in an aerodynamic balance the lift forces taken into account are all of them that work in all the span of the blade, that is the main difference with the Galbraith, in their paper they calculate the lift force by an integration of the pressure difference in the centre of the blade but in this case the resultant of the lift force is the integration of all the lift forces in the blade. And, since the lift forces at the boundaries of the blade are smaller than the ones in the centre [15], that is why the lift forces measured by the aerodynamic balance could be smaller than the theoretical ones.

Finally there was a last fact that could make the measured lift forces were smaller, the aspect ratio, i.e, the ratio between the span wise and the chord length. As it agrees with what is displayed in the *figure 60* the lift losses due to the boundaries of the blade are severe. Even for aspect ratios bigger than 6.

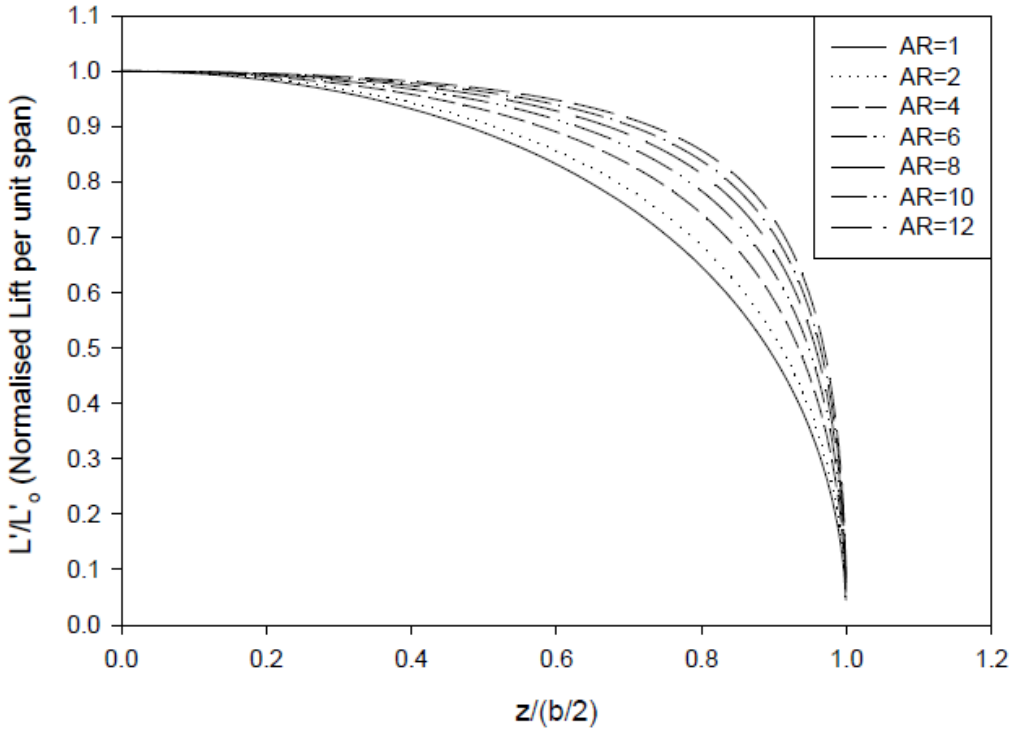

Figure 60 - Lift mitigation along the span wise in function of the aspect ratio. [15]

In this case, the aspect ratio hardly achieves the value of 2.4; so according to the figure above the measured lift forces are much lower than real. We tried to compensate this low aspect ratio by adding the two plates of the angle of attack system that would

prevent the wind circulation from the suction to the pressure side. According to the fact that an aspect ratio of at least 6 would be more acceptable, that would suppose building a blade with a 10cm chord, what would suppose building a really small model that would have been harder to construct accurately, more over, the measured lift force would have been much smaller, and maintaining the accuracy of the balance unchanged the accuracy of the measurements would have been considerably worse.

Despite the explained factors could in some way affect to the measurements, the differences between the curves in the Galbraith paper and the experimental ones were still too large, and since the results were not the expected ones, another test were performed in order to improve the curves.

5.2 EXPERIMENT 2

5.2.1 SET UP

Since the measurements did not agree with nor Galbraith's results nor with our intuition, in this experiment we investigate looking for some facts that could explain these differences.

So, the idea was measuring again lift forces from the -6 degrees of the angle of attack system to 24 degrees in steps of 2 degrees, and check if in that range of angle of attack both curves, the Galbraith ones and the experimental ones matched. More over, there was another fact in the angle of attack issue; the blade itself was twisted, as it can be seen in the *figure 61*.

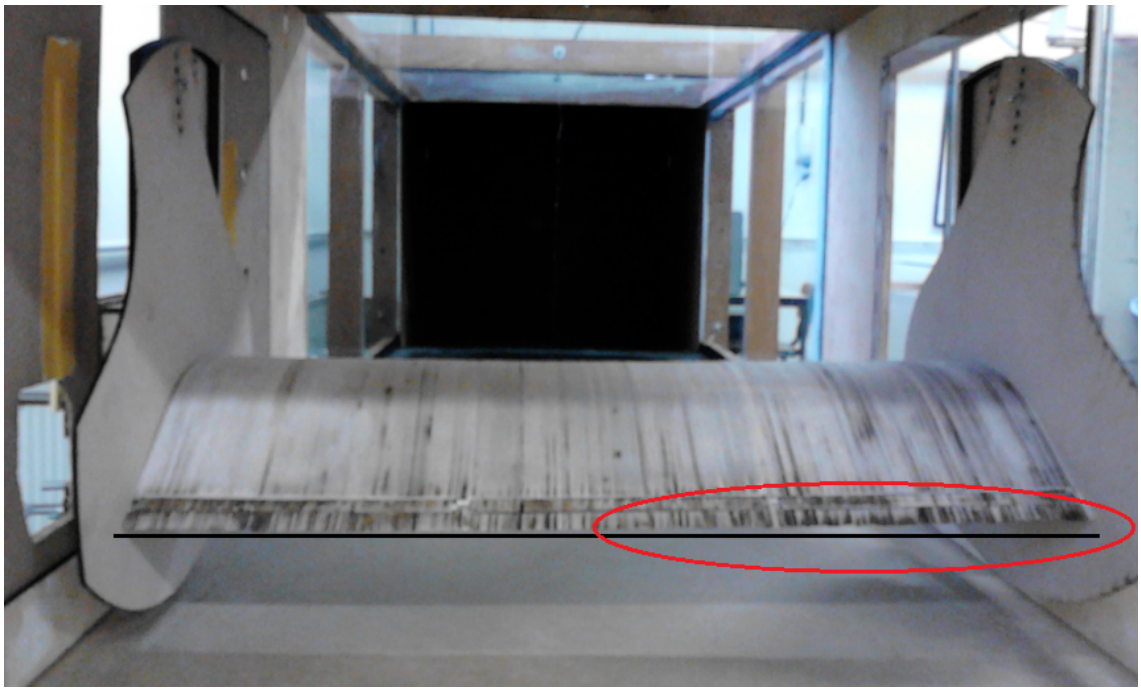

Figure 61 – Blade twist

This twist added to the previous offset another one, we tried to measure it by fixing one side of the blade to the angle of attack system, and change the other side's angle till the twist disappeared. The offset due to the blade twist happened to be 2.5 degrees. So the total offset would be at least 2.5 degrees, this was too much offset since 2 degrees difference in the lift coefficient graphics has a lot of influence, but if this could be kept under control the problem would de diminished.

The twist is not only a problem of offset but also of a variation in angle of attack for the different profiles along the span. The result is a sort of average lift over the span.

So, the experiments were going to be repeated with and without microtabs for different Reynolds numbers, and then the obtained curves were going to be compared with the Galbraith's ones.

5.2.2 RESULTS

The measurements were repeated but now instead of going from 0 degrees to 24 degrees, we made them from -6 degrees to 24 degrees in steps of 2 degrees. The goal of this experiment is plotting the experimental curves with different offsets and comparing with the Galbraith's ones, focusing on the intercept of the lift curves whether they match.

The following graphics show the experimental and the Galbraith's paper curves for different Reynolds numbers.

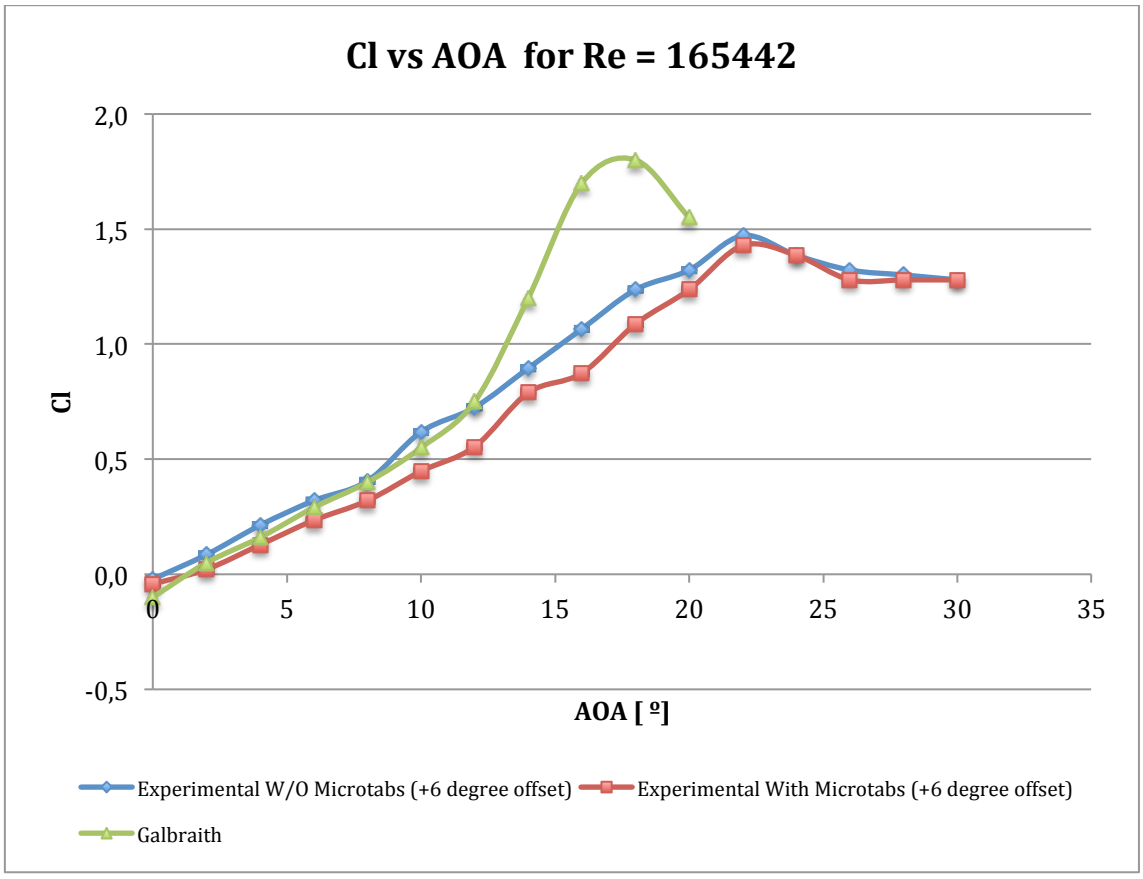

Graphic 4 – Lift coefficient curves for Re = 165442. The experimental ones with an offset of +6 degrees

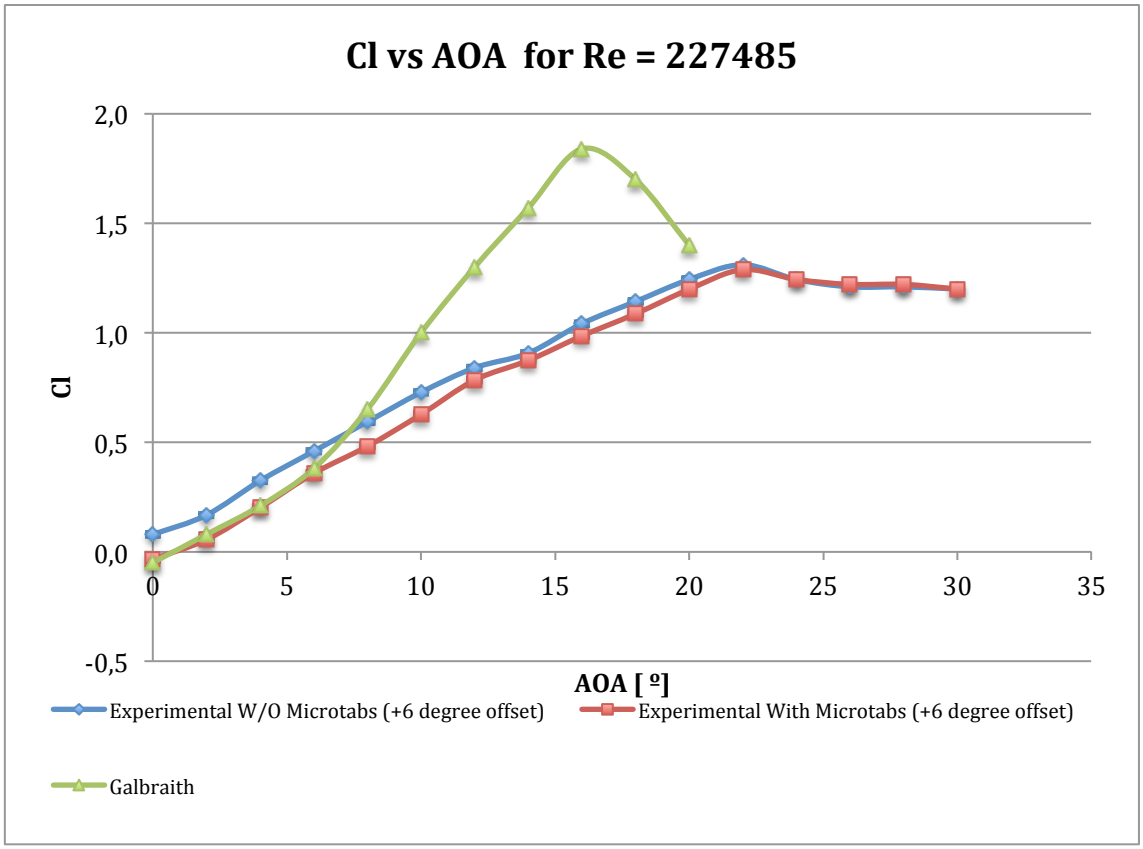

Graphic 5 - Lift coefficient curves for Re = 227485. The experimental ones with an offset of +6 degrees

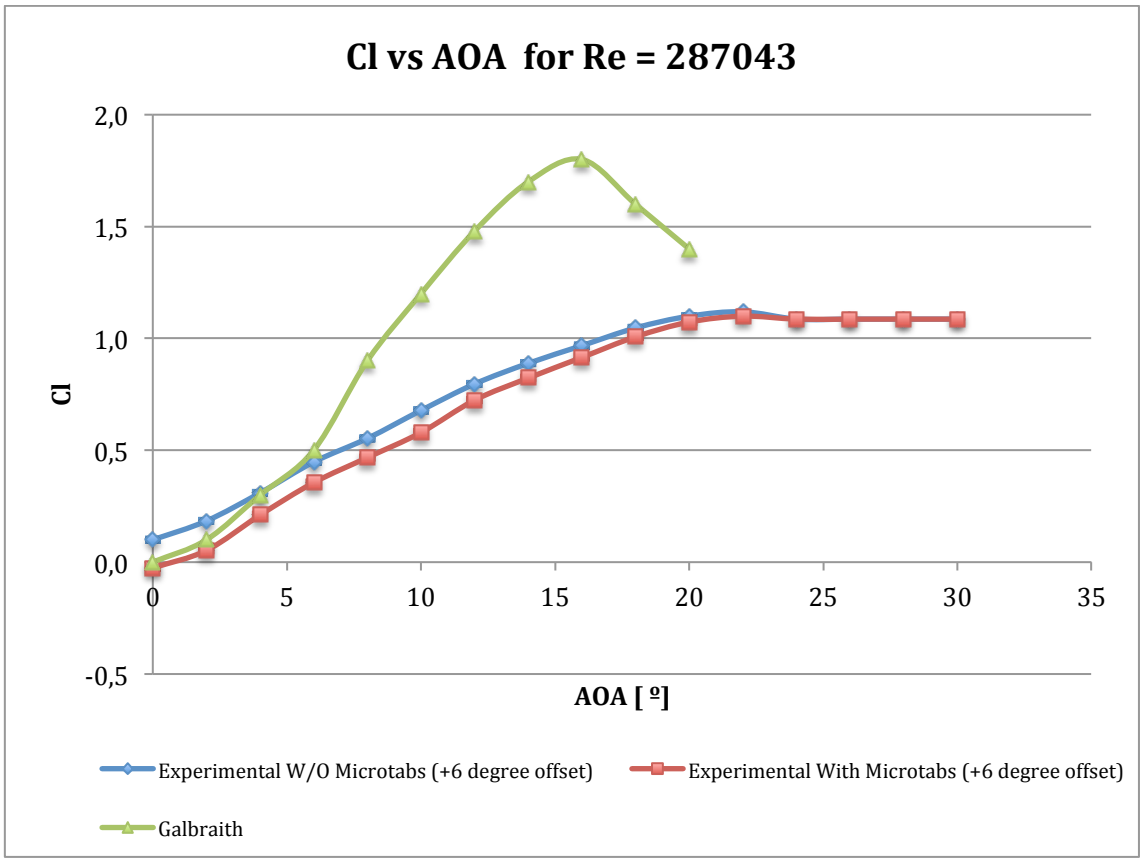

Graphic 6 - Lift coefficient curves for Re = 227485. The experimental ones with an offset of +6 degrees

5.2.3 DISCUSSION AND CONCLUSIONS

Regarding to the experimental curves, in this cases there is a positive offset between the experimental curves and the ones from Galbraith, and the slopes match better than in the previous experiment. Actually in this case for the lowest Reynolds number curves, both the slope and curves match till 12 degrees of angle of attack. So it can be appreciated that with this offset in the experimental curves we have been able to make a better comparison with the Galbraith's curves.

These results could mislead to the idea that the only fact the changes the curves of the graphic is the +6 degree offset. But there are another factors such as the fact that the blade itself is twisted 2.5 degrees, so the measurements of the balance are not accurate since instead of making one measurement for every fixed angle of attack, the measurements are done for an average of angle of attack.

But there are still some differences between the experimental curves and the theoretical ones. The first one is the achieved maximum lift coefficient values that in the experimental ones are lower. The explanations about the mitigation in lift measurements in aerodynamic balances in comparison with the measurements with pressure tabs that were explained in the previous experiment could explain in some level this effect.

More experiments were planned, in order to explain the different behaviour between the Galbraith paper curves and the experimental ones.

5.3 EXPERIMENT 3

5.3.1 SET UP

The wind flow speed was the next factor we investigated for making an improvement in the curves.

- ✓ In the first experiment, the lift measurements and the lift coefficient calculations were made with an average wind speed measured for every Reynolds number tested. But the same wind speed was used for all the angle of attacks.
- ✓ In the second experiment the angle of attack system was checked without especial regards to the wind speed.

In the third experiment the lift measurements were repeated and lift coefficients calculated, but this time, instead of using an average wind speed for all the angle of attacks for the different Reynolds numbers tested, an average wind speed was measured for every angle of attack and for every Reynolds number tested, and then the lift coefficients calculated.

The measurements were taken from an angle of attack of -6 degrees to 24 degrees in steps of 2 degrees.

The anemometer measurements were made using the holes located in different heights in the tests section located before the blade, as it is shown in the *figure 62*.

Figure 62 – Holes at different heights (10-20-30-40 cm) located before the blade in the tests section

5.3.2 RESULTS

The following graphics show the lift coefficient curves compared with the Galbraith ones, for every Reynolds number tested and for the cases with and without microtabs.

The goal of the experiment was to check if using these new average wind speeds the obtained maximum lift coefficients were bigger. For this reason the results of this experiment are going to be compared with the results of the previous experiment. After that, as in the other experiments, some graphics comparing the experimental results of this experiment with the results in Galbraith are going to be compared, but in this the experimental graphics would have an offset of +6 degrees in the angle of attack for a better comparison with the Galbraith's curves.

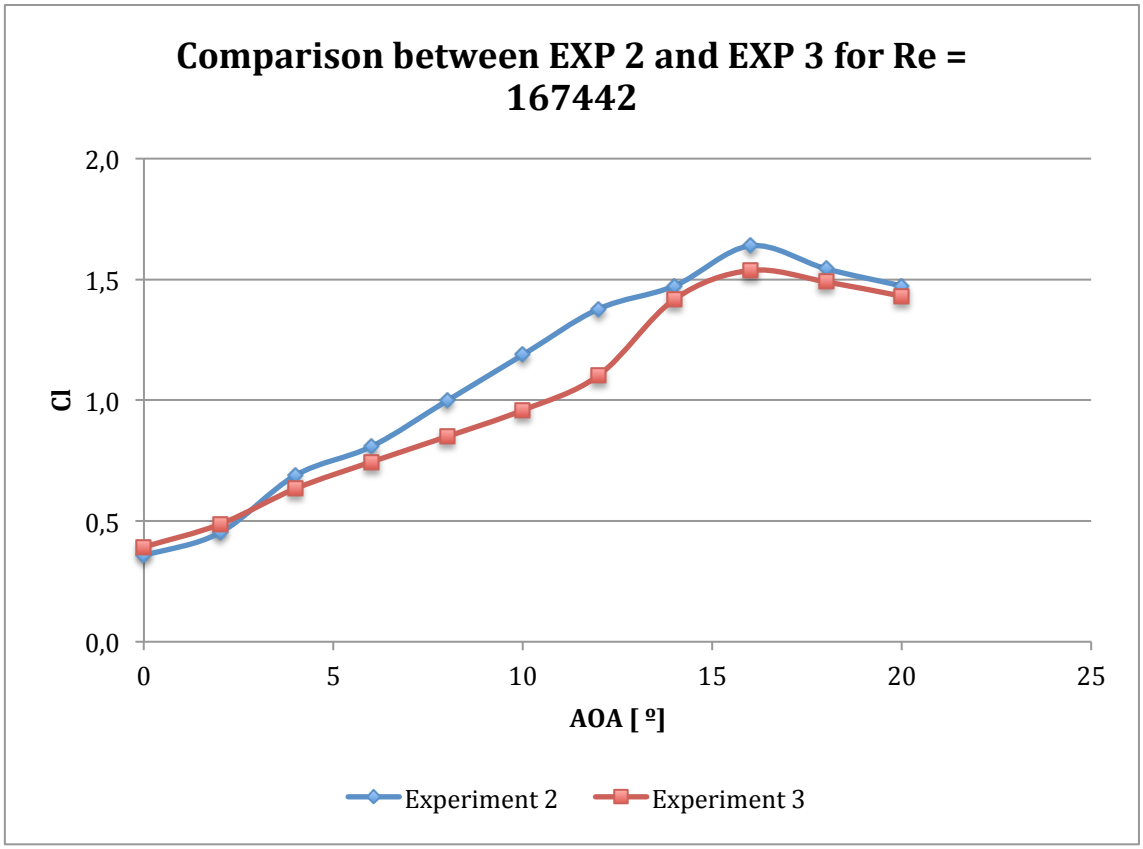

Graphic 7 – Comparison between experiment 2 and 3 for Re = 165442

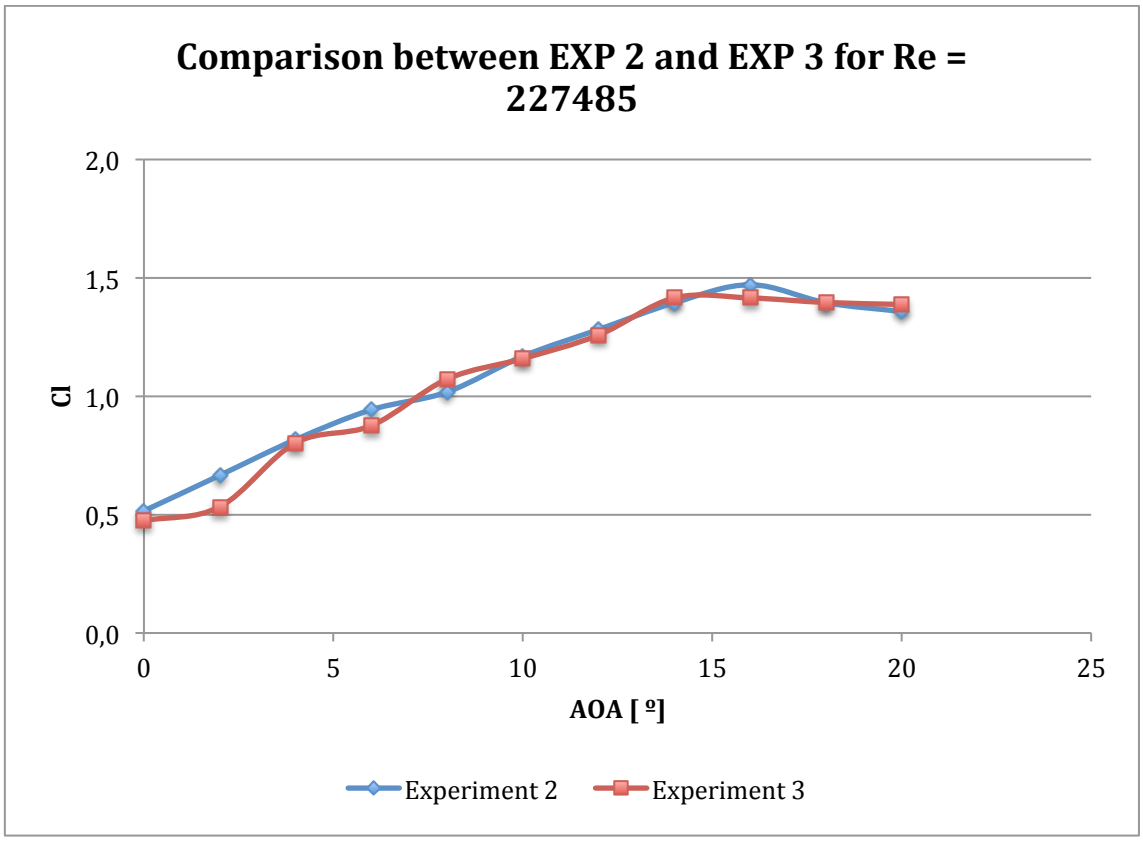

Graphic 8 - Comparison between experiment 2 and 3 for Re = 227485

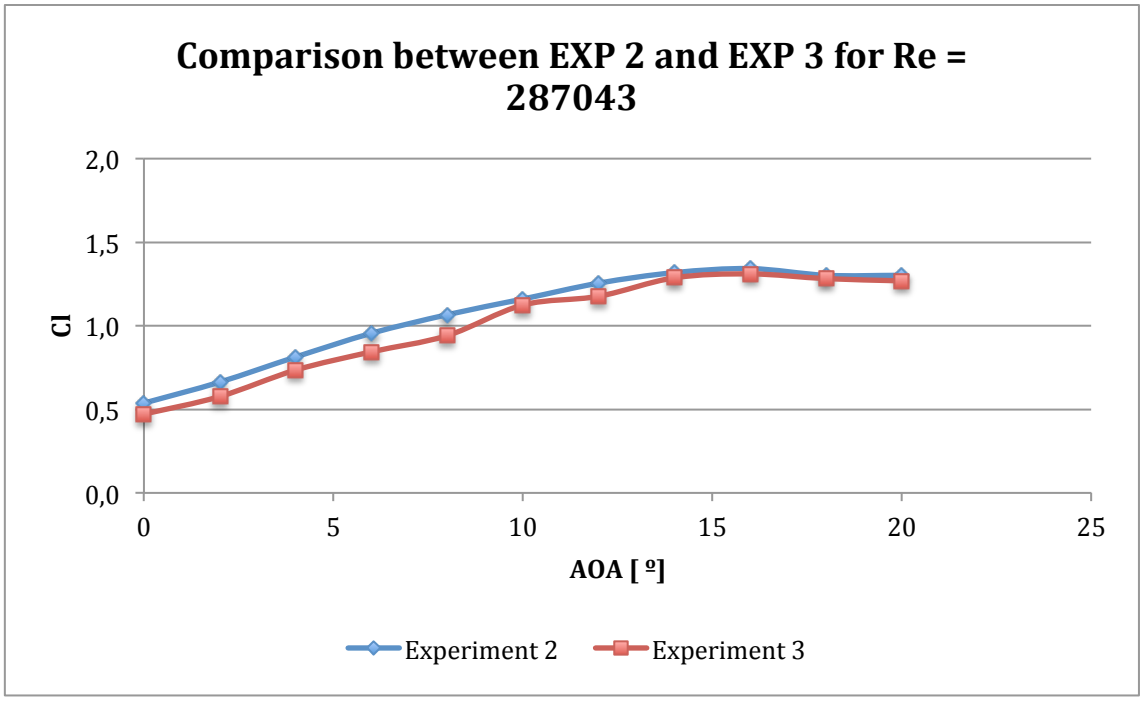

Graphic 9 – Comparison between experiment 2 and 3 for Re = 287043

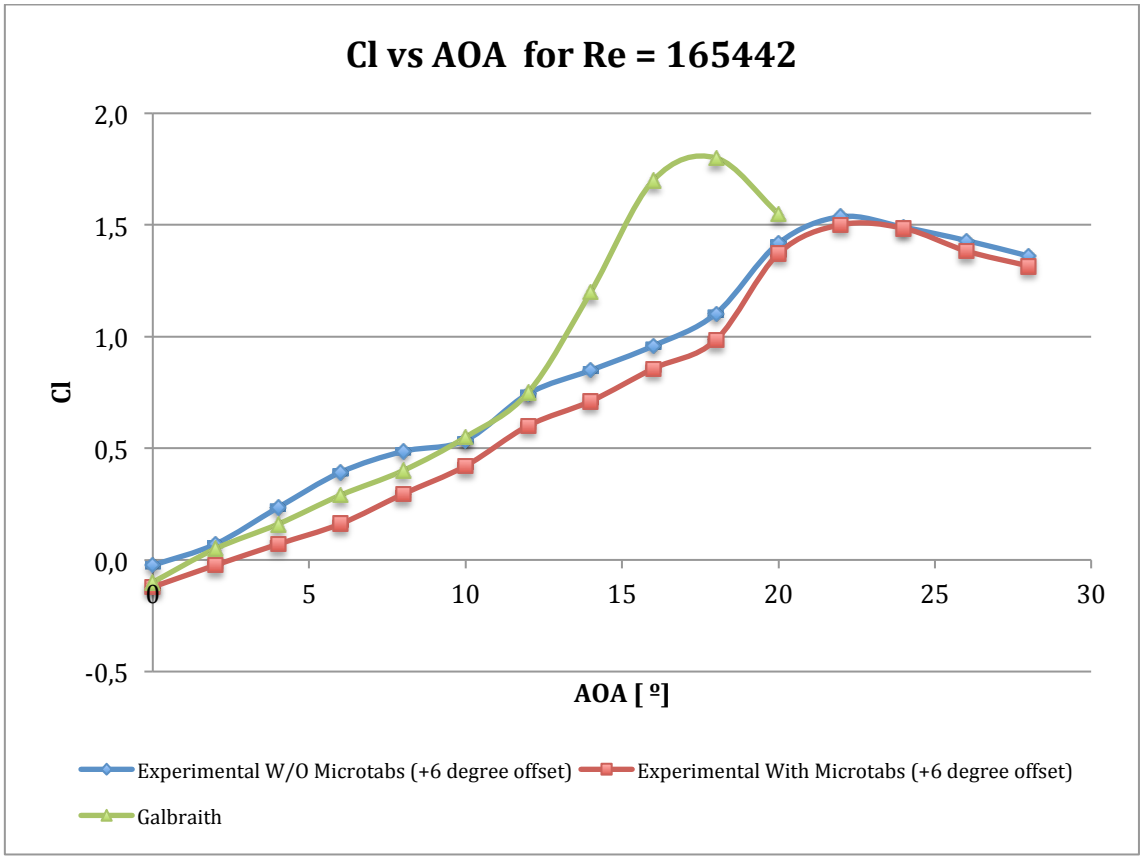

Graphic 10 - Lift coefficient curves for Re = 165442. The experimental ones with an offset of +6 degrees

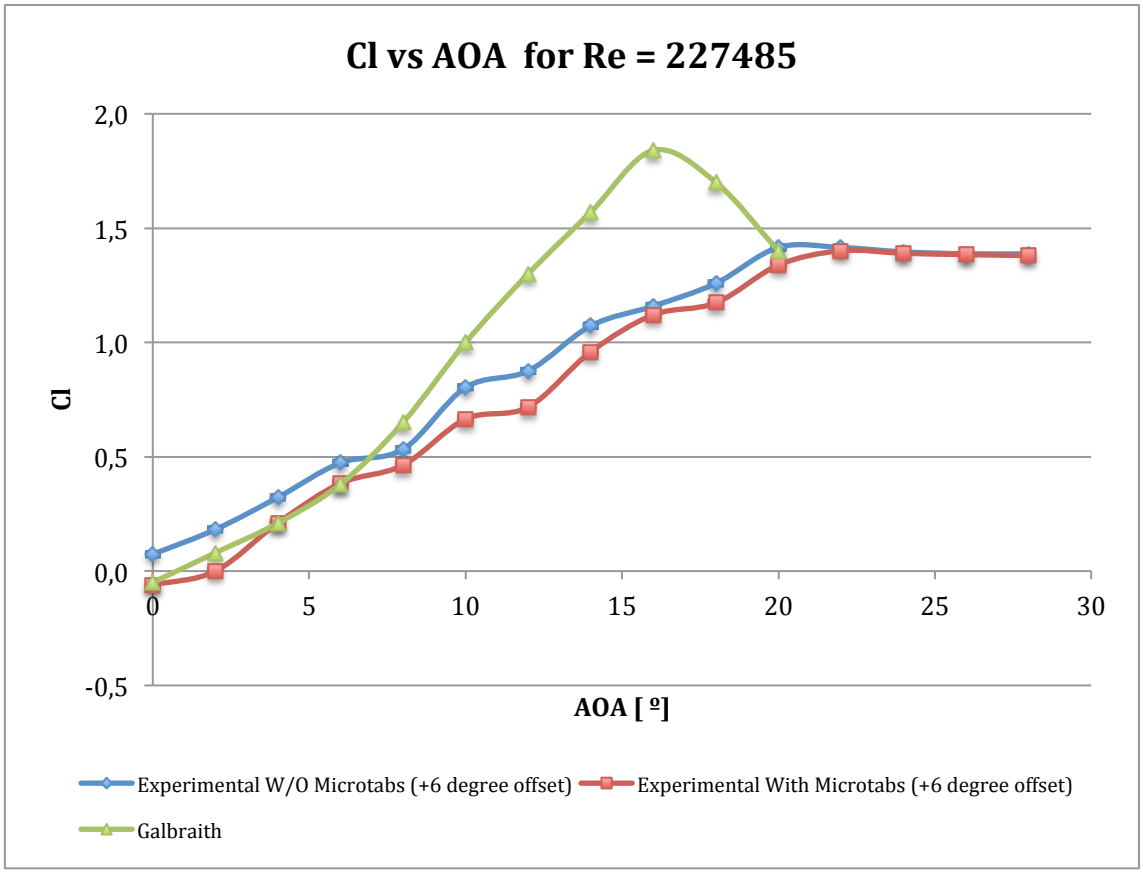

Graphic 11 - Lift coefficient curves for Re = 227485. The experimental ones with an offset of +6 degrees

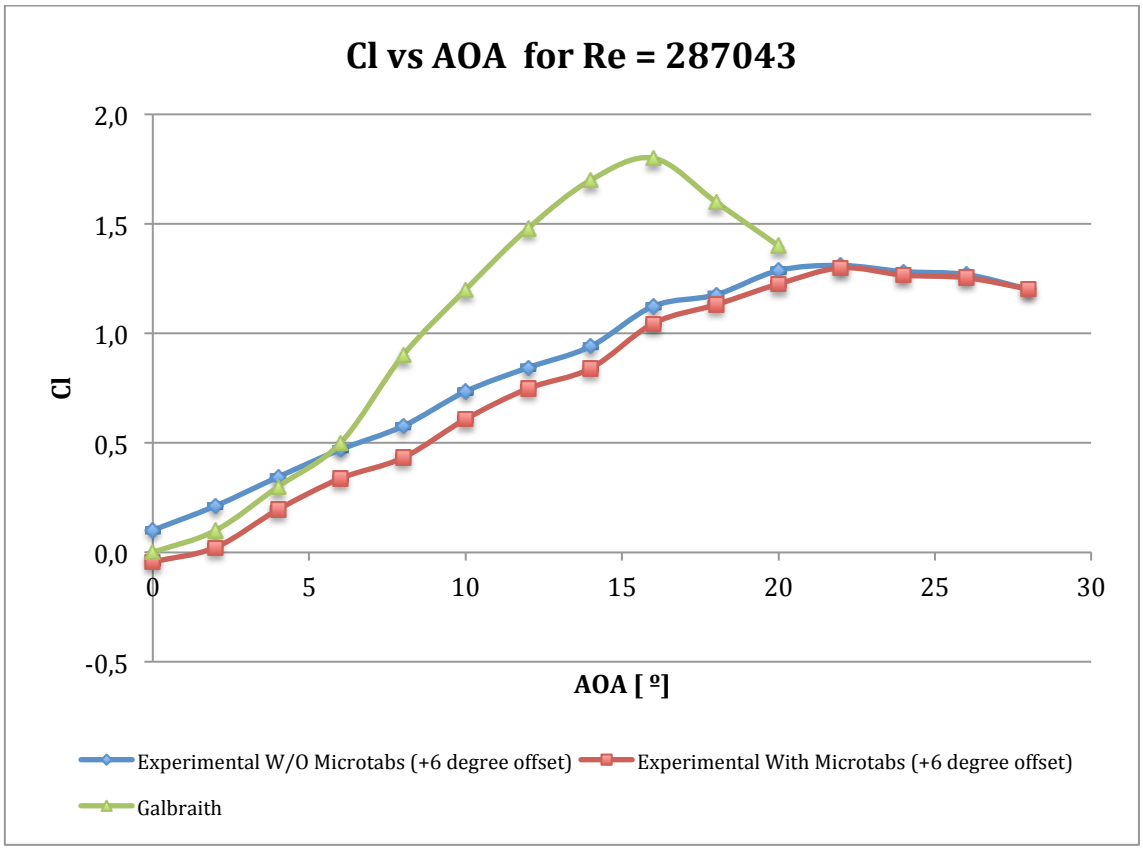

Graphic 12 - Lift coefficient curves for Re = 287043. The experimental ones with an offset of +6 degrees

5.3.3 DISCUSSION AND CONCLUSIONS

As it can be appreciated in the *graphics 7, 8 and 9* with these two different measurement procedures the intersects are more or less the same, but in all the cases the obtained maximum lift coefficients are equal or bigger in the second experiment than in the third one, and in any case the differences are too small for taking them into account, so we can conclude that this measurement technique, with an average speed measured for every angle of attack and Reynolds number tested is not better than the previous ones and there is no need of measuring the average speed for every angle of attack.

As it have been explained in the experiment one, the blockage effect of the blade makes alterations in the wind flow speed increasing the values, and in *the graphics 7, 8 and 9*, can be appreciated that the experiment 2 shows generally higher lift coefficient values, this is because the lift forces measured in both experiments match, but due to the blockage effect the wind speed used in the third experiment for the calculate the lift coefficient is higher than the used in the second experiment, so the lift coefficients are always bigger or at least equal in the second experiment than in the third one.

Finally, for the performance of the last experiment some ideas about the effect of the turbulence intensity will be explained.

5.4 EXPERIMENT 4

5.4.1 SET UP

In this experiment the effect of the turbulence intensity in airfoil measurements will be studied. The turbulence intensity of a wind tunnel is the standard deviation of the wind flow speed expressed in percentages.

$$TI = \frac{\sigma_V}{\overline{V}}$$

Equation 16 – Turbulence intensity

The idea of studying this effect comes from comparing the curves of the previous experiments with the curves obtained by Stijn Van Gysel in his thesis last year. [16]

The wind tunnel used in the Galbraith paper has a turbulence intensity of 0.5% [14], and VUB wind tunnel, where Stijn Van Gysel made the tests, has a turbulence intensity of 1% [16], bigger than the Galbraith's one. Finally the turbulence intensity of the EhB wind tunnel is between the 5 and 15 % [17], much bigger than the other ones. So it seems to be a factor that could affect to the behaviour of the curves of this thesis.

So, the idea for this experiment was either increase or decrease the turbulence intensity of the EhB and check what happens to the lift curves. Since it is much easier to increase the turbulence intensity we decided on it and expected with this experiment obtaining lift curves with a more delayed stalls than the ones in the previous experiments and with lower maximum lift coefficients.

For the performance of this experiment, another tests section was added between the tests section with the blade and the exit of the wind tunnel (Figure 59a). In this section there were set up some blocks that would increase the turbulence intensity (Figure 63b, 63c and 63d).

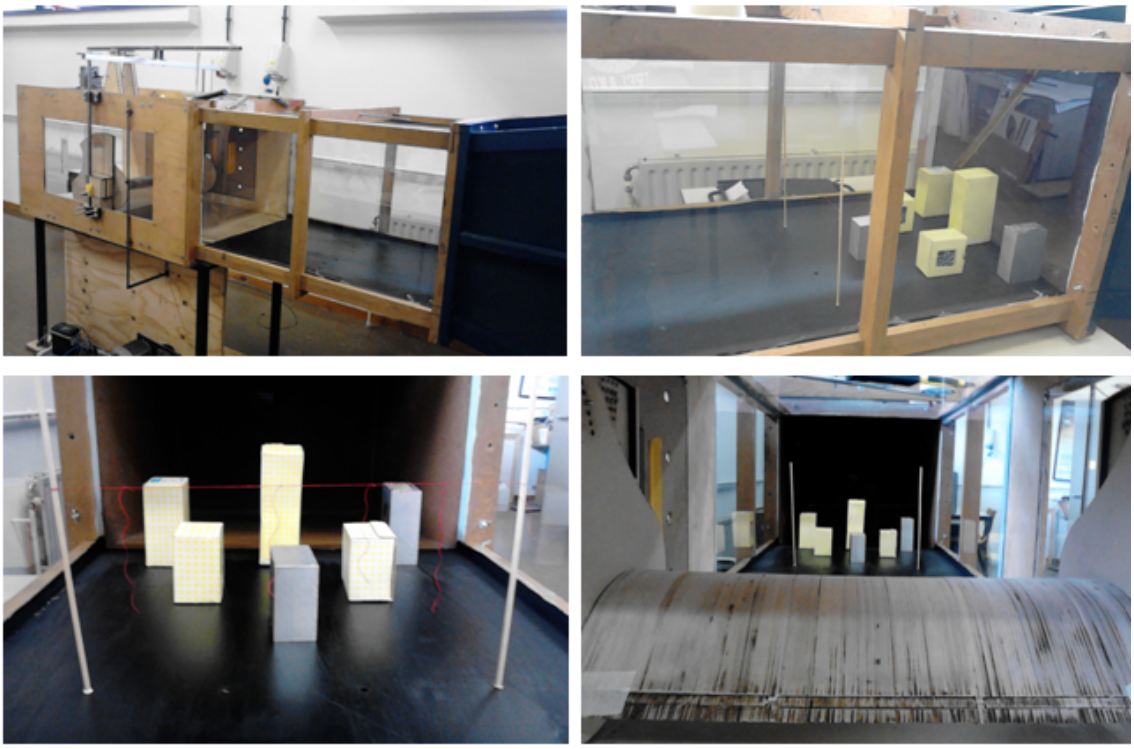

Figure 63 – Set up for the test of increased turbulence

Once the turbulence intensity was increased, new test were made for Reynolds numbers 165442, 227485 and 287043, and for every angle of attack for a range from -6º to 24º in a step of two degrees.

5.4.2 RESULTS

In the following graphics are shown a comparison between the Galbraith paper's curves, the Stijn Van Gysel thesis' curves, the experimental curves of the previous experiments and the experimental curves with increased turbulence intensity for different Reynolds numbers.

In these cases the experimental curves are plotted with the +6 degree offset for a better comparison with the Galbraith's and Stijn Van Gysel thesis' ones.

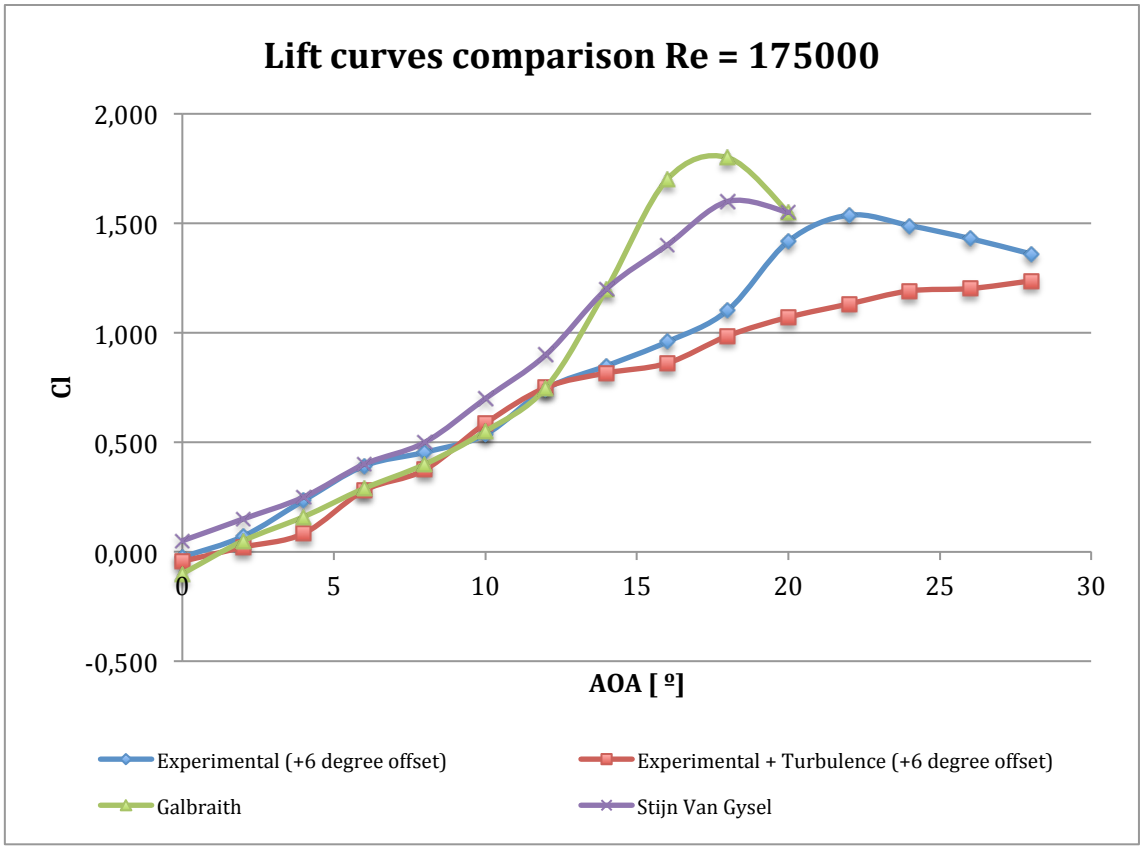

Graphic 13 – Lift comparison curves, Galbraith – Stijn Van Gysel – Experimental – Experimental + T for Re = 175000. The experimental ones with +6 degree offset

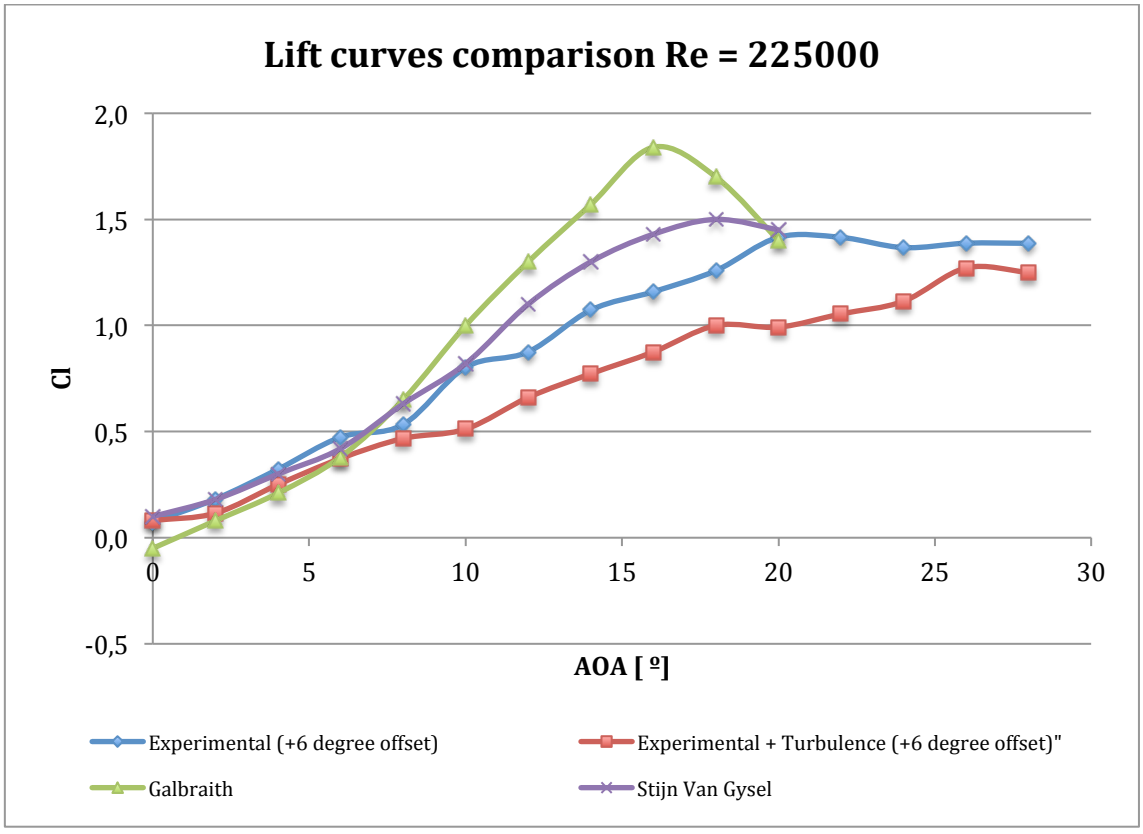

Graphic 14 - Lift comparison curves, Galbraith – Stijn Van Gysel – Experimental – Experimental + T for Re = 225000. The experimental ones with +6 degree offset

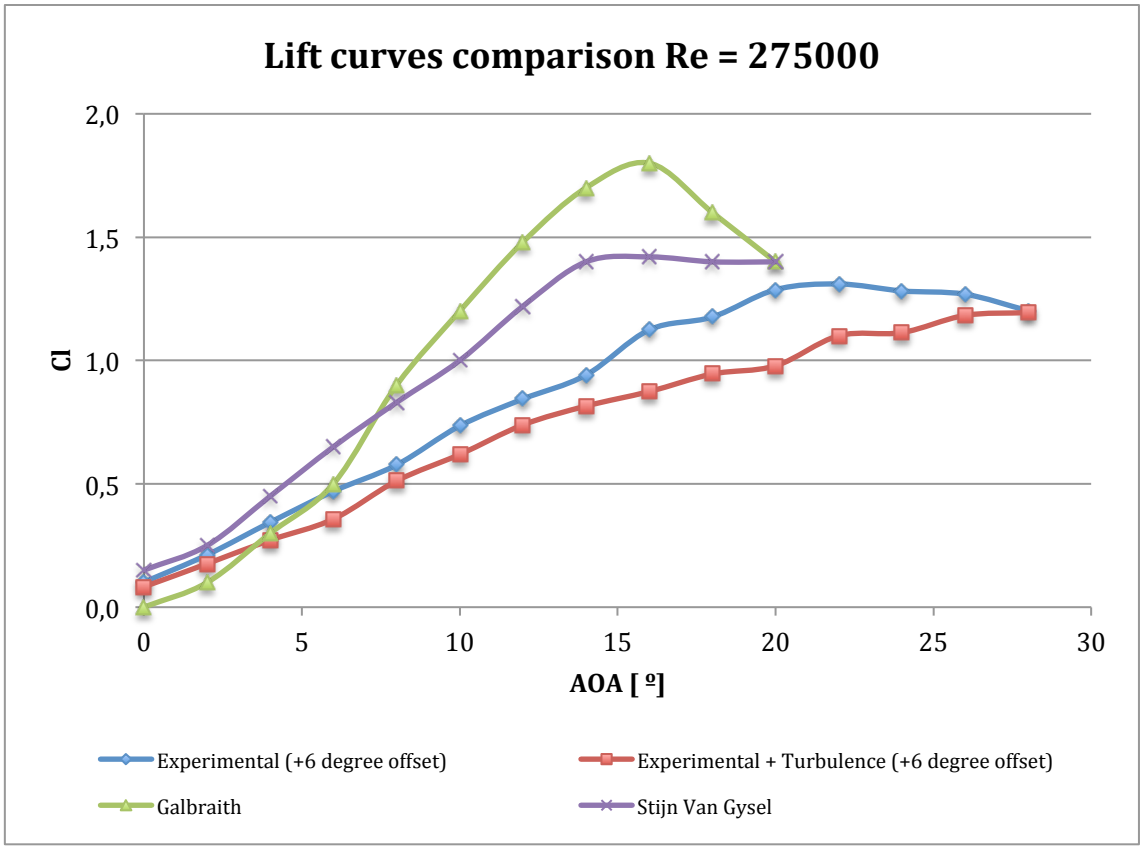

Graphic 15 - Lift comparison curves, Galbraith – Stijn Van Gysel – Experimental – Experimental + T for Re = 225000. The experimental ones with +6 degree offset

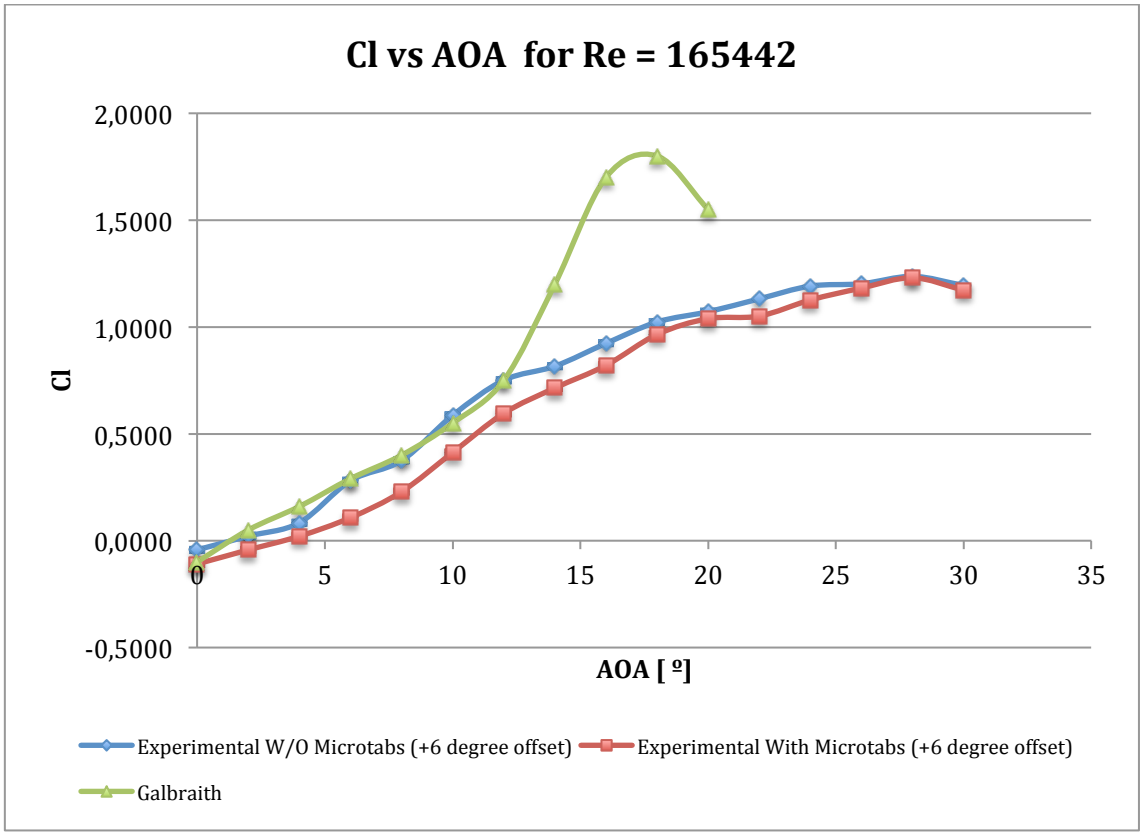

Graphic 16 – Lift coefficient curves for Re = 165442. The experimental ones with an offset of +6 degrees

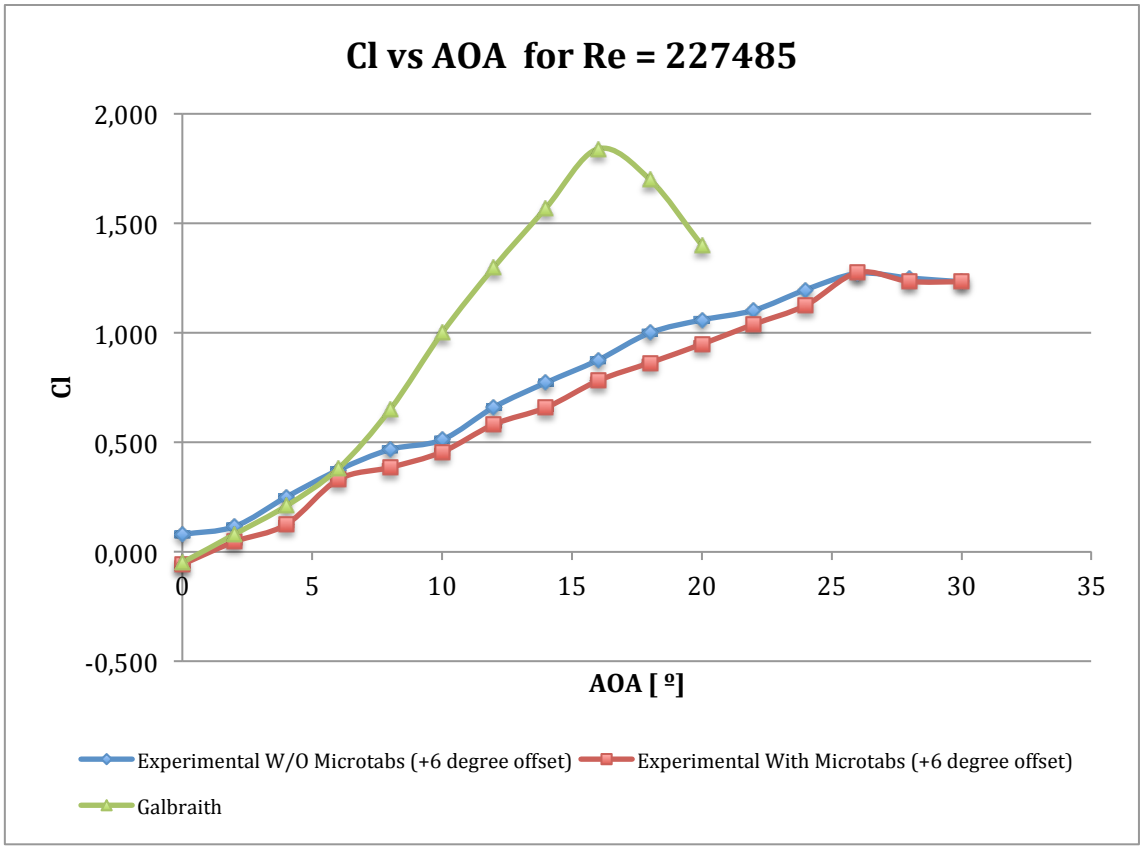

Graphic 17 - Lift coefficient curves for Re = 227485. The experimental ones with an offset of +6 degrees

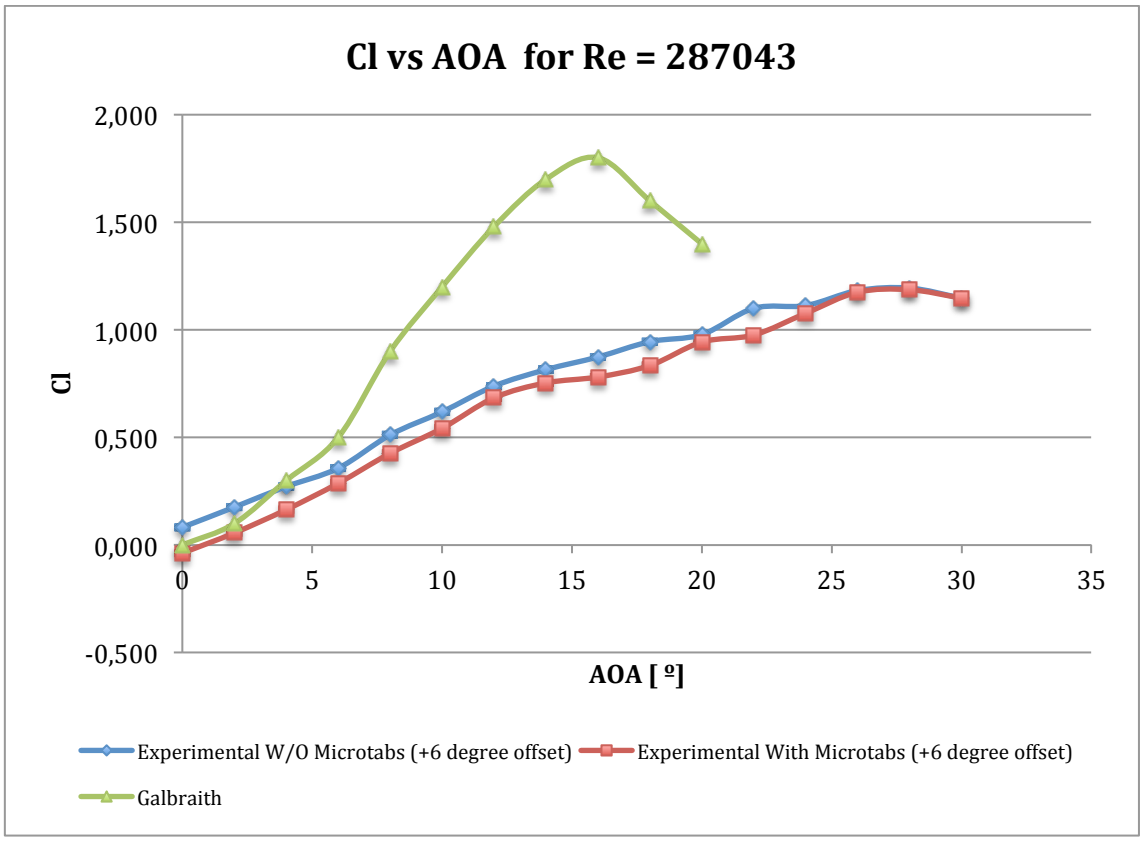

Graphic 18 - Lift coefficient curves for Re = 287043. The experimental ones with an offset of +6 degrees

5.4.3 DISCUSSION AND CONCLUSIONS

There can be appreciated some similarities in our experimental curves and the ones of Stijn Van Gysel's thesis, they have the same differences with the Galbraith curves. Both curves have less lift coefficient values than the Galbraith ones and the slope of the curves remain more or less constant, what differs with the Galbraith ones since when the pressure bubble start to develop at an angle of attack of 10-12 degrees, and the wind flow goes into turbulent, the Galbraith paper's curves change the slope to a bigger on and in Stijn Van Gysel's thesis and in the curves of these experiments the slope remain constant.

But, although both curves have the same differences with the Galbraith, the experimental curves in these experiments show pronounced effect of differing from the Galbraith one curves, so there should be a fact that enhances the difference with the Galbraith paper's curves and one fact could be the intensity of the turbulence.

As it was expected the curves in this test have been displaced pronouncing the effect of going to the bottom right side of the Galbraith curves, as it can be appreciable in *graphics 14, 15 and 16*.

This effect was also studied on a NACA 65_4-421 aerofoil in *"Experimental study of wind turbine airfoil aerodynamics in high turbulence"* [18] in order to examine the influence of the turbulence intensity on the aerodynamic behaviour of the aerofoil. The conclusion was made that higher turbulence intensity reduces the slope of the linear portion of the CL graph, increases the maximum CL value and delays stall, as it can be appreciated in the *graphics 14, 15 and 16.*

6. CONCLUSIONS

The goals of this thesis were to test a smart blade with microtabs by performing wind tunnel tests on the blade and to examine various properties.

Once the wind tunnel of the EhB was chosen for the performance of the tests, the first achievement was to build a smart blade using the material and machines available in the FabLab. In comparison with last year Stijn Van Gysel's setup [16] there was no need of building a hollow blade because in our case all the actuator system would be placed outside the blade since we bet on the rotating actuation system (Section 4.2).

Next achievement was the design and construction of a system for controlling and setting in accurate enough way the angle of attack of the blade. This system must be accurate enough for setting the angle of attack with an error less than half degree, since, as it can be appreciated in all the graphics of this thesis, the lift coefficient varies considerably with small changes of the angle of attack.

After that, the design and setup of the aerodynamic balance for the measurement of the lift forces was achieved. This balance should be accurate enough for measuring small changes in lift forces with especial regard to the static friction of the balance that would affect to the measurements. Despite we did not entirely achieve the set goals, in the aerodynamic balance setup section (section 4.4) some solutions are proposed and explained, and in the next chapter, some improvements for the aerodynamic balance are proposed.

Once the setup was completed, the next step was to start with the measurements and calculations, and plotting the lift coefficient curves. As it is shown in the graphics of the first experiment (section 5.1) there are large differences between the experimental curves and the curves of the literature (Galbraith paper [14]), so, as it could not be possible obtaining the same curves as in the literature, the next achievement was presenting and studying facts that could explain these differences. Among all the factors that could affect the results these were proposed:

- ✓ Instead of using pressure tabs, an aerodynamic balance was used for measuring the lift forces, with the consequent tip losses explained in experiment 1. (Section 5.1)
- ✓ The blade was not as perfect as it should be, it was twisted with the consequent problems explained in experiment 2. (Section 5.2)
- ✓ The much bigger turbulence intensity of the EhB wind tunnel in comparison with the one used in the Galbraith paper as it is explained in experiment 4 (section 5.4)

One of the last achievements was to understand the effect of increasing the turbulence intensity in the measurement of the lift forces. In experiment 4 an artificial increase of the turbulence intensity of the EhB wind tunnel was performed and the effect studied. The fact of increasing instead of not increasing the turbulence intensity relies on the easiness of increase the turbulence in comparison with the decrease. The results come up with the ones in the literature, and it was proved that an increase in the turbulence intensity provokes a decreasing in the lift coefficient slope. [18]

Finally, as it has been commented in the beginning of this chapter, the main goal of the thesis was to study the effect of the microtabs of load alleviation in wind turbines. For this, it was necessary constructing microtabs and implementing them in the smart blade as it is explained in section 4.2. The effect of lift mitigation can be appreciated in all the graphics of the experimental results chapter, as it was expected from the literature [7]. Nevertheless, a study about the variation of mitigation effect with the Reynolds numbers would be appropriate for enclosing the study.

7. FUTURE RESEARCH

In this chapter some future goals and improvements to this thesis are going to be explained in order to guide the reader going one with the lines of this work.

- ✓ Improvements in the blade
  - ➢ Using other (and more accurate) manufacturing techniques, such as milling machine or 3D printing.

- ✓ Improvements in the aerodynamic balance
  - ➢ Decrease the static friction substituting the lift carriage with linear bearing displacing along a cylindrical rod system, by a lift carriage with wheels that rotate in a plain surface. (Linear rail system)
  - ➢ Implement strain gauges instead of a dynamometer based on a spring for the lift measurements that would allow connect the balance to a computer. This would allow for a better data handling.
  - ➢ Design a way for a better interchange ability in order to make easier testing different blades in the balance without too much effort spent in the setting up
  - ➢ Sharpen the pivot point of the balance that would decrease the friction in that point.

- ✓ Improvements in the microtabs
  - ➢ The study and implementation of different actuator system
  - ➢ Design of the control loop for controlling the microtabs deployment ensuring an optimal effectiveness of the microtab in terms of lift reduction and maintaining a good lift-to-drag ratio.

- ✓ Improvement in the experiments
  - ➢ Study the blockage effect
  - ➢ Study a way for reducing the turbulence of intensity in the EhB wind tunnel in order to develop the conclusion about the turbulence intensity effect.

BIBLIOGRAPHY

[1] Joseba Ripa, *Energía eólica*. Universidad Pública de Navarra, 2009.

[2] Vincent Gray, *The causes of global warming*. Frontier Centre for Public Policy, 2001.

[3] Commision of the European communities, *Communication of the European commision about limiting global climate change and the way ahead for 2020 and beyond*. Commision of European communities, 2007.

[4] Ignacion Cruz, *Avances tecnológicos y perspectivas de la tecnología eólica*. Ciemat - Ministerio de economia y competitividad, Gobierno de España, 2012.

[5] J. L. Rodriguez Amenedo, J. C. Burgos Díaz, and S. Arnalte Gómez, *Sistemas eólicos de producción de energía eléctrica*. Rueda SL, 2003.

[6] Global Wind Energy Councyl, *Global Wind Statistics 2012*. GWEC, 2013.

[7] S. J. Johnson, C. P. van Dam, and D. Berg, *Active load control techniques for wind turbines*. Technical report, Sandia national laboratories, 2008.

[8] D. T. Yen, C. P. van Dam, F. Bräuche, R. L. Smith, and S. D. Collins, *Active Load Control and Lift Enhancement Using MEM Translational Tabs*. 2000.

[9] UIUC, *Airfoil cordinates database*. Department of aerospace energy - University of Illinois.

[10] D. T. Y. Nakafuji, C. P. van Dam, R. L. Smith, and S. D. Collins, *Active load control for airfoils using microtabs*. Journal of Solar Energy Engineering, 2001.

[11] Iñigo Solana Arocena and Asier Herreo Barandica, *Experimental study of the performance of microtabs for load alleviation in wind turbines*. EhB Master thesis, 2012.

[12] Michael S. Selig, Robert W. Deters, and Gregory A. Williamson, *Wind tunnel testing airfoils at low Reynolds numbers*. University of Illinois, 2011.

[13] Michael S. Selig, James J. Guglielmo, Andy P. Broeren, and Philippe Giguere, *Summary of Low-Speed Airfoil Data*. University of Illinois, 1985.

[14] R. A. McD. Galbraith, "The aerodynamic characteristics of a GU25-5(11)8 aerofoil for low Reynolds numbers," *Experiments in fluids*, 1985.

[15] Sagar Sanjeev Sathaye, *Lift districutions on low aspect ratio wings ay low reynolds numbres*. Worcester polytechnic institute, 2004.

[16] Stijn Van Gysel, *Load alleviation on wind turbine blades using microtabs: an experimental approach*. EhB Master thesis, 2012.

[17] Ivan Werkhoven, *Kalibreren van een lagesnelheidswindtunnel*. EhB Master thesis, 2013.

[18] P. Devinant, T. Laverne, and J. Hureau, *Experimental study of wind turbine airfoil aerodynamics in high turbulence*. Journal of wind engineering and industrial aerdynamics, 2002.